Title
Genetic and Biochemical Characterization of Early Carotenoid Biosynthesis Mutants of Chlamydomonas reinhardtii

Author
Tran, Phoi T

Publication Date
2011

Peer reviewed|Thesis/dissertation

Genetic and biochemical characterization of early carotenoid biosynthesis mutants of *Chlamydomonas reinhardtii*

By

Phoi Thi Tuyet Tran

A dissertation submitted in partial satisfaction of the

requirements for the degree of

Doctor of Philosophy

in

Plant Biology

in the

Graduate Division

of the

University of California, Berkeley

Committee in charge:

Professor Krishna K. Niyogi, Chair
Professor Anastasios Melis
Professor Jasper Rine

Spring 2011

Abstract

Genetic and biochemical characterization of early carotenoid biosynthesis mutants

of *Chlamydomonas reinhardtii*

by

Phoi Thi Tuyet Tran

Doctor of Philosophy in Plant Biology

University of California, Berkeley

Professor Krishna K. Niyogi, Chair

Carotenoids are isoprenoid pigment molecules with a long hydrocarbon skeleton distinguished by its system of conjugated double bonds. They are essential to photosynthetic organisms because of their ability to prevent photo-oxidative damage, and they also harvest light energy for photosynthesis. *Chlamydomonas reinhardtii* carotenoid-deficient mutants were generated using UV and DNA insertional mutagenesis and screened for pigment accumulation. Mutants that accumulate phytoene, ζ-carotene, or prolycopene were isolated and found to be genetically linked to the predicted phytoene desaturase (*PDS1*), zeta-carotene desaturase (*ZDS1*), and carotene isomerase (*CRTISO1*) genes, respectively.

The first *C. reinhardtii pds1* mutant isolated, *pds1-1*, is a weak allele for phytoene desaturation; it is light-green and accumulates phytoene and downstream colored carotenoids. Two white mutants that appear to be null alleles of PDS1, *pds1-2* and *pds1-3*, were identified by their phytoene accumulation and complete lack of colored carotenoids. Compared to white *psy* mutants, which also lack all colored carotenoids, phytoene-accumulating mutants exhibited slower growth rates in the dark and reduced plating efficiencies, indicating that phytoene accumulation may be deleterious. Three classes of *pds1-2* suppressor mutants were identified that synthesized elevated levels of colored carotenoids and were less light sensitive than their parental strain. The *pds1-2* suppressor mutants had mutations affecting amino acids at positions 64, 90, and 143 in the predicted PDS protein: *pds1-4* (L64P), *pds1-5* (L64F and E143K), and *pds1-6* (L64P, K90M, E143K). Characterization of *pds1-2* intragenic suppressors coupled with computational structure prediction of PDS suggest that amino acids at positions 64 and 90 help maintain the structural stability and/or activity of the PDS enzyme.

Dark-grown *C. reinhardtii zds1* and *crtiso1* mutants are yellow in the dark and accumulate ζ-carotenes or prolycopene, respectively, but with gradual illumination they can turn green and accumulate higher levels of xanthophylls. In the case of *crtiso1*, dark-accumulated prolycopene can be photoisomerized and efficiently converted to downstream photoprotective carotenoids in the light. The presence of xanthophylls in dark-grown *zds1* and *crtiso1* null mutants provides evidence for an alternative carotene desaturase in *C. reinhardtii*. A suppressor of the *zds1*

mutant, zSup63, with a dominant very-green-in-low-light phenotype was isolated. Transcript levels for a putative protein (protein ID 516552) with homology to plant and algal CRTISO proteins were elevated at least ten-fold in light-grown zSup63 cells compared to the parental *zds1* strain. A low light-sensitive, dark-green DNA insertional mutant (CAL028.02.09) with a disruption in the gene encoding protein 516552 has been identified and analysis of double mutants will determine if this protein is responsible for xanthophyll synthesis in dark-grown *zds1* and *crtiso1* mutants.

The collection of early carotenoid biosynthetic mutants reported here, which accumulate *cis*-configured carotenes, conclusively demonstrate that carotenoids in *C. reinhardtii* are primarily synthesized by a plant-type poly-*cis* carotene desaturation pathway, making *C. reinhardtii* ideal for investigating carotenoid biosynthesis and regulation (and the processes that intersect with them).

DEDICATION

To my parents

My mother, Hia T. Quach (July 7, 1940 - July 18, 2010) will always be the strongest woman in my life. She single-handedly raised six daughters in a foreign country. Her life's work is manifest in this work, and in the post-baccalaureate degrees of each of her children. Her love and support were unconditional.

My father, Tai V. Tran (November 1, 1938 to June 14, 1984) was a fearless follower of dreams. No matter his life situation, he lived joyously and gave generously.

TABLE OF CONTENTS

Abstract 1

Dedication i

Table of Contents ii

List of Figures iii

List of Tables v

Acknowledgements vi

Chapter 1: Introduction-Early carotenoid biosynthesis in plants and green algae 1

Chapter 2: Intragenic enhancers and suppressors of phytoene desaturase mutations in *Chlamydomonas reinhardtii* 16

Chapter 3: Light conditional mutants affecting conversion of zeta-carotene to lycopene in *Chlamydomonas reinhardtii* 45

Chapter 4: A mutant that improves the greening phenotype of *zds1* identifies a light-induced, CRTISO-like protein as a possible second ζ-carotene desaturase in *Chlamydomonas reinhardtii* 70

Chapter 5: Conclusions of Dissertation 94

LIST OF FIGURES

Figure 1.1: Carotenoid biosynthesis in plants and green algae 3

Figure 2.1: Structural features of the linearized pBC1 vector used to generate insertional mutant *pds1-3* 22

Figure 2.2: Phenotype of wild-type Chlamydomonas cells grown norflurazon 23

Figure 2.3: Light sensitivity of wild-type, *lts1* and *pds1* mutants 25

Figure 2.4: Chlorophyll and carotenoid profiles of PDS-activity deficient mutants 26

Figure 2.5: The *PDS1* gene is genetically linked to the *pds1-1* mutant phenotype 28

Figure 2.6: Multiple sequence alignment of PDS protein sequences 29

Figure 2.7: Analysis of enhancer strain P3-84 (*lts 1-301 pds1-2)* and intragenic suppressors of *pds1-2* mutants 30

Figure 2.8: Analysis of *pds1*-3 DNA insertional mutant 33

Figure 2.9: Results of plating assays of wild-type, *lts1-201*, *pds1-3*, and *pds1-1* 35

Figure 2.10: Analysis of intragenic suppressors of *pds1-2* mutants 37

Figure 3.1: The poly-*cis* carotene desaturation pathway found in plants 47

Figure 3.2: Light sensitivity and "greening" phenotype of *zds1* and *crtiso1* mutants 51

Figure 3.3: Chlorophyll and carotenoid profiles of *zds1-1* and *crtiso1-1* mutants under dark and light conditions 52

Figure 3.4: Genetic linkage analyses of *zds1* mutants 56

Figure 3.5: Mutations found in *zds1* mutants 57

Figure 3.6: Molecular analysis of *zds1-1* and *crtiso1-1* DNA insertional mutants. 59

Figure 3.7: Mutations identified in *crtiso1* mutants 61

Figure 4.1: Desaturation of 15-*cis*-phytoene to all-*trans*-lycopene by PDS/ZDS-type and CrtI-type phytoene desaturases 72

Figure 4.2: Light sensitivity and "greening" phenotype of *zds1-1* mutants 77

Figure 4.3: Effect of light and cycloheximide on carotenoid accumulation in *zds1-1* mutants. 78

Figure 4.4: Double mutant *zds1-1 crtiso1-1* still accumulates xanthophylls. 80

Figure 4.5: Example of color phenotypes of non-greening *zds1-1* mutants. 81

Figure 4.6: Selection/screening for *zds1-1* mutants that are greener in the light. 82

Figure 4.7: Mutants derived from *zds1-1* that have a dominant very-green-in-LL phenotype 83

Figure 4.8: Phylogenetic tree of carotenoid desaturases and isomerases from plants, algae, bacteria, and a fungus. 87

Figure 4.9: Transcript expression levels of a candidate carotene desaturase, Au5.g6551_t1 (516552), in *zds1-1* mutants with a dominant, very-green-in-LL phenotype. 89

LIST OF TABLES

Table 2.1: Tetrad analysis of *pds1-1* and *pds1-3* crossed to wild-type 27

Table 2.2: Quantification of chlorophyll, carotenoid, and α-tocopherol content of *lts1* and *pds1* mutants 31

Table 3.1: Timeline of gradually increasing light intensities used in "greening" assay. 48

Table 3.2: Quantification of chlorophyll, xanthophyll, and α-tocopherol levels in *zds1-1* and *crtiso1-1* mutants 54

Table 3.3: Genetic analyses of *crtiso1* and *zds1* mutants. 62

Table 4.1. Levels of ζ-carotene isomers in *zds1-1* mutants treated with cycloheximide and light 79

ACKNOWLEDGEMENTS

I understood Dr. Krishna Niyogi to be an excellent adviser before I joined his lab. As a new graduate student, I tried to avoid meeting with him because his questions consistently stumped me. Over the years, I have come to enjoy discussing science with Kris, and I try very hard to anticipate his questions. He still stumps me with his questions, but now they function as platforms for new experiments. I will strive to emulate his integrity and thoroughness in my own research career. Finally, I am especially grateful for Kris' kindness and patience during exceptionally trying times in my life. His no nonsense attitude and encouragement has helped me complete research that I am proud of.

I would also like to recognize my undergraduate adviser at Cornell University, Dr. William E. Fry, and Dr. Guangping Gao, for whom I worked, at the University of Pennsylvania. Dr. Fry gave me a job in his lab and in the process introduced me to the field of research. I also thank Dr. Fry for the five drafts of my undergraduate thesis that I had to write—I learned so much about writing from Dr. Fry. Dr. Gao really took me under his wing. From Dr. Gao, I learned the finite details and controls required to carry out a reliable experiment; all those lessons in front of the white board, all the calculations, and hands-on demonstrations were invaluable. I have used those lessons Dr. Gao taught me countless times during my dissertation.

From my dissertation committee, I have received valuable guidance. In addition to serving on my committee, Dr. Anastasios Melis acted as the chair during my qualifying exams. Dr. Melis is a great teacher to whom I owe much of my understanding of photosynthesis and plant biochemistry. The *zds1-1* suppressor screen in Chapter 4 was the result of Dr. Jasper Rine's thoughtful questions and advice. I have saved time and have promising results because of his counsel.

To the members of the Niyogi lab, thank you for your support. You have been there to commiserate or make me laugh when my experiments failed, to cheer me on when things finally worked, and for saving my cultures when I was house-bound in Philly. Setsuko Wakao, Rachel Dent, Zhirong Li, Robbie Calderon, and Graham Peers are my go-to people for friendship and fun conversations on science, food, and life. Setsuko is an amazing teacher and I envy the undergraduates that have been lucky enough to be trained by her. She has taught me qPCR and her advice on how to culture *Chlamydomonas* has made the difference between a successful or failing experiment. I am indebted to Rachel for creating and isolated the insertional mutants mentioned in this dissertation and for bringing them to my attention. Marilyn Kobayashi is a super lab manager—supplies are consistently stocked and organized and equipment running. I know that I can rely on Zhirong and Marilyn fix the HPLC machine whenever it breaks. I also want to thank Brian Chin and to Sarah McCarthy for showing me the ropes during my first year in the lab.

To my five sisters, brothers-in-law, my nieces and nephews and Daniel…

The language of love
Was never the worse
For some overstatement.
--Antonio Machado

Thank you for seeing me through everything, I couldn't have asked for a better family. Daniel, you are my comfort and sanity management (Toot Toot).

CHAPTER 1
Early carotenoid biosynthesis in plants and green algae

INTRODUCTION

Carotenoids are a diverse and large class of lipid-soluble pigments with important functions in nature and in human life. In plants and green algae they are C_{40} molecules distinguished by their system of conjugated double bonds that can absorb light energy and quench harmful molecules such as triplet chlorophylls and singlet oxygen. The number of conjugated double bonds and other modifications lend carotenoids their characteristic colors and biological activities. Plants synthesize carotenoids in chloroplasts for harvesting light energy, photoprotection, and maintaining the structure and function of photosynthetic membranes [1,2,3]. In photosynthetic tissues most carotenoids are bound to and help stabilize proteins localized in the thylakoid membrane [4,5,6,7]. In the absence or reduction of carotenoids, chlorophyl-binding proteins are less stable, and the proteins as well as the chlorophylls that bind to them accumulate poorly or hardly at all in cells [7,8]. As photoprotectants, carotenoids perform several functions. They harmlessly dissipate excess absorbed light energy as heat by de-exciting the singlet excited state of chlorophyll (^{1}Chl) in a process measured as nonphotochemical quenching of chlorophyll fluorescence (NPQ) [7,9,10]. They are also quenchers of reactive molecules of chlorophyll in the triplet excited state (^{3}Chl) and oxygen in the singlet excited state ($^1O_2$), which forms when ^{3}Chl interacts with molecular oxygen [3,9,11].

Besides their role in photosynthesis, carotenoids also act as attractants for pollination and seed dispersal in plants. Carotenoids, in addition to two other pigment groups, betalin and anthocyanins, give flowers and plants their many different colors [12,13]. Carotenoids can also be cleaved to form the plant hormone, abscisic acid (ABA), which promotes seed dormancy and inhibits germination [14,15,16,17]. In seeds, elevated carotenoids levels are also associated with seed viability and aging [13,17,18]. Additionally, carotenoid cleavage products also control shoot branching in plants [19,20]. In the green alga *Chlamydomonas reinhardtii,* carotenoids in the eyespot assist in phototaxis [21]. Dietary carotenoids provide some animals such as flamingos, salmon, and lobsters their familiar pink or blue coloration. In the human diet, carotenoids have many functions and uses as antioxidants, coloring agents, and as precursors to vitamin A [22,23,24]. Carotenoid production, in particular for astaxanthin and lutein, for commercial fish and poultry farming, respectively, is a multi-million dollar business [25,26,27,28]. A diet rich in carotenoids helps prevent eye diseases and reduce the risk of cancers and UV damage to skin in humans [13,22,28,29,30,31,32,33].

General steps of carotenoid biosynthesis in plants and algae

Carotenoids in oxygenic photosynthetic organisms are synthesized in plastids from isopentylpyrophosphate (a C_5 molecule) formed in the 1-deoxyxylulose 5-phosphate (DOXP) or methylerythritol 4-phosphate (MEP) pathway [34,35,36,37]. Carotenoid biosynthesis (Figure 1.1) is carried out in four types of reactions: (1) condensation of two colorless C_{20} geranylgeranylpyrophosphate (GGPP) molecules to form the colorless 15-*cis*-phytoene carotenoid molecule, (2) desaturation and isomerization of 15-*cis*-phytoene to form red-colored all-*trans*-lycopene, (3) cyclization of all-*trans*-lycopene to form cyclic carotenes, beta-carotene (β-carotene) and alpha-carotene (α-carotene) and (4) addition of oxygen groups to form xanthophylls [34,38]. Non-oxygenated carotenoids are referred to as carotenes. The purpose of this chapter is to provide an overview of the early steps of carotenoid biosynthesis, focusing on the poly-*cis* carotene desaturation pathway in plants and algae along with a brief review of bacterial-type phytoene desaturation found in archaea, fungi, anoxygenic photosynthetic and non-photosynthetic bacteria for comparison [39,40,41,42].

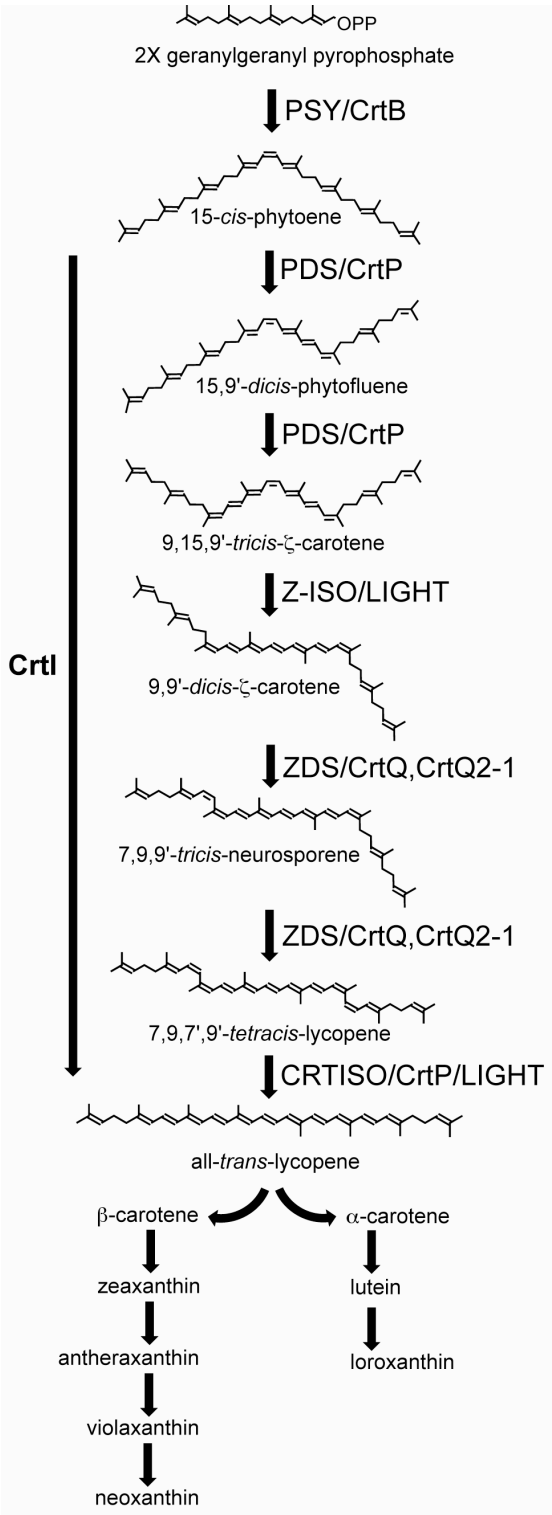

Figure 1.1. Carotenoid biosynthesis in plants and green algae.
Geranylgeranyl pyrophosphate, phytoene, and phytfluene are all colorless compounds Colored carotenoids include ζ-carotene and all carotenoids downstream. Xanthophylls include zeaxanthin, antheraxanthin, violaxanthin, neoxanthin, lutein, and loroxanthin (found in *C. reinhardtii*). "Crt" prefix denote prokaryotic carotenoid biosynthesis proteins.

Phytoene synthesis

In plants and green algae the first committed step of carotenoid biosynthesis is catalyzed by phytoene synthase (PSY), which joins two molecules of the C_{20} compound GGPP to form the colorless C_{40} compound, 15-*cis*-phytoene. 15-*cis*-phytoene is produced by all C_{40} carotenogenic organisms [37,39,40,43,44]. Phylogenetic studies based on protein sequence show that phytoene synthases, PSY and CrtB, from photosynthetic and non-photosynthetic eukaryotes and prokaryotes are highly conserved [41,45]. Plant-type PDS/CrtP proteins can efficiently use the phytoene substrate generated by *Escherichia coli* expressing the *crtB* gene from *Erwinia* [46,47,48].

Toledo-Ortiz *et al.* recently showed that during photomorphogenesis, carotenoid biosynthesis was up-regulated by the transcription factors phytochrome-interacting factors (PIFs) directly targeting the *Arabidopsis thaliana PSY* gene [49]. Red light was shown to active the Pfr form of phytochrome, causing it to move to the nucleus where it promotes the degradation of PIFs, which negatively regulate *PSY* expression by binding to its promoter [49]. Studies measuring *PSY* mRNA levels and transgenic plants overexpressing *PSY* support the idea that *PSY* is the primary target (other rate-limiting steps are also present in the pathway) of carotenoid regulation (for reviews on carotenoid regulation see [28,50,51,52]). Light was shown to increase *PSY* and *crtB* transcripts in *A. thaliana*, *Sinapis alba* L. (white mustard), *Oryza sativa*, *Synechococcus* PCC7942, and *C. reinhardtii* [53,54,55,56]. Overexpression of *A. thaliana* and maize PSY led to increased carotenoid content in non-green tissues [57,58] while overexpression of *PSY1* led to dwarf phenotypes in tobacco and tomato plants [59,60,61]. Multiple homologs of the *PSY* gene occur in some plants and have been shown to have non-exclusive but tissue-specific activities. Chromoplast carotenogenesis in tomato (pTOM5) and maize was associated with increased transcript levels of *PSY1*, whereas leaf carotenogenesis was associated with increased levels of *PSY2* mRNA [62,63,64,65]. Elevated expression levels of *PSY1* and *PSY2* from *Oryza sativa* were both associated with leaf carotenogenesis [56]. A third *PSY* (*PSY3*) was identified in both *Oryza sativa* and maize whose expression was elevated during drought- and salt-induced stress [56,62]. Because phytoene synthase may be the main rating-limiting step in carotenoid biosynthesis, manipulation of *crtB* and *PSY* genes has been a major target in metabolic engineering to create crop plants with improved carotenoid content [28,58,66,67].

Phytoene desaturation

Next, four double bonds are added to 15-*cis*-phytoene to form all-*trans*-lycopene—extending the number of conjugated double bonds from three to eleven [68]. Two systems for desaturation of phytoene to lycopene have been identified in nature, the bacterial CrtI-type enzyme and the plant-type PDS/Z-ISO/ZDS/CRTISO enzymes. Plant-type phytoene desaturation is distinguished from bacterial-type or CrtI-type phytoene desaturation by the *cis*-configured intermediates accumulated by mutants with blocks in each step of phytoene desaturation. Organisms with CrtI-type desaturases exhibit all-*trans* isomers of phytofluene, ζ-carotenes, neurosporene, and lycopene [37,40,43,69,70,71]. Plant-type phytoene desaturation or poly-*cis*-carotene pathway results in 7,9,7',9'-*tetracis*-lycopene (prolycopene) via *cis*-isomers of phytofluene, ζ-carotenes, neurosporene [39,40,42,46]. Phylogenetic analyses based on protein structural similarity show that the bacterial-type and the plant-type phytoene desaturases are evolutionarily unrelated [41,45]: CrtI-type desaturases form one group while

PDS(CrtP)/ZDS(CrtQ,CrtQ-1)-type form another group. However, CRTISO(CrtH), which functions in plant-type desaturation, is more related to bacterial-type than plant-type desaturases [41,45,72,73].

CrtI-type or bacterial-type phytoene desaturases

Fungi, archaea, and heterotrophic and anoxygenic bacteria require only one enzyme, the CrtI-type desaturases, to convert 15-*cis*-phytoene to all-*trans*-lycopene [37,43]. In the process of introducing four double bonds, CrtI-type desaturases also isomerize the central *cis*-configured double bond at C15 to *trans*-configuration. Among the CrtI-type desaturases there can be variations in the number of desaturation steps introduced and types of substrates used. The ones described below have relevance to the following chapters, so they are mentioned. The anoxygenic photosynthetic bacterium, *Rhodobacter capsulatus,* has a CrtI that catalyzes a three-step desaturation to form neurosporene [69,74,75]. The heterotrophic bacterium, *Myxococcus xanthus* has two functional CrtI-like proteins, CrtIa and CrtIb [76]. *M. xanthus crtIb* mutants accumulate all-*trans*-configured phytoene and phytofluene, whereas mutants for *crtIa* accumulate only 15-*cis*-phytoene [76]. Functional complementation in *E. coli* determined that CrtIa was a two-step desaturase with *cis*-to-*trans* isomerase activity that can either convert *cis*-phytoene to *trans*-ζ-carotene or *cis*-ζ-carotene to *trans*-neurosporene while CrtIb, also a two-step desaturase, could only use *trans*-configured carotenes. *In vivo*, CrtIa isomerizes 15-*cis*-phytoene to all-*trans*-phytoene, which then permits CrtIb to catalyze the formation of all-*trans*-lycopene [76]. *Gloeobacter violaceus*, unlike other characterized cyanobacteria, which have plant-type phytoene desaturases, has an active CrtI-like four-step desaturase and does not have genes for *CrtP, CrtQ, or CrtH* [77,78].

PDS-type or plant-type phytoene desaturases

In green algae and higher plants at least four known enzymes are required to complete the same reaction catalyzed by CrtI desaturases. Both PDS/CrtP and ZDS/CrtQ/CrtQ-1, are two-step desaturases compared to CrtI desaturases. PDS adds one *trans*-double bond at C-11 to 15-*cis*-phytoene creating 9,15-*dicis*-phytofluene and then a second *trans*-double bond at C-11' to generate 9,15,9'-*tricis*-ζ -carotene [42,79,80]. The introduction of *trans*-double bonds at the 11 positions was observed to cause *trans*-double bonds at C-9 and C-9' to become *cis*-configured [39,42,46]. 9,15,9'-*tricis*-ζ -carotene was established as the product of PDS desaturation, but not as the substrate for ZDS desaturation in *in vitro* experiments.

When daffodil chromoplast homogenates were incubated with ^{14}C-labeled 15-*cis*-phytoene in the dark, 15-*cis*-phyfluene and a 15-*cis* isomer of ζ-carotene accumulated [81]. Lycopene was formed in chromoplast incubation experiments only after illumination of the 15-*cis* isomer of ζ-carotene. *E. coli* expressing *A. thaliana PDS* and *ZDS,* when grown in the dark, accumulated mostly a C-15 *cis*-configured ζ-carotene isomer, but when shifted into light accumulated lycopene, a decrease in 9,15,9'-*tricis*-ζ-carotene, and an increase in 9,9'-*dicis*-ζ-carotene [46]. Breitenbach and Sandmann [79] further established these findings with purified *Capsicum annum* (pepper) ZDS proteins incubated with individual *cis*- and *trans*-isomers of ζ-carotene. From these experiments, they concluded that 9,15,9'-*tricis*-ζ-carotene and 15,9'-*dicis*-phytofluene as an intermediate were the enzymatic products of PDS. They also confirmed that light could photoisomerize the central C-15 *cis*-configured double bond in 9,15,9'-*tricis*-ζ-

carotene to a *trans*-configuration and that 9,9'-*dicis*-ζ-carotene was the primary substrate of ZDS.

Phytoene-accumulating white tissues of *A. thaliana* and tomato with mutations in genes for plastoquinone (PQ) biosynthesis [82] or for an *IMMUTANS*-type plastid terminal oxidase (PTOX) [83,84] revealed that PDS activity requires an oxidized PQ pool and a PTOX. In models for carotene desaturation, electrons generated by the PDS and ZDS desaturation reactions are used to reduce the PQ pool ([85,86,87]; reviewed in [88,89]). PTOX then oxidizes the PQ pool by transferring electrons to molecular oxygen.

A. thaliana [82,90], *Nicotiana tabacum* [59], *Zea mays* [91], and *O. sativa* [92] plants with transcriptional silencing or mutations affecting PDS activity exhibit severe phenotypes, including stunted growth and albino coloring or photobleaching. Moreover, homozygous *pds* mutants are lethal at the seedling stage and require growth on Murashige and Skoog medium supplemented with sugar [82,92]. *Z. mays* (*vp5*, [91]) and *O. sativa* (*phs1*, [92]) *pds* mutants also have viviparous or precocious germination due to ABA deficiency.

Some, though not all, studies have concluded that PDS is also a rate-limiting step in carotenoid biosynthesis. Some studies have noticed that increased *PDS* transcript expression correlated with increased carotenoid levels and/or light exposure [24,55,64,93]. In contrast, studies by Wetzel *et al.* [94] and Simkin *et al.* [95] did not find *PDS* mRNA levels correlated with carotenoid content.

15-cis-ζ-carotene isomerase

In dark-grown and non-photosynthetic tissues a ζ-carotene isomerase, Z-ISO, is required for carotenogenesis. *Z. mays* and *A. thaliana Z-ISO* expressed in dark-grown *E. coli* was shown to carry out a *cis*-to-*trans* isomerization of the 9,15,9'-*tricis*-ζ-carotene PDS product to 9,9'-*dicis*-ζ-carotene, the substrate for ZDS [96]. Unlike CRTISO carotene isomerases which have similarity to CrtI-type desaturases, the Z-ISO protein was more related to bacterial nitrite and nitric oxide reductase U (NnrU), a protein active in bacterial denitrification [96]. *Z. mays* (*y9*) and *A. thaliana* (*zic1*) mutants with a deficiency in Z-ISO activity have non-lethal phenotypes. Etiolated seedlings of both mutants appeared more yellow than wild type seedlings and accumulated 9,15,9'-*tricis*-ζ-carotene [96,97]. Under light conditions, mutants exhibited delayed greening and accumulated xanthophylls, and green and white striping in homozygous mutants [97].

ζ-carotene desaturase

Plant-type ZDS is also a two-step desaturase. It introduces *cis*-configured double bonds to the C-7 (7,9,9'-*tricis*-neurosporene) and C-7'positions of 9,9'-*dicis*-ζ-carotene to produce a poly-*cis* lycopene or 7,9,7'9'-*tetracis*-lycopene (prolycopene) [46,79,81,98]. Analysis of *crtiso* mutants (tomato *tangerine* [39,72], *A. thaliana ccr2*, and *Scenedesmus* C-6D [42]) that accumulate prolycopene, as well as experiments with *E. coli* expressing plant-type *PDS* and *ZDS* genes and substrate feeding experiments using purified ZDS proteins [46,79,98,99], showed that prolycopene was the final product of ZDS activity. Two types of ζ-carotene desaturases have been characterized from cyanobacteria, the CrtQ/CrtQ-2 ζ-carotene desaturase related to the plant-type ZDS and the CrtQ-1/CrtQa related to bacterial CrtI desaturases [99,100]. CrtQ-1 from *Nostoc* PCC7120 (formerly *Anabaena* PCC7120) was the first ζ-carotene desaturase cloned from

any organism [101]. Functional characterization of CrtQ-1 expressed in *E. coli* accumulating phytoene desaturation products from *Rhodobacter capsulatus* CrtI or from *Synechococcus* (CrtP) determined that CrtQ-1 was a two-step desaturase that could use both *cis*- and *trans*-configured carotenes [102].

Plants with *ZDS* gene mutations have severe phenotypes similar to those found in *pds* mutants. Mutant phenotypes displayed by *A. thaliana* (*spc1*, [103]), *Helianthus annum* L (*nd-1*, [104]), *Zea mays* (*vp9*, [105]), and *O. sativa* (*phs2,* [92]) include vivipary, albino and photobleached leaves/seedlings, seedling lethality, and ζ-carotene accumulation.

Carotene isomerase

The last step of plant and algal carotene desaturation is defined by the *cis*-to-*trans*-isomerization of prolycopene to all-*trans*-lycopene. In non-green, carotenoid-producing cells, this final step is catalyzed by CRTISO. Similar to *z-iso* mutants that accumulate 9,15,9'-tricis-ζ-carotene, the presence of light allows cells with blocks in CRTISO activity to synthesize cyclic carotenes and xanthophylls. Functional expression in *E. coli* showed that CRTISO does not possess any desaturase activity and that its *cis*-to-*trans* isomerase activity was responsible for the conversion of all four *cis* double bonds in prolycopene to *trans* double bonds [72,73,106]. *In vitro* biochemical assays with purified tomato CRTISO demonstrated that CRTISO belongs to a class of flavoproteins that catalyzes non-redox reactions that require a bound, reduced FAD [106]. The same study also found that CRTISO could isomerize monocyclic carotenoids (γ-carotene) and form 5-*cis*-lycopene by catalyzing a *trans*-to-*cis* isomerization to poly-*cis* carotenoids [106]. Anaerobic conditions [72,106] also enhanced CRTISO activity in contrast to PDS whose activity requires molecular oxygen [81]. Yu *et al.* suggested that the anaerobic requirement of CRTISO may be a reflection of its evolution in an anoxygenic environment [106].

Plant and algal mutants with defects in CRTISO activity are viable in the light, unlike carotene desaturase mutants. In general, *crtiso/crth* mutants in plants (tomato *tangerine* [39,72], *A. thaliana ccr2* [73], rice *zebra2* and *phs3* [92,107]), green algae (*Scenedesmus obliquus* C-6D [42]), and cyanobacteria (*Synechocystis* PCC6803 *sll0033* [108]) have light-induced/delayed greening phenotypes. Mutants grown in the dark have orange- to yellow-colored leaves and pale-green cells (algae) that accumulate *cis*-carotenes, in particular prolycopene [42,72,73,92,107,108,109]. After transfer to the light, both plant and algal *crtiso/crth* mutants accumulate wild-type carotenoids and prolycopene disappeared. The plant *crtiso* mutants also experienced delayed greening in the light: yellow to orange-colored seedlings and newly formed leaves turned green, accumulated chlorophyll, but at a delayed rate compared to wild-type plants [72,73,107].

In vitro experiments with extracts of ζ-carotene substrates and *E. coli* expressing PDS, which produces 9,15,9'-*tricis*-ζ-carotene, showed that the isomer 9,15,9'-*tricis*-ζ-carotene is very efficiently isomerized to 9,9'-*dicis*-carotene in the light [46,79,81,96]. Prolycopene, in contrast, seems to be less efficiently photoisomerized without photosynthetic tissue. When the *E. coli* cells expressing *PDS* and *ZDS* were grown in the light, prolycopene was unchanged [72] or changed only slightly [46]. Prolycopene-accumulating chromoplasts of fruits and flowers also were unchanged by illumination [72]. In contrast, prolycopene accumulated in photosynthetic tissues in plants and algae can be efficiently converted to all-*trans*-lycopene in the light [42,73,80,107,108].

In *L. esculentum*, *A. thaliana*, and *O. sativa crtiso* mutants, lutein accumulation in green leaves was noticeably reduced compared to wild-type levels [72,73,107]. In *O. sativa* mutants, defects in CRTISO activity resulted in green and white sectors reflecting photo-oxidative bleaching of leaves [92,107].

Chlamydomonas reinhardtii as a model system

The unicellular green alga *Chlamydomonas reinhardtii* is well suited for studying carotenoid biosynthesis and other photosynthesis-related functions as it can grow either photoautotrophically or heterotrophically on exogenous carbon sources [110,111,112]. This has permitted the culturing of photosynthesis mutants that would otherwise be lethal or infertile in plants. Mutants in the early steps of carotenoid biosynthesis in plants frequently have severe phenotypes that include seedling lethality, sterility, albinism, vivipary, and dwarfism. *C. reinhardtii* is also an ideal model organism for photosynthesis-related studies because of its short doubling time and it requires less space than plants. Genetic analyses are simplified by its haploid nature and the 13x sequencing coverage of its genome [111].

Because carotenoids have such vital roles in nature and in human life, understanding their synthesis and regulation is of vital importance. In the last several decades, much information concerning carotenoid biosynthesis has been produced, but because carotenoid biosynthesis is closely linked to photosynthetic processes and light, there is still little information regarding carotenoid regulation in plants. The collection of *C. reinhardtii mutants,* described in the following three chapters, with defects in early carotenoid biosynthesis will hopefully contribute to future studies in carotenoid biosynthesis, evolution, and regulation.

REFERENCES

1. Niyogi KK, Björkman O, Grossman AR (1997) The roles of specific xanthophylls in photoprotection. Proceedings of the National Academy of Sciences 94: 14162-14167.
2. Plumley FG, Schmidt GW (1987) Reconstitution of chlorophyll a/b light-harvesting complexes: xanthophyll-dependent assembly and energy transfer. Proceedings of the National Academy of Sciences 84: 146-150.
3. Demmig-Adams B, Adams WW (1992) Photoprotection and other responses of plants to high light stress. Annual Review of Plant Physiology and Plant Molecular Biology 43: 599-626.
4. Bassi R, Pineau B, Dainese P, Marquardt J (1993) Carotenoid-binding proteins of photosystem II. European Journal of Biochemistry 212: 297-303.
5. Havaux M (1998) Carotenoids as membrane stabilizers in chloroplasts. Trends in Plant Science 3: 147-151.
6. Yamamoto HY, Bassi R (2004) Carotenoids: Localization and Function. In: Ort DR, Yocum CF, Heichel IF, editors. Oxygenic Photosynthesis: The Light Reactions: Springer Netherlands. pp. 539-563.
7. Frank HA, Cogdell RJ (1996) Carotenoids in Photosynthesis. Photochemistry and Photobiology 63: 257-264.
8. Herrin DL, Battey JF, Greer K, Schmidt GW (1992) Regulation of chlorophyll apoprotein expression and accumulation. Requirements for carotenoids and chlorophyll. Journal of Biological Chemistry 267: 8260-8269.
9. Niyogi KK (1999) Photoprotection revisited: genetic and molecular approaches. Annual Review of Plant Physiology and Plant Molecular Biology 50: 333-359.
10. Demmig-Adams B, Gilmore A, Adams W (1996) Carotenoids 3: in vivo function of carotenoids in higher plants. The FASEB Journal 10: 403-412.
11. Asada K (2006) Production and scavenging of reactive oxygen species in chloroplasts and their functions. Plant Physiology 141: 391-396.
12. Grotewold E (2006) The genetics and biochemistry of floral pigments. Annual Review of Plant Biology 57: 761-780.
13. Howitt CA, Pogson BJ (2006) Carotenoid accumulation and function in seeds and non-green tissues. Plant, Cell & Environment 29: 435-445.
14. Rock CD, Zeevaart JAD (1991) The *aba* mutant of *Arabidopsis thaliana* is impaired in epoxy-carotenoid biosyntheis. Proceedings of the National Academy of Sciences 88: 7496-7499.
15. Schwartz SH, Tan BC, Gage DA, Zeevaart JAD, McCarty DR (1997) Specific oxidative cleavage of carotenoids by VP14 of maize. Science 276: 1872-1874.
16. Taylor HF, Smith TA (1967) Production of plant growth inhibitors from xanthophylls: a possible source of dormin. Nature 215: 1513-1514.
17. Nambara E, Marion-Poll A (2005) Abscisic acid biosynthesis and catabolism. Annual Review of Plant Biology 55: 165-185.
18. Calucci L, Capocchi A, Galleschi L, Ghiringhelli S, Pinzino C, et al. (2004) Anitoxidants, free radicals, storage proteins, puroindolines, and proteolytic activities in bread wheat (*Triticum aestivum*) seeds during accelerated aging. Journal of Agricultural and Food Chemistry 52: 4274-4281.

19. Auldridge ME, McCarty DR, Klee HJ (2006) Plant carotenoid cleavage oxygenases and their apocarotenoid products. Current Opinion in Plant Biology 9: 315-321.
20. Ohmiya A (2009) Carotenoid cleavage dioxygenases and their apocarotenoid products in plants. Plant Biotechnology 26: 351-358.
21. Kreimer G (2009) The green algal eyespot apparatus: a primordial visual system and more? Current Genetics 55: 19-43.
22. Fraser PD, Bramley PM (2004) The biosynthesis and nutritional uses of carotenoids. Progress in Lipid Research 43: 228-265.
23. Mann V, Harker M, Pecker I, Hirschberg J (2000) Metabolic engineering of astaxanthin production in tobacco flowers. Nature Biotechnology 18: 888-892.
24. Steinbrenner J, Sandmann G (2006) Transformation of the green alga *Haematococcus pluvialis* with a phytoene desaturase for accelerated astaxanthin biosynthesis. Applied Environmental Microbiology 72: 7477-7484.
25. Eonseon J, Polle JE, Lee HK, Hyun SM, Chang M (2003) Xanthophylls in microalgae: from biosynthesis to biotechnological mass production and application. Journal of Microbiology and Biotechnology 13: 165-174.
26. Higuera-Ciapara I, Félix-Valenzuela L, Goycoolea FM (2006) Astaxanthin: A review of its chemistry and applications. Critical Reviews in Food Science and Nutrition 46: 185 - 196.
27. Lorenz RT, Cysewski GR (2000) Commercial potential for *Haematococcus* microalgae as a natural source of astaxanthin. Trends in Biotechnology 18: 160-167.
28. Farré G, Sanahuja G, Naqvi S, Bai C, Capell T, et al. (2010) Travel advice on the road to carotenoids in plants. Plant Science 179: 28-48.
29. Aluru M, Xu Y, Guo R, Wang Z, Li S, et al. (2008) Generation of transgenic maize with enhanced provitamin A content. Journal of Experimental Botany 59: 3551-3562.
30. van den Berg H, Faulks R, Granado HF, Hirschberg J, Olmedilla B, et al. (2000) The potential for the improvement of carotenoid levels in foods and the likely systemic effects. Journal of the Science of Food and Agriculture 80: 880-912.
31. Ye X, Al-Babili S, Klöti A, Zhang J, Lucca P, et al. (2000) Engineering the provitamin A (β-carotene) biosynthetic pathway into (carotenoid-free) rice endosperm. Science 287: 303-305.
32. Fraser PD, Enfissi EMA, Bramley PM (2009) Genetic engineering of carotenoid formation in tomato fruit and the potential application of systems and synthetic biology approaches. Archives of Biochemistry and Biophysics 483: 196-204.
33. Giovannucci E (1999) Tomatoes, tomato-based products, lycopene, and cancer: review of the epidemiologic literature. Journal of the National Cancer Institute 91: 317-331.
34. Hirschberg J (2001) Carotenoid biosynthesis in flowering plants. Current Opinion in Plant Biology 4: 210-218.
35. DellaPenna D, Pogson BJ (2006) Vitamin synthesis in plants: tocopherols and carotenoids. Annual Review of Plant Biology 57: 711-738.
36. Lichtenthaler HK (1999) The 1-deoxy-d-xylulose-5-phosphate pathway of isoprenoid biosynthesis in plants Annual Review of Plant Physiology and Plant Molecular Biology 50: 47-65.
37. Sandmann G (1994) Carotenoid biosynthesis in microorganisms and plants. European Journal of Biochemistry 223: 7-24.

38. Cunningham FX, Gantt E (1998) Genes and enzymes of carotenoid biosynthesis in plants. Annual Review of Plant Physiology and Plant Molecular Biology 49: 557-583.
39. Clough JM, Pattenden G (1983) Stereochemical assignment of prolycopene and other poly-Z-isomeric carotenoids in fruits of the tangerine tomato *Lycopersicon esculentum* var. 'Tangella'. Journal of the Chemical Society, Perkin Transactions 1: 3011-3018.
40. Sandmann G (2009) Evolution of carotene desaturation: the complication of a simple pathway. Archives of Biochemistry and Biophysics 483: 169-174.
41. Sandmann G (2002) Molecular evolution of carotenoid biosynthesis from bacteria to plants. Physiologia Plantarum 116: 431-440.
42. Ernst S, Sandmann G (1988) Poly-*cis* carotene pathway in the *Scenedesmus* mutant C-6D. Archives of Microbiology 150: 590-594.
43. Misawa N, Nakagawa M, Kobayashi K, Yamano S, Izawa Y, et al. (1990) Elucidation of the *Erwinia uredovora* carotenoid biosynthetic pathway by functional analysis of gene products expressed in *Escherichia coli*. Journal of Bacteriology 172: 6704-6712.
44. Beyer P, Weiss G, Kleinig H (1985) Solubilization and reconstitution of the membrane-bound carotenogenic enzymes from daffodil chromoplasts. European Journal of Biochemistry 153: 341-346.
45. Klassen JL (2010) Phylogenetic and evolutionary patterns in microbial carotenoid biosynthesis are revealed by comparative genomics. PLoS ONE 5: e11257.
46. Bartley GE, Scolnik PA, Beyer P (1999) Two *Arabidopsis thaliana* carotene desaturases, phytoene desaturase and & z-carotene desaturase, expressed in *Escherichia coli,* catalyze a poly-*cis* pathway to yield pro-lycopene. European Journal of Biochemistry 259: 396-403.
47. Pecker I, Chamovitz D, Linden H, Sandmann G, Hirschberg J (1992) A single polypeptide catalyzing the conversion of phytoene to zeta-carotene is transcriptionally regulated during tomato fruit ripening. Proceedings of the National Academy of Sciences of the United States of America 89: 4962-4966.
48. Chamovitz D, Misawa N, Sandmann G, Hirschberg J (1992) Molecular cloning and expression in *Escherichia coli* of a cyanobacterial gene coding for phytoene synthase, a carotenoid biosynthesis enzyme. FEBS Letters 296: 305-310.
49. Toledo-Ortiz G, Huq E, Rodr√≠guez-Concepci√≥n M (2010) Direct regulation of phytoene synthase gene expression and carotenoid biosynthesis by phytochrome-interacting factors. Proceedings of the National Academy of Sciences 107: 11626-11631.
50. Bramley PM (2002) Regulation of carotenoid formation during tomato fruit ripening and development. Journal of Experimental Botany 53: 2107-2113.
51. Cazzonelli CI, Pogson BJ (2010) Source to sink: regulation of carotenoid biosynthesis in plants. Trends in Plant Science 15: 266-274.
52. Lu S, Li L (2008) Carotenoid metabolism: biosynthesis, regulation, and beyond. Journal of Integrative Plant Biology 50: 778-785.
53. von Lintig J, Welsch R, Bonk M, Giuliano G, Batschauer A, et al. (1997) Light-dependent regulation of carotenoid biosynthesis occurs at the level of phytoene synthase expression and is mediated by phytochrome in *Sinapis alba* and *Arabidopsis thaliana* seedlings. The Plant Journal 12: 625-634.
54. Schäfer L, Sandmann M, Woitsch S, Sandmann G (2006) Coordinate up-regulation of carotenoid biosynthesis as a response to light stress in *Synechococcus* PCC7942. Plant, Cell & Environment 29: 1349-1356.

55. Bohne F, Linden H (2002) Regulation of carotenoid biosynthesis genes in response to light in *Chlamydomonas reinhardtii*. Biochimica et Biophysica Acta (BBA) 1579: 26-34.
56. Welsch R, Wust F, Bar C, Al-Babili S, Beyer P (2008) A third phytoene synthase Is devoted to abiotic stress-induced abscisic acid formation in rice and defines functional diversification of phytoene synthase genes. Plant Physiology 147: 367-380.
57. Maass D, Arango J, Wüst F, Beyer P, Welsch R (2009) Carotenoid crystal formation in *Arabidopsis* and carrot roots caused by increased phytoene synthase protein levels. PLoS ONE 4: e6373.
58. Paine JA, Shipton CA, Chaggar S, Howells RM, Kennedy MJ, et al. (2005) Improving the nutritional value of Golden Rice through increased pro-vitamin A content. Nature Biotechnology 23: 482-487.
59. Busch M, Seuter A, Hain R (2002) Functional analysis of the early steps of carotenoid biosynthesis in tobacco. Plant Physiology 128: 439-453.
60. Fray RG, Wallace A, Fraser PD, Valero D, Hedden P, et al. (1995) Constitutive expression of a fruit phytoene synthase gene in transgenic tomatoes causes dwarfism by redirecting metabolites from the gibberellin pathway. The Plant Journal 8: 693-701.
61. Fraser PD, Enfissi EMA, Halket JM, Truesdale MR, Yu D, et al. (2007) Manipulation of phytoene levels in tomato fruit: effects on isoprenoids, plastids, and intermediary metabolism. Plant Cell 19: 3194-3211.
62. Li F, Vallabhaneni R, Wurtzel ET (2008) *PSY3*, a new member of the phytoene synthase gene family conserved in the poaceae and regulator of abiotic stress-induced root carotenogenesis. Plant Physiology 146: 1333-1345.
63. Bramley P, Teulieres C, Blain I, Bird C, Schuch W (1992) Biochemical characterization of transgenic tomato plants in which carotenoid synthesis has been inhibited through the expression of antisense RNA to pTOM5. Plant Journal 2: 343-349.
64. Giuliano G, Bartley GE, Scolnik PA (1993) Regulation of carotenoid Biosynthesis during tomato development. Plant Cell 5: 379-387.
65. Bartley GE, Scolnik PA (1993) cDNA cloning, expression during development, and genome mapping of *PSY2*, a second tomato gene encoding phytoene synthase. Journal of Biological Chemistry 268: 25718-25721.
66. Diretto G, Al-Babili S, Tavazza R, Papacchioli V, Beyer P, et al. (2007) Metabolic engineering of potato carotenoid content through tuber-specific overexpression of a bacterial mini-pathway. PLoS ONE 2: e350.
67. Shewmaker CK, Sheehy JA, Daley M, Colburn S, Ke DY (1999) Seed-specific overexpression of phytoene synthase: increase in carotenoids and other metabolic effects. The Plant Journal 20: 401-412.
68. Britton G, Liaaen-Jensen S, Pfander H (2004) *Carotenoids Handbook*. Basel, Switzerland: Birkhäuser Verlag.
69. Giuliano G, Pollock D, Scolnik PA (1986) The gene crtI mediates the conversion of phytoene into colored carotenoids in *Rhodopseudomonas capsulata*. Journal of Biological Chemistry 261: 12925-12929.
70. Scolnik PA, Walker MA, Marrs BL (1980) Biosynthesis of carotenoids derived from neurosporene in Rhodopseudomonas capsulata. Journal of Biological Chemistry 255: 2427-2432.

71. Fraser PD, Misawa N, Linden H, Yamano S, Kobayashi K, et al. (1992) Expression in *Escherichia coli*, purification, and reactivation of the recombinant *Erwinia uredovora* phytoene desaturase. Journal of Biological Chemistry 267: 19891-19895.
72. Isaacson T, Ronen G, Zamir D, Hirschberg J (2002) Cloning of *tangerine* from tomato reveals a carotenoid isomerase essential for the production of β-carotene and xanthophylls in plants. Plant Cell 14: 333-342.
73. Park H, Kreunen SS, Cuttriss AJ, DellaPenna D, Pogson BJ (2002) Identification of the carotenoid isomerase provides insight into carotenoid biosynthesis, prolamellar body formation, and photomorphogenesis. Plant Cell 14: 321-332.
74. Armstrong GA, Alberti M, Leach F, Hearst JE (1989) Nucleotide sequence, organization, and nature of the protein products of the carotenoid biosynthesis gene cluster of *Rhodobacter capsulatus*. Molecular and General Genetics MGG 216: 254-268.
75. Bartley GE, Scolnik PA (1989) Carotenoid biosynthesis in photosynthetic bacteria. Genetic characterization of the *Rhodobacter capsulatus* CrtI protein. Journal of Biological Chemistry 264: 13109-13113.
76. Iniesta AA, Cervantes M, Murillo FJ (2007) Cooperation of two carotene desaturases in the production of lycopene in *Myxococcus xanthus*. FEBS Journal 274: 4306-4314.
77. Steiger S, Jackisch Y, Sandmann G (2005) Carotenoid biosynthesis in *Gloeobacter violaceus* PCC4721 involves a single crtI-type phytoene desaturase instead of typical cyanobacterial enzymes. Archives of Microbiology 184: 207-214.
78. Tsuchiya T, Takaichi S, Misawa N, Maoka T, Miyashita H, et al. (2005) The cyanobacterium *Gloeobacter violaceus* PCC 7421 uses bacterial-type phytoene desaturase in carotenoid biosynthesis. FEBS Letters 579: 2125-2129.
79. Breitenbach J, Sandmann G (2005) ζ-Carotene cis isomers as products and substrates in the plant poly-cis carotenoid biosynthetic pathway to lycopene. Planta 220: 785-793.
80. Isaacson T, Ohad I, Beyer P, Hirschberg J (2004) Analysis in vitro of the enzyme CRTISO establishes a poly-cis-carotenoid biosynthesis pathway in plants. Plant Physiology 136: 4246-4255.
81. Beyer P, Mayer M, Kleinig H (1989) Molecular oxygen and the state of geometric isomerism of intermediates are essential in the carotene desaturation and cyclization reactions in daffodil chromoplasts. European Journal of Biochemistry 184: 141-150.
82. Norris SR, Barrette TR, DellaPenna D (1995) Genetic dissection of carotenoid synthesis in *Arabidopsis* defines plastoquinone as an essential component of phytoene desaturation. Plant Cell 7: 2139-2149.
83. Wetzel CM, Jiang C-Z, Meehan LJ, Voytas DF, Rodermel SR (1994) Nuclear-organelle interactions: the *immutans* variegation mutant of *Arabidopsis* is plastid autonomous and impaired in carotenoid biosynthesis. The Plant Journal 6: 161-175.
84. Mackinney (1956) The phytoene content of tomatoes. Proceedings of the National Academy of Sciences.
85. Wu D, Wright DA, Wetzel C, Voytas DF, Rodermel S (1999) The IMMUTANS variegation locus of *Arabidopsis* defines a mitochondrial alternative oxidase homolog that functions during early chloroplast biogenesis. Plant Cell 11: 43-56.
86. Carol P, Stevenson D, Bisanz C, Breitenbach J, Sandmann G, et al. (1999) Mutations in the *Arabidopsis* gene *IMMUTANS* cause a variegated phenotype by inactivating a chloroplast terminal oxidase associated with phytoene desaturation. Plant Cell 11: 57-68.

87. Josse E-M, Simkin AJ, Gaffé J, Labouré A-M, Kuntz M, et al. (2000) A plastid terminal oxidase associated with carotenoid desaturation during chromoplast differentiation. Plant Physiology 123: 1427-1436.
88. Aluru MR, Rodermel SR (2004) Control of chloroplast redox by the IMMUTANS terminal oxidase. Physiologia Plantarum 120: 4-11.
89. Carol P, Kuntz M (2001) A plastid terminal oxidase comes to light: implications for carotenoid biosynthesis and chlororespiration. Trends in Plant Science 6: 31-36.
90. Qin G, Gu H, Ma L, Peng Y, Deng XW, et al. (2007) Disruption of phytoene desaturase gene results in albino and dwarf phenotypes in *Arabidopsis* by impairing chlorophyll, carotenoid, and gibberellin biosynthesis. Cell Research 17: 471-482.
91. Hable WE, Oishi KK, Schumaker KS (1998) *Viviparous -5* encodes phytoene desaturase, an enzyme essential for abscisic acid (ABA) accumulation and seed development in maize. Molecular and General Genetics MGG 257: 167-176.
92. Fang J, Chai C, Qian Q, Li C, Tang J, et al. (2008) Mutations of genes in synthesis of the carotenoid precursors of ABA lead to pre-harvest sprouting and photo-oxidation in rice. The Plant Journal 54: 177-189.
93. Chamovitz D, Sandmann G, Hirschberg J (1993) Molecular and biochemical characterization of herbicide-resistant mutants of cyanobacterial reveals that phytoene desaturation is a rate-limiting step in carotenoid biosynthesis. The Journal of Biological Chemistry 268: 17348-17353.
94. Wetzel CM, Rodermel SR (1998) Regulation of phytoene desaturase expression is independent of leaf pigment content in *Arabidopsis thaliana*. Plant Molecular Biology 37: 1045-1053.
95. Simkin AJ, Breitenbach J, Kuntz M, Sandmann G (2000) In vitro and in situ Inhibition of carotenoid biosynthesis in *Capsicum annuum* by bleaching herbicides. Journal of Agricultural and Food Chemistry 48: 4676-4680.
96. Chen Y, Li F, Wurtzel ET (2010) Isolation and characterization of the *Z-ISO* gene encoding a missing component of carotenoid biosynthesis in plants. Plant Physiology 153: 66-79.
97. Li F, Murillo C, Wurtzel ET (2007) Maize *Y9* encodes a product essential for 15-cis-{zeta}-carotene isomerization. Plant Physiology 144: 1181-1189.
98. Albrecht M, Klein A, Hugueney P, Sandmann G, Kuntz M (1995) Molecular cloning and functional expression in *E. coli* of a novel plant enzyme mediating ζ--carotene desaturation. FEBS Letters 372: 199-202.
99. Breitenbach J, Fernández-González B, Vioque A, Sandmann G (1998) A higher-plant type ζ-carotene desaturase in the cyanobacterium *Synechocystis* PCC6803. Plant Molecular Biology 36: 725-732.
100. Linden H, Misawa N, Saito T, Sandmann G (1994) A novel carotenoid biosynthesis gene coding for ζ-carotene desaturase: functional expression, sequence and phylogenetic origin. Plant Molecular Biology 24: 369-379.
101. Linden H, Vioque A, Sandmann G (1993) Isolation of a carotenoid biosynthesis gene coding for ζ-carotene desaturase from *Anabaena* PCC 7120 by heterologous complementation. FEMS Microbiology Letters 106: 99-103.
102. Albrecht M, Linden H, Sandmann G (1996) Biochemical characterization of purified ζ-carotene desaturase from *Anabaena* PCC 7120 after expression in *Escherichia coli*. European Journal of Biochemistry 236: 115-120.

103. Dong H, Deng Y, Mu J, Lu Q, Wang Y, et al. (2007) The *Arabidopsis Spontaneous Cell Death1* gene, encoding a [zeta]-carotene desaturase essential for carotenoid biosynthesis, is involved in chloroplast development, photoprotection and retrograde signalling. Cell Research 17: 458-470.
104. Conti A, Pancaldi S, Fambrini M, Michelotti V, Bonora A, et al. (2004) A deficiency at the gene coding for ζ-carotene desaturase characterizes the sunflower *non dormant-1* mutant. Plant Cell Physiology 45: 445-455.
105. Matthews PD, Luo R, Wurtzel ET (2003) Maize phytoene desaturase and {zeta}-carotene desaturase catalyse a poly-Z desaturation pathway: implications for genetic engineering of carotenoid content among cereal crops. Journal of Experimental Botany 54: 2215-2230.
106. Yu Q, Ghisla S, Hirschberg J, Mann V, Beyer P (2011) Plant carotene *cis-trans* isomerase CRTISO. Journal of Biological Chemistry 286: 8666-8676.
107. Chai C, Fang J, Liu Y, Tong H, Gong Y, et al. (2011) *ZEBRA2*, encoding a carotenoid isomerase, is involved in photoprotection in rice. Plant Molecular Biology 75: 211-221.
108. Masamoto K, Wada H, Kaneko T, Takaichi S (2001) Identification of a gene required for cis-to-trans carotene isomerization in carotenogenesis of the cyanobacterium *Synechocystis sp.* PCC 6803. Plant and Cell Physiology 42: 1398-1402.
109. Römer S, Humbeck K, Senger H (1991) Dark reactions following photoisomerization of prolycopene*. Photochemistry and Photobiology 53: 535-538.
110. Lohr M, Im C-S, Grossman AR (2005) Genome-Based Examination of Chlorophyll and Carotenoid Biosynthesis in *Chlamydomonas reinhardtii*. Plant Physiology 138: 490-515.
111. Merchant SS, Prochnik SE, Vallon O, Harris EH, Karpowicz SJ, et al. (2007) The *Chlamydomonas* genome reveals the evolution of key animal and plant functions. Science 318: 245-250.
112. Grossman AR, Lohr M, Im CS (2004) *Chlamydomonas reinhardtii* in the landscape of pigments Annual Review of Genetics 38: 119-173.
113. Wang T, Iyer LM, Pancholy R, Shi X, Hall TC (2005) Assessment of penetrance and expressivity of RNAi-mediated silencing of the *Arabidopsis phytoene desaturase* gene. New Phytologist 167: 751-760.
114. Li Q, Farre G, Naqvi S, Breitenbach J, Sanahuja G, et al. (2010) Cloning and functional characterization of the maize carotenoid isomerase and β-carotene hydroxylase genes and their regulation during endosperm maturation. Transgenic Research 19: 1053-1068.
115. Sandmann G (1991) Light-dependent switch from formation of poly-cis carotenes to all-trans carotenoids in the *Scenedesmus mutant* C-6D. Archives of Microbiology 155: 229-233.

CHAPTER 2
Intragenic enhancers and suppressors of phytoene desaturase mutations in *Chlamydomonas reinhardtii*

SUMMARY

Photosynthetic organisms synthesize carotenoids for harvesting light energy, photoprotection, and maintaining the structure and function of photosynthetic membranes. A light-sensitive, phytoene-accumulating mutant, *pds1-1,* was isolated in *Chlamydomonas reinhardtii* and found to be genetically linked to the phytoene desaturase (*PDS*) gene. PDS catalyzes the second step in carotenoid biosynthesis—the conversion of phytoene to ζ-carotene. Accumulation of reduced amounts of downstream colored carotenoids suggest that the *pds1-1* mutant is leaky for PDS activity. A screen for enhancers of the *pds1-1* mutation yielded the *pds1-2* allele, which completely lacks PDS activity. A second independent null mutant (*pds1-3*) was identified using DNA insertional mutagenesis. Both null mutants accumulate only phytoene and no other carotenoids. All three phytoene-accumulating mutants exhibited slower growth rates and reduced plating efficiency compared to wild-type cells and white phytoene synthase mutants. Insight into amino acid residues important for PDS activity was obtained through the characterization of intragenic suppressors of *pds1-2* suppressor mutants. The suppressor mutants fell into three classes: revertants of the *pds1-1* point mutation, mutations that changed PDS amino acid residue Pro64 to Phe, and mutations that converted PDS residue Lys90 to Met. Characterization of *pds1-2* intragenic suppressors coupled with computational structure prediction of PDS suggest that amino acids at positions 90 and 143 are in close contact in the active PDS enzyme and have important roles in its structural stability and/or activity.

PREFACE

Marina Sharifi and Subhajit Poddar contributed to the work described in this chapter. Marina Sharifi isolated and performed genetic and molecular characterization of the *pds1-3* mutant, while Subhajit Poddar isolated *pds1-1*.

INTRODUCTION

In plants and green algae, the first committed step of carotenoid biosynthesis is catalyzed by phytoene synthase (PSY), which joins two molecules of the colorless C_{20} compound geranylgeranyl diphosphate (GGPP) to form the colorless C_{40} carotene, 15-*cis*-phytoene. Two conjugated double bonds are then added to 15-*cis*-phytoene by phytoene desaturase (PDS), lending ζ-carotenes their characteristic light-yellow color. PDS catalzyes two successive dehydrogenation reactions, converting 15-*cis*-phytoene via the intermediate 15,9'-*dicis*-phytofluene to 9,15,9'-*tricis*-ζ-carotene. Plant and algal mutants affecting PSY and PDS activity accumulate GGPP and phytoene, respectively, resulting in albino seedlings for plants [1,2,3,4,5] and white-colored cells in algae [6].

C. reinhardtii lts1 mutants impaired in PSY were previously characterized by McCarthy *et al.* [6], who isolated eleven "white" or carotenoid-less mutants, all of which were found to be affected in PSY activity and did not accumulate phytoene as would be expected for mutants with defects in PDS activity [6]. Vila *et al.* attempted to generate phytoene-accumulating mutants by post-transcriptional silencing of *PDS* expression through small interfering RNA (siRNA) and antisense cDNA targeted to *PDS* [7]. Although they showed that *PDS* mRNA levels were reduced, carotenoid levels were unaffected, and phytoene did not accumulate [7]. Compared to *lts1* mutants, isolation of *pds1 C. reinhardtii* mutants seem to be rare events. This chapter describes the successful isolation and characterization of *pds* mutants and offers an explanation as to why previous screens were unsuccessful.

MATERIALS AND METHODS

Strains and growth conditions

Strains: The wild-type *C. reinhardtii* strains used in this work, 4A+ (*mt*+) and 4ax5.2- (*mt*-), are in the 137c genetic background [8]. The polymorphic wild-type strain, S1D2 (*mt*-), was used in genetic linkage tests [9]. The *lts1-210* mutant has a null mutation in the *PSY* gene [6]. Cells were maintained on Tris-acetate-phosphate (TAP) agar medium [10] at 25°C in complete darkness. For experimental purposes, cells were grown in liquid TAP in complete darkness with shaking at 120 rpm as described [6].

Norflurazon and light sensitivity assays: For norflurazon assays cells were first grown in 50 ml of liquid TAP with shaking at 120 rpm to a density of ~$5x10^6$ cells ml^{-1} then spotted onto 35 ml of TAP-agar either with or without norflurazon. TAP-agar plates with norflurazon concentrations of 0.5 μM, 1 μM, 5 μM, 10 μM, 50 μM and 100 μM were prepared by first dissolving norflurazon into methanol. 100 μl of the norflurazon/methanol solution was used per 35 ml of TAP-agar. TAP-only plates contained 100 μl of methanol. Cells were either grown in the dark or at 100 μmol photons m^{-2} sec^{-1} for 2 weeks at 25°C prior to high performance liquid chromatography (HPLC) analysis. 4A+ cells were grown in 50 ml TAP plus 0 μM, 5 μM, or 10 μM norflurazon to a density of ~$5x10^6$ cells ml^{-1} before $4x10^7$ cells were harvested for HPLC analysis. For light sensitivity assays, a toothpick swab of cells was used to inoculate 150 μl of TAP in 96-well plates and allowed to grow for 2 days in the dark at 25°C. 5 μl of cells were then spotted onto TAP-agar and grown for 5 days in the dark. After 5 days of dark growth, cells were moved to 10 μmol photons m^{-2} sec^{-1} (vLL), 100 μmol photons m^{-2} sec^{-1} (LL), or 500 μmol

photons m^{-2} sec^{-1} (HL). Cells were grown at each light intensity for 7 days at 25°C. Dark-only cells were grown completely in the dark for 12 days.

Growth rate determination and plating tests: Cells were grown to $2x10^6$ cells/ml in the dark and then counted using a hemacytometer. Since *pds1-3* mutants tend to stick together in clumps, all strains were incubated in 30 ml of water for 2 hours prior to cell counting allowing them to become single cells. After water incubation, cells were again checked under a microscope for clumps and then centrifuged at 3000 X g for 5 min. The cell pellet was gently suspended in liquid TAP and plated onto TAP-agar plates using glass beads. The plates were incubated in the dark at 25°C for 2 weeks before colony forming units (CFUs) were counted. Growth of white mutants compared to dark green wild-type cells was tested by mixing *lts1* or *pds1* cells in equal ratio to wild-type cells and plating onto TAP-agar. Plates were inoculated so that 500 CFUs of each cells type would grow after 2 weeks of growth in the dark.

To determine growth rate, 1 ml of TAP media was inoculated with 4A+, *lts1*, *pds1-3*, and *pds1-1* cells and incubated at 25ºC overnight in the dark. After 24 hours, the 1 ml culture was used to inoculate 50 ml of TAP and allowed to grow with shaking at 120 rpm in the dark at 25ºC. After 2 days, cell densities were measured with a Multisizer3 Coulter Counter (Beckman Coulter, Fullerton, CA). This 50 ml culture of each sample was used to inoculate three 100 ml TAP cultures at a concentration of 10,000 cells/ml for biological triplicates. The cultures were allowed to grow in the dark at 25ºC with shaking at 120 rpm and counted every 12 hours for 1 week.

Mutagenesis

UV mutagenesis: *pds1-1*, *pds1-2*, P3-84, and *pds1-2* suppressor mutants were all generated using UV mutagenesis [6]. 4A+ cells were mutagenized to create *pds1-1* mutants, and *pds1-1* in turn, was mutagenized to generate the P3-84 strain. The *pds1-2* suppressor mutants were generated by mutagenizing P3-84 cells. For each mutagenesis, 20 mls of cells (~$5x10^6$ cells ml^{-1}) in an open 150 mm glass Petri dish were exposed to 90,000 μJ UV light cm^{-2}. Cells were then permitted to recover overnight in the dark before being plated with glass beads onto TAP-agar and allowed to grow in the dark at 25°C until colonies became visible. For *pds1* enhancer mutants, light green, green brown, and white mutants were picked and further screened via HPLC for phytoene accumulation. To isolate suppressor mutants, P3-84 cells were UV mutagenized at 55,000 μJ UV light cm^{-2}. A total of 35 TAP-agar plates were generated with 12,500,000 mutagenized cells/plate. After plating onto TAP-agar, mutagenized cells were allowed to grow in the dark for 5 days followed by 2 weeks at a light intensity of 1 μmol photons m^{-2} sec^{-1}. Any green colonies that grew were picked in the suppressor screen.

DNA insertional mutagenesis: The mutant *pds1-3* was generated by DNA insertional mutagenesis [8] using the pBC1 plasmid conferring paromomycin resistance. pBC1 was linearized with *Xba*I and 0.5 μg of the plasmid was used per transformation. Following transformation cells were resuspended in liquid TAP and placed in the dark with shaking at 120 rpm at 25°C to recover overnight. Following recovery, mutagenized cells were centrifuged and resuspended in 300 μl TAP before being plated onto TAP-agar containing 10 μg/ml paromomycin. The cells were then kept in the dark at 25°C for 4 weeks to select for paromomycin-resistant colonies.

HPLC analysis

Carotenoid, tocopherol, and chlorophyll extraction and analysis: Pigments were extracted and analyzed via HPLC from dark-grown liquid TAP cultures or from cells grown on TAP-agar as described previously [6]. Pigments were extracted using approximately 0.05 mg of cells or by cell number. For quantitative comparison of chlorophyll, biological triplicates of each strain were grown to a density of $5x10^6$ cells/ml prior to HPLC analysis. Pigments were extracted from $1x10^8$ cells by first centrifuging cells at 20,000 X g for 5 minutes, discarding the supernatant, and then vortexing the pellet in 200 μl of acetone for 30 seconds. After centrifugation at 20,000 X g for 1 min, the supernatant was filtered through a 0.45-μm nylon filter. The acetone-extracted samples were stored in the dark until HPLC analysis, when 25 μl of the pigment extract was separated into individual pigments on a reverse-phase C18 Spherisorb S5 ODS1 4.6- X 250-mm cartridge column (Waters, Milford, MA) at 30°C. The carotenoids and chlorophylls were identified by their absorbance at 445 and 296 nm using a diode array detector. A standard curve of known concentrations of each purified compound was used for calculating chlorophyll and carotenoid concentrations. Since no commercially purified phytoene was available to create a standard curve, phytoene levels were compared using peak areas derived from HPLC analysis. α-Tocopherol levels were measured by fluorescence at excitation of 295 nm and emission at 325 nm.

Genetic analysis

Crosses and genetic linkage tests: All crosses were carried out according to Harris 1989 [10]. Because *pds1* mutants were extremely light sensitive, zygospores derived from *pds1* mutants were only exposed to 5 hours of vLL to induce germination. Germinated zygospores were dissected, and the resulting progeny were grown in complete darkness at 25°C on TAP-agar plates until colonies could be detected. The *pds1-1* (*mt+*), *pds1-3* (*mt+*), and P3-84 (*mt+*) strains were crossed to 4ax5.2 (*mt-*). Progeny produced from crosses between 4ax5.2 and *pds1-3* were tested for paromomycin-resistance by growing the cells on TAP-agar plus 10 μg/ml paromomycin for 2 weeks in the dark.

For genetic linkage analyses, the *pds1-1* mutant was crossed to the S1D2 (mt -) strain. Genomic DNA was extracted from progeny resulting from this cross and used to amplify a 268-bp DNA fragment of the *PDS1* gene with primers PDS4 (5'–ACCTTTCTGTTACACAAACCATGC-3') and PDS7 (5'-TACACTGGTTTGGCACTCGTAGA-3'). The 268-bp PCR product was digested with *ScrFI* overnight before being run on a 3% Metaphor agarose gel (Cambrex, East Rutherford, NJ).

Dominance tests: Vegetative diploids were generated by crossing *pds1-1* to an arginine-deficient strain with the *arg7-8* mutation [11]. Progeny from this cross were maintained on TAP-agar supplemented with 50 μg/ml of L-arginine. The *pds1-1 arg7-8* (*mt-*) double mutants were selected by their light green color and their inability to grow on TAP-agar without arginine and then crossed to an arginine-deficient strain with the *arg7-1* allelic mutation. The mating mix was plated directly on TAP-agar without arginine plates and grown in LL at 25°C. After 10 days in the light, surviving colonies were picked and tested for their ploidy using mating-type PCR [11].

DNA analysis

DNA isolation: For both DNA and RNA extractions, cells were grown to a density of ~$5x10^6$ cells/ml in 50 ml TAP with shaking at 120 rpm in the dark at 25°C. For restriction enzyme site-directed amplification (RESDA)-PCR analysis, DNA was extracted from cells grown on TAP-agar plates for 14 days in the dark. DNA was extracted from cells as described previously [12], but without CsCl purification.

DNA sequencing: The *PDS1* and *PSY* genes were sequenced from genomic DNA isolated from 4A+, *pds1-1,* P3-84*,* and *pds1-2* suppressor mutants. Sequencing primers were designed using Primer3 software [13] against the annotated *PDS1* and *PSY* genes in the *Chlamydomonas* nuclear genome sequence from the DOE Joint Genome Institute (JGI, http://genome.jgi-psf.org/Chlre4/Chlre4.home.html). PCR fragments were sequenced using the DYEnamic ET Terminator Cycle Sequencing kit (Amersham Biosciences, Piscataway, NJ) and then analyzed using an ABI 3100 automated DNA sequencer (Applied Biosystems, Foster City, CA). Primer pairs used to amplify and sequence regions carrying mutations in the *PDS1* locus were: 1) C490019_17A (5'-GGACACCACCCAATCGTTCT-3') and C490019_17B (5'-CTACAGCCGCCCTTACTGAC-3') and 2) C490019_4A (5'-ATACGAACATATATACGTGGCACACT-3') and C490019_4B (5'-ATGTTTAGCTCCTTGAAGACATTCAT-3'). Primers T-PSYF1 and PSYR2 [6] were used to amplify and sequence mutations in the *PSY* locus.

RNA analysis

RNA isolation: Total RNA for quantitative PCR (qPCR) and reverse-transcriptase (RT) PCR was prepared by first centrifuging cultures for 5 min at 3000 rpm followed by RNA extraction using 2 ml of Trizol reagent (Invitrogen, Carlsbad, CA) per 50 ml culture. Total RNA was resuspended in 30 μl DEPC-H_20 and treated with 1.5 μl RQ Rnase-free DNAse (Promega, Madison, WI) for 1 hour at 37°C, and RNA was purified from the reaction using RNAeasy columns (Qiagen, Valencia, CA).

Reverse-transcriptase (RT-PCR): First-strand cDNA was synthesized using Superscript Reverse Transcriptase III (Invitrogen, Carlsbad, CA). The first-strand synthesis reaction was set up with 1 μl of 50 μM oligo-$dT_{(20)}$ primer, 1 μl 10 mM dNTPs, and 500 ng total RNA in a total volume of 13 μl. The cDNA synthesis reaction was incubated at 65°C for 5 minutes and quenched on ice for 1 minute before adding 4 μl 5X FS buffer, 1 μl 0.1M DTT, 1 μl RnaseOUT, and 200 U enzyme. This was followed by a 50°C incubation for 1 hour, and finally 70°C for 15 min. 1 μl RnaseH was added to the reaction and incubated at 37° C for 20 min. 2 μl of the first-strand cDNA reaction was used as template for PCR amplification of specific transcripts with specific primers. Primers used for the amplification of tubulin as a positive control were tub-3 (5'-CGCCAAAGTACATCTCCATCC-3') and tub-4 (5'-TAGGGGCTCTTCTTGGACA-3') which produce a 285 bp fragment from genomic DNA and a 107 bp fragment from cDNA. Primers used to amplify the *PDS1* transcript were PDSF_4 (5'-CTGCATGGAAGGATGAGGAT-3') and MS069 (5'- TTGATCTCGGTGGGAAACA-3').

Quantitative PCR (qPCR): First-strand cDNA was synthesized from 1 μg total RNA with random primers (5'NNNNNNNNN) using Omniscript reverse transcriptase (Qiagen, Valencia, CA) according to the manufacturer's protocol. qPCR reactions were set up using 1 μl cDNA synthesis reaction diluted to 5 μl with sterile water as template, 2 μl of each primer at 2.5 μM concentration, and 10 μl 2X Sybr-green master mix (Qiagen, Valencia, CA) in a final volume of 20 μl. qPCR reactions were run on an ABI-7300 qPCR machine, with standard cycling. Transcript levels were quantified using the delta-delta Ct method. *CblP* was selected as the endogenous control gene, amplified with primers SWQ43 (5'-CAAGACCATCAAGCTGTGGA-3') and SWQ44 (5'-ACACGATGATGGGGTTGGT-3') which targeted the third exon. Primer pairs in the second exon of *PDS1*, PDSF_4 (5'-CTGCATGGAAGGATGAGGAT-3') and PDSR_4 (5'GAGTCGGGCATAGCAAAGAT-3'), and in the 3' UTR, PDSF_3 (5'-ATCCGGAGGATTCAGGAGAC-3') and PDSR_3 (5'-CAGAAGTCCGCACACTCAAA-3'), with approximately 150 bp amplicons were used for *PDS1* expression analysis. Transcript levels were quantified using the delta-delta Ct method.

Isolation of flanking genomic sequences

RESDA-PCR: The insertion site of pBC1 in the DNA insertional mutant, *pds1-3*, was identified using RESDA-PCR [14]. A set of primary and secondary specific nested primers was designed to amplify genomic DNA flanking the vector insert. Flanking sequence was isolated with primary primer MS010 (5'- AATGCGGGCGTTGCAAGTCAAATC-3') and secondary primer MS011A (5'-AATCTGCAAGCACGCTGCCTGATC-3'). Degenerate primers and the Q_0 specific primer were those described in González-Ballester *et al* .[14], with the addition of a fifth degenerate primer constructed identically to the original four, replacing the original restriction enzyme cutting sites with the *StyI* site (Figure 2.1).

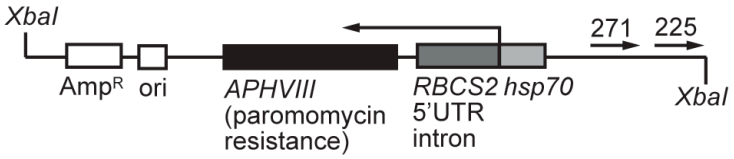

Figure 2.1. Structural features of the linearized pBC1 vector used to generate DNA insertional mutant *pds1-3.*
271 and 225 indicate position of the vector-specific primers used for amplifying flanking sequence in RESDA-PCR.

Two sequential PCR reactions were required to amplify the flanking sequence. The primary RESDA-PCR reaction was set up in a volume of 25 µl as follows: 5 pmol specific primary primer, 15 pmol degenerate primer, 2.5 µl Eppendorf 10x PCR Buffer Advanced, 2.5 µl 200 µM dNTPs, 0.3 µl Eppendorf Taq polymerase, and ~80 ng genomic DNA template suspended in TE buffer. Primary reactions were diluted 1:25 and used as template in secondary RESDA-PCR reactions which were set up in a volume of 25 µl as follows: 5 pmol specific secondary primer, 5 pmol Q_0 specific primer, 2.5 µl Eppendorf 10x PCR Buffer Advanced, 2.5 µl 200 µM dNTPs, 0.3 µl Eppendorf Taq polymerase, and 1.5 µl diluted primary reaction. RESDA-PCR primary cycling parameters were as described in Dent *et al.* [8] while secondary cycling parameters were as described in González-Ballester *et al.* [14]. Secondary RESDA-PCR reactions were separated on 1% agarose gels, and reactions with amplification product(s) were purified for sequencing using either the Qiagen MinElute PCR purification kit (Qiagen, Valencia, CA), or the QIAquick gel extraction kit (Qiagen, Valencia, CA) for reactions that amplified multiple bands. 40-50 ng of the DNA obtained was sequenced with the plasmid specific primer RMD225 (5'-ATAAGCTTGATATCGAATTC-3').

PCR analysis of the pBC1 insertion site: RESDA-PCR of *pds1-3* yielded *Chlamydomonas* genomic DNA flanking sequence was used to design the primer MS039 (5'-GCCACGCCCTTGTAGTTGTA-3') for further analysis of the insertion site. PCR with primer MS039 and RESDA-PCR secondary vector specific primers RMD225, RMD 271 (5'-CGAGCTCCCCGCTCGAGGTCGACG-3'), and MS011A (5'-AATCTGCAAGCACGCTGCCTGATC-3') was performed. Primers were also designed within the *PDS1* gene model at two locations upstream of the recovered flanking sequence: MS041A (5'-CTCCCTAACTCCCGCTCTTC-3') and MS041B (5'-GTCCACGGTGGTCAGCTT-3') were designed 500 bp upstream while MS031A (5'-GGTGGGTCATTTAGCACCTC-3') and MS031B (5'-ATCCTCATCCTTCCATGCAG-3') were designed 2.5 kb upstream (Fig 2.8C).

Bioinformatics and structural modeling

Transit peptide prediction: ChloroP 1.1 (http://www.cbs.dtu.dk/services/ChloroP/) was used to predict the presence and length of potential chloroplast transit peptides from translated protein sequences [15].

Multiple sequence alignment: PDS protein sequences from *C. reinhardtii* (GenBank ID XP_001690859.1), *Synechocystis* sp. PCC 6803 (GenBank ID CAA44452.1) and *Arabidopsis thaliana* (GenBank ID AAA20109.1) were retrieved from NCBI protein database at http://www.ncbi.nlm.nih.gov/sites/entrez?db=protein [16]. *Ostreococcus tauri* PDS protein

sequence was from the Joint Genome Institue (JGI, http://genome.jgi-psf.org/Ostta4/Ostta4.home.html, protein ID 21852). The protein sequences were aligned using ClustalW version 1.83 [17] at http://www.ch.embnet.org/cgi-bin/clustalw_parser and shaded according to Blosum 62 matrix.

Protein structure prediction: The *C. reinhardtii* PDS protein (GenBank ID XP_001690859.1) was submitted to 3DLigandSite web server (Ligand binding site prediction Server) at http://www.sbg.bio.ic.ac.uk/3dligandsite/ [18].

RESULTS

C. reinhardtii wild-type cells (4A+) were grown on norflurazon to predict the phenotype of *pds1* mutants. Norflurazon is a bleaching herbicide that specifically inhibits PDS activity and therefore carotenoid biosynthesis [19,20,21,22]. When wild-type cells were grown on norflurazon, dark green cells became light green to almost white with increasing concentrations of norflurazon (Figure 2.2A). Cell growth was inhibited by norflurazon concentrations above 10 µM in the dark, whereas in low light cell growth was completely inhibited at 5 µM and higher. HPLC analysis of dark-grown cells showed that cells treated with norflurazon accumulated phytoene and had about a 5-fold reduction in chlorophyll and carotenoids levels (Figure 2.2B). Phytoene was identified by its absorbance spectrum at 296 nm and a retention time of 16.25 minutes (Figure 2.2B). Chlorophylls and other carotenoids were detected at 445 nm and also identified by their absorbance spectra and retention times (Figure 2.2B).

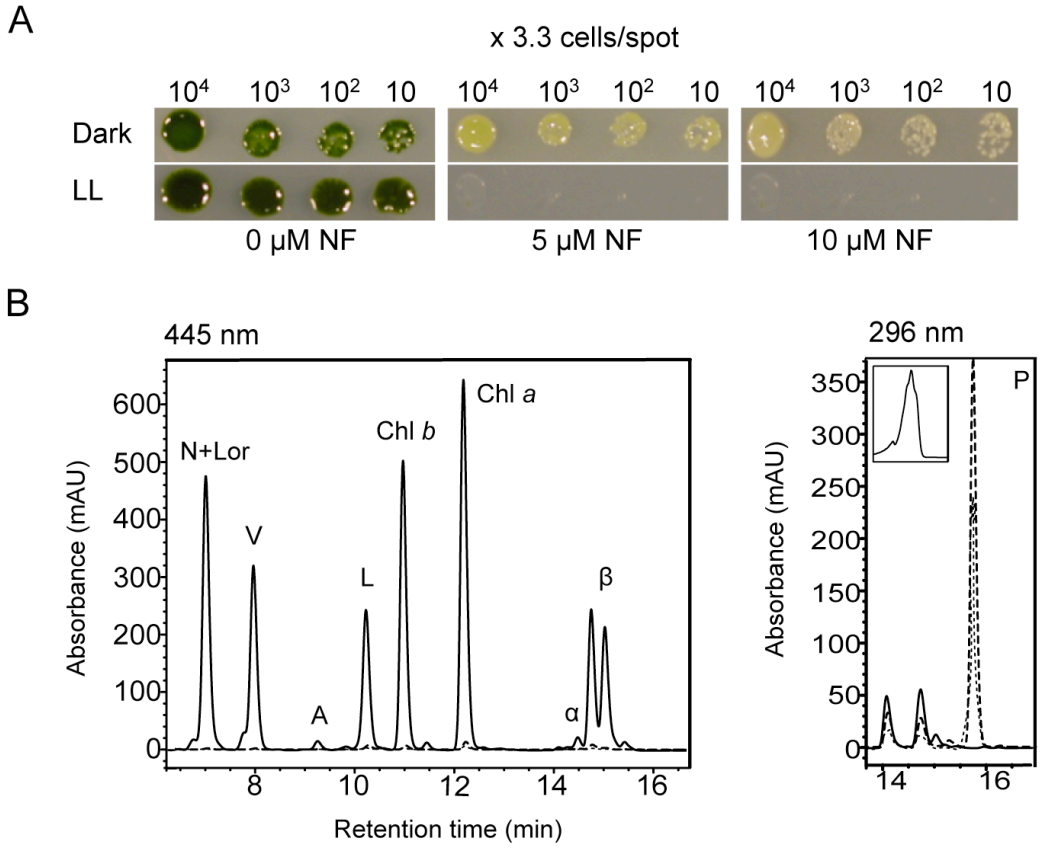

Figure 2.2. Phenotype of wild-type Chlamydomonas cells grown norflurazon.
A). Growth of wild-type *C. reinhardtii* cells on 0, 5, and 10 µM of norflurazon (NF) in LL (100 µmol photons m^{-2} sec^{-1}) or in the dark with decreasing cell numbers. Number above cells indicate the quantity of cells inoculated per spot at the start of the assay.
B). Overlay of HPLC results of carotenoid and chlorophyll pigments detected in dark-grown wild-type cells treated with 0 µM (solid lines), 5 µM (dashed lines), and 10 µM (dotted lines) of NF at absorbance 445 nm and 296 nm. N+Lor (neoxanthin + loroxanthin); V (violaxanthin); A (antheraxanthin); L (Lutein); Chl *a* and Chl *b* (chlorophyll *a* and *b*); α-, β- (α- and β-carotenes); P (phytoene). Inset shows absorbance spectrum of phytoene peak at 296 nm.

A phytoene accumulating mutant: *pds1-1*

Based on the results of norflurazon inhibition, *C. reinhardtii* mutants that are defective in PDS activity were predicted to have a light to very pale green color. From a UV mutagenesis screen, 135 light green, pale green, white, and green/brown color mutants were picked and analyzed by HPLC for pigment abnormalities. The *pds1-1* mutant was identified from this screen—it was light green and accumulated phytoene (Figure 2.3 and 2.4B). However, *pds1-1* still produced carotenoids downstream of phytoene including β-carotene, lutein, antheraxanthin, violaxanthin, and neoxanthin (Figure 2.4A) at ~5% the levels found in wild-type cells (Figure 2.4A and Table 2.2). The *pds1-1* mutant accumulated 5-fold more chlorophyll than *lts1* mutants but only ~12% the level detected in wild-type cells. The chlorophyll to colored carotenoid ratio for wild-type cells was 3.19:1, whereas in *pds1-1* the ratio was 8.74:1. Wild-type and *lts1* mutants did not accumulate any phytoene, whereas *pds1-1* mutants accumulated significant levels of phytoene (Figure 2.4B).

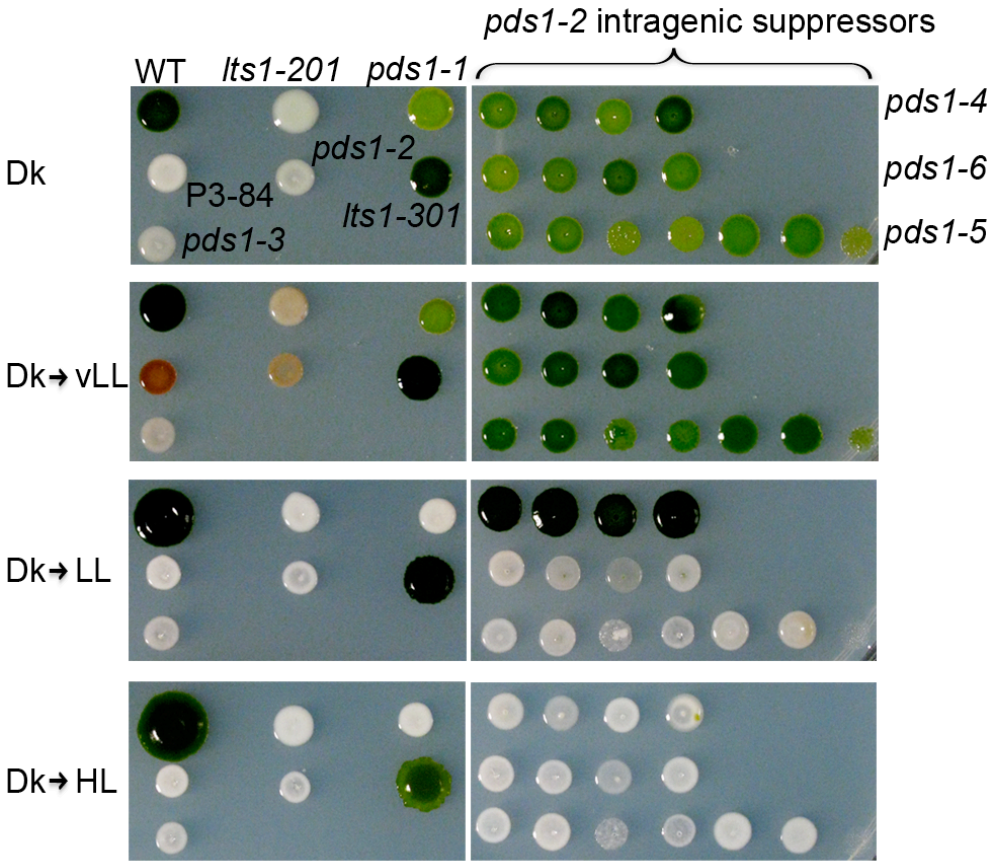

Figure 2.3. Light sensitivity of wild-type, *lts1* and *pds1* mutants.
Cells were spotted onto TAP-agar and grown for 5 days in the dark before being exposed to increasing light intensities. All cells were grown for a total of 19 days.
WT (wild-type), *lts1-201* (null *psy*), *pds1-1* (leaky *pds1*), P3-84 (*lts1-301 pds1-2*), *pds1-2*, *lts1-301* (leaky *psy*), and *pds1-3* (null *pds1*) are in the left column. In the right column, intragenic suppressors of *pds1-2* mutants (*pds1-4*, *pds1-5*, *pds1-6*) all in the *lts1-301* genetic background.
Light intensities: Dk (dark), vLL (10 µmol photons m^{-2} sec^{-1}), LL (100 µmol photons m^{-2} sec^{-1}), HL (500 µmol photons m^{-2} sec^{-1})

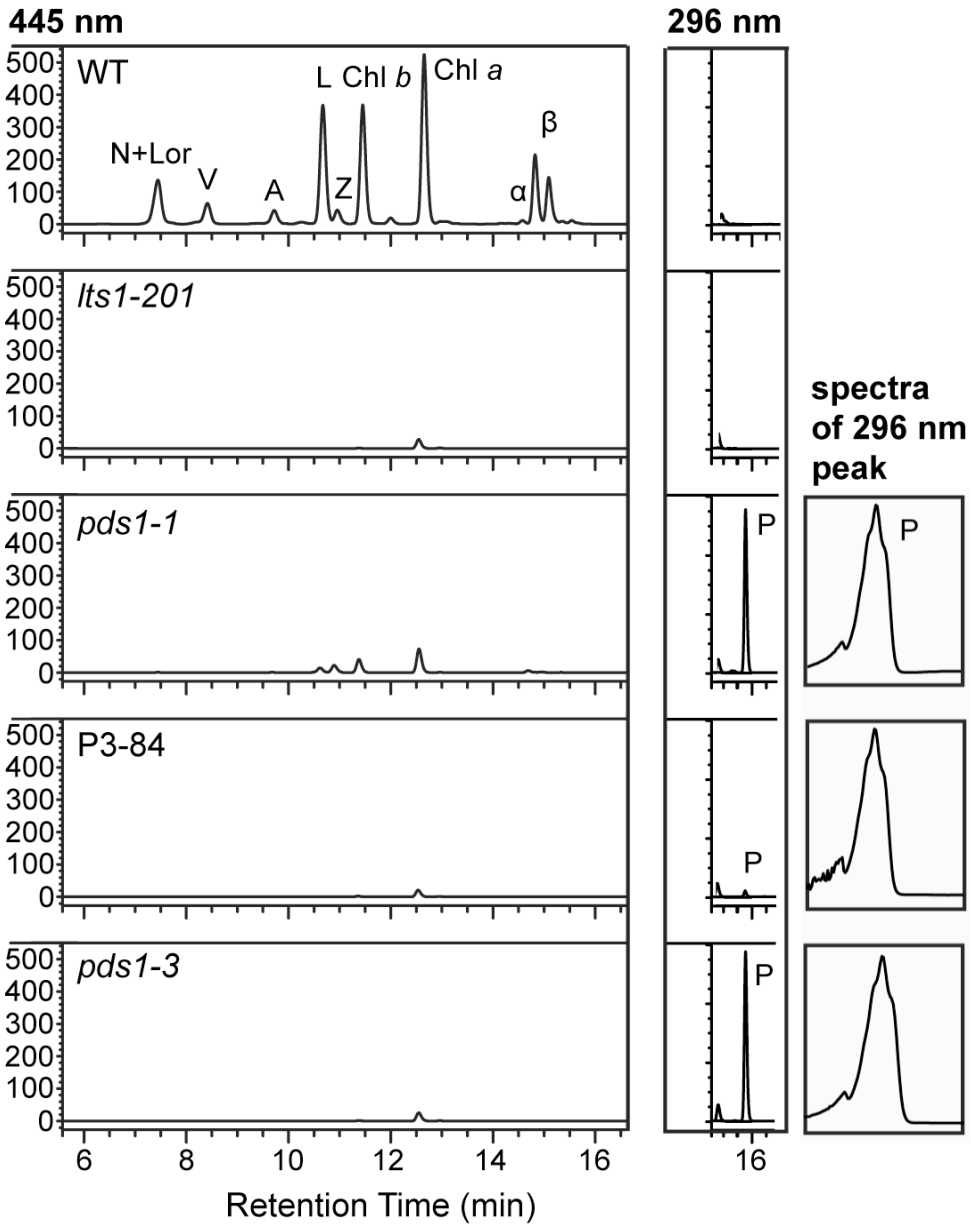

Figure 2.4. Chlorophyll and carotenoid profiles of PDS-activity deficient mutants. Chlorophylls and carotenoids were detected at 445 nm and phytoene was detected at 296 nm. Absorbance spectra are shown for the 296 nm phytoene peak present in both *pds1-1* and *pds1-3* mutants and small peak detected in P3-84. Pigments were extracted from a total of $1x10^8$ cells for each sample and analyzed via HPLC coupled with a diode array detector. N+Lor (neoxanthin + loroxanthin); V (violaxanthin); A (antheraxanthin); L (lutein); Z (zeaxanthin); Chl *a* and Chl *b* (chlorophyll *a* and *b*); α-, β- (α- and β-carotenes); P (phytoene).

Similar to *lts1* mutants, *pds1-1* mutants were found to be very light sensitive. After growth in the dark for four days, *pds1-1* died after being exposed to more than 24 hours of vLL

(Figure 2.3). In vLL cells died and turned brown, while at higher light intensities (LL and HL) cells bleached completely and turned white (Figure 2.3). In contrast, wild-type cells grew well at all light intensities including HL.

Genetic analysis of *pds1-1* revealed that the *pds1* phenotype is caused by a single, recessive nuclear mutation. Crosses between *pds1-1* and wild-type cells produced tetrads that segregated 2:2 for the *pds1-1* mutant phenotype (light colored, phytoene accumulation, and reduced levels of colored carotenoids) and the wild-type phenotype (dark green, no phytoene, and normal levels of carotenoids) (Table 2.1). Dominance testing using heterozygous *pds1-1/PDS1* vegetative diploids showed the *pds1-1* mutation is recessive.

Table 2.1. Tetrad analysis of *pds1-1* and *pds1-3* crossed to wild-type.

	PD:NPD (complete tetrads)	Total Progeny	WT progeny	Mutant progeny	Mutant progeny recombinant for paromomycin marker
pds1-1 (mt+) x WT (mt-)	10:0	106	54	52	N/A
pds1-3 (mt+) x WT (mt-)	7:0	145	88	57	0

WT = wild-type (4ax5.2), PD = parental ditype, NPD = non-parental ditype.

The *pds1-1* mutant was crossed to the polymorphic wild-type strain S1D2 in order to map the mutation relative to the annotated *PDS1* gene. A total of 21 progenies were isolated from this cross: 12 from complete tetrads and 9 from incomplete tetrads. A marker for the *PDS1* locus on chromosome 12 was designed to amplify a 268 bp PCR product from both *pds1-1* and S1D2. Digestion of the 268 bp PCR product with *ScrFI* yielded 215 and 52 bp fragments from *pds1-1*, whereas 111, 104, 26, and 25 bp fragments were produced from S1D2. DNA fragments smaller than 100 bp could not be visualized. When the *PDS1* marker was tested on DNA isolated from the progenies, the light green phenotype cosegregated with the polymorphism found in *pds1-1* (215 and 52 bp) while dark green progeny yielded fragments similar to S1D2 (111, 104, 26, and 25 bp) (Figure 2.5). This result shows that the light green phenotype is linked to the *PDS1* locus and that a mutation in *PDS1* is likely to be responsible for the light green color and phytoene accumulation in *pds1-1*.

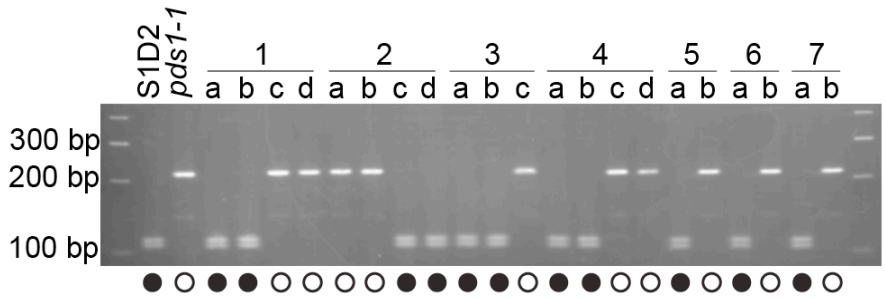

Figure 2.5. The *PDS1* gene is genetically linked to the *pds1-1* mutant phenotype. A marker located within the *PDS1* locus cosegregated with the light green, phytoene accumulating mutant phenotype of *pds1-1*. Amplification and *ScrFI* digestion of a 268 bp fragment of the *PDS1* gene containing the single nucleotide polymorphism in exon 2 was used to score progeny from crosses between *pds1-1* and polymorphic wild-type strain (S1D2). Seven full and partial tetrads were scored: individual progeny within tetrads are labeled "a, b, c, d". Solid circles indicate dark green progeny with wild-type carotenoid composition while open circles indicate light green progeny with phytoene accumulation.

The *PDS1* locus was sequenced from *pds1-1* to discover if a mutation in this locus was responsible for the phytoene accumulating, light green phenotype. The *Chlamydomonas* nuclear genome sequence of *PDS1* is 4030 bp and the predicted protein is 564 amino acids long. Amplification and sequencing of the *PDS1* locus with primers C490019_17A and C490019_17B identified a single base pair change in exon two of *pds1-1*. The point mutation consisted of a G/C to A/T transition, resulting in an E143K missense change in deduced PDS protein sequence (Figure 2.6). A multiple sequence alignment (MSA) of predicted PDS protein sequences from wild-type *C. reinhardtii*, *O. tauri*, *Synechocystis* sp PCC6803, and *A.thaliana* and revealed that the amino acid change occurred in the conserved dinucleotide [FAD or NAD(P)] dependent oxidoreductase/amine oxidase domain of the PDS protein (Figure 2.6).

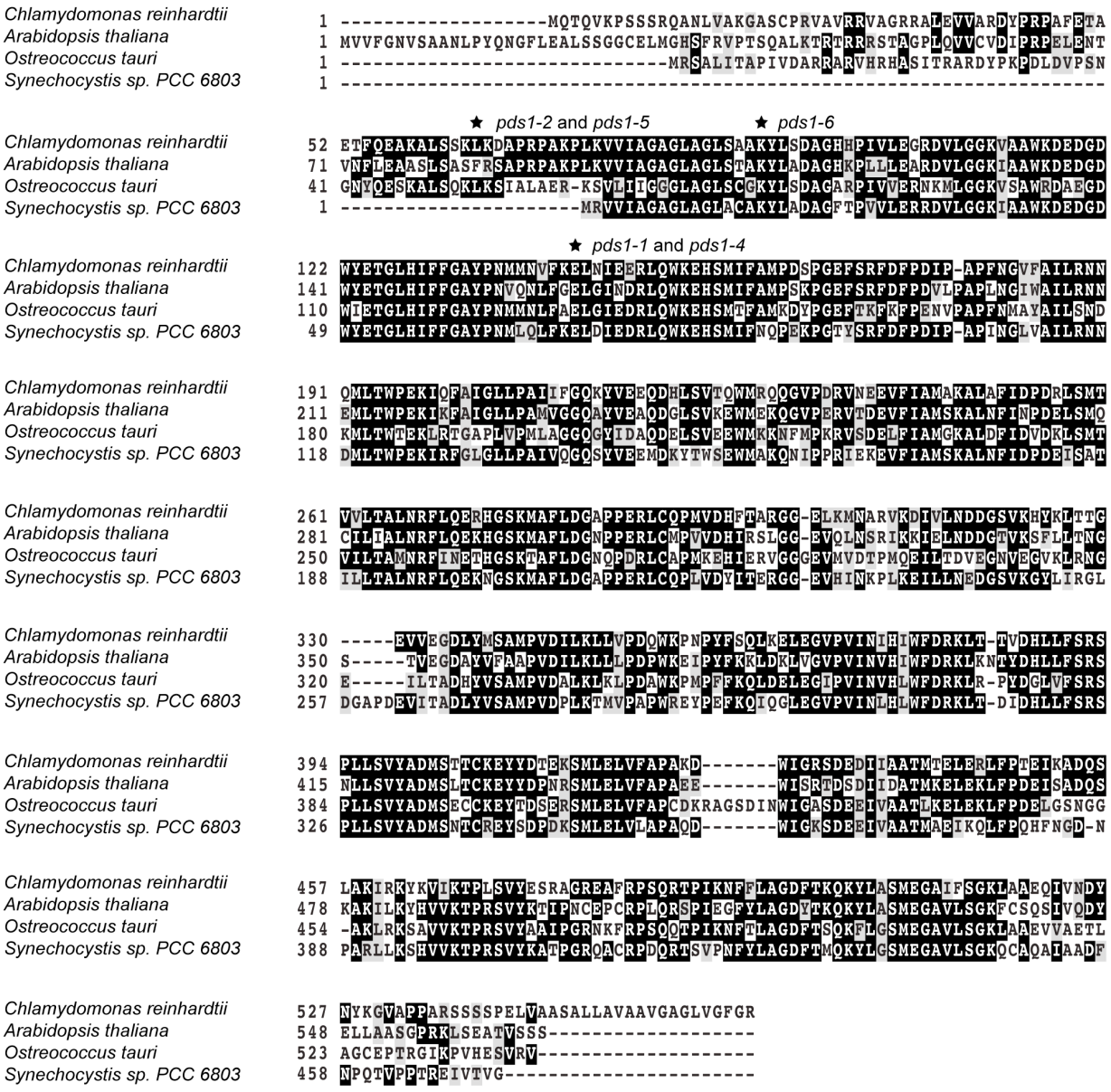

Figure 2.6. Multiple sequence alignment of PDS protein sequences.
Alignment of PDS amino acid sequences from eukaryotic green algae, *Chlamydomonas* and *Ostreococcus*; a plant, *Arabidopsis;* and a cyanobacterium, *Synechocystis sp.* PCC6803. Conserved residues were scored using Blosum 62 matrix, with darker shading indicating higher conservation and no shading low conservation. Asterisks mark positions of mutations in *pds1* alleles.

Isolation of *pds1-2* as an intragenic enhancer of *pds1-1*

Because *pds1-1* still synthesizes colored carotenoids, a second UV mutagenesis was conducted to find enhancer mutants that eliminated PDS activity. For the enhancer screen, light green *pds1-1* cells were mutagenized, and a white mutant, P3-84, was isolated (Figure 2.3 and

Figure 2.7A) that had a similar pigment profile as null *psy* (*lts1-201*) mutants, except that P3-84 accumulated a low level of phytoene (Figure 2.4). When P3-84 was crossed to wild-type cells, the tetratype tetrad progeny gave unexpected pigment phenotypes: two white mutants with phytoene and no other carotenoids, one dark green mutant with wild-type carotenoid composition and levels, and one light green mutant with wild-type carotenoid composition and levels (Figure 2.7B). The original light green, phytoene accumulating *pds1-1* pigment phenotype was not recovered. To determine if the P3-84 mutant phenotype was due to mutations in either the *PSY* or *PDS1* gene, both genes were sequenced. Sequencing results revealed new mutations in both *PSY* and *PDS1* genes in P3-84. An in-frame deletion of 24 bp removed eight amino acid residues from positions 7 to 14 (H_7SAQTCPA$_{14}$) in the putative chloroplast transit peptide of PSY (Figure 2.7C). This new allele of *PSY* was named *lts1-301*. The *PDS1* locus was found to carry two point mutations: the original *pds1-1* mutation (E143K) and an additional T to C transition resulting in the conversion of a leucine residue at position 64 to a proline residue (L64P) (Figure 2.7D). This double mutant allele of *PDS* was named *pds1-2*.

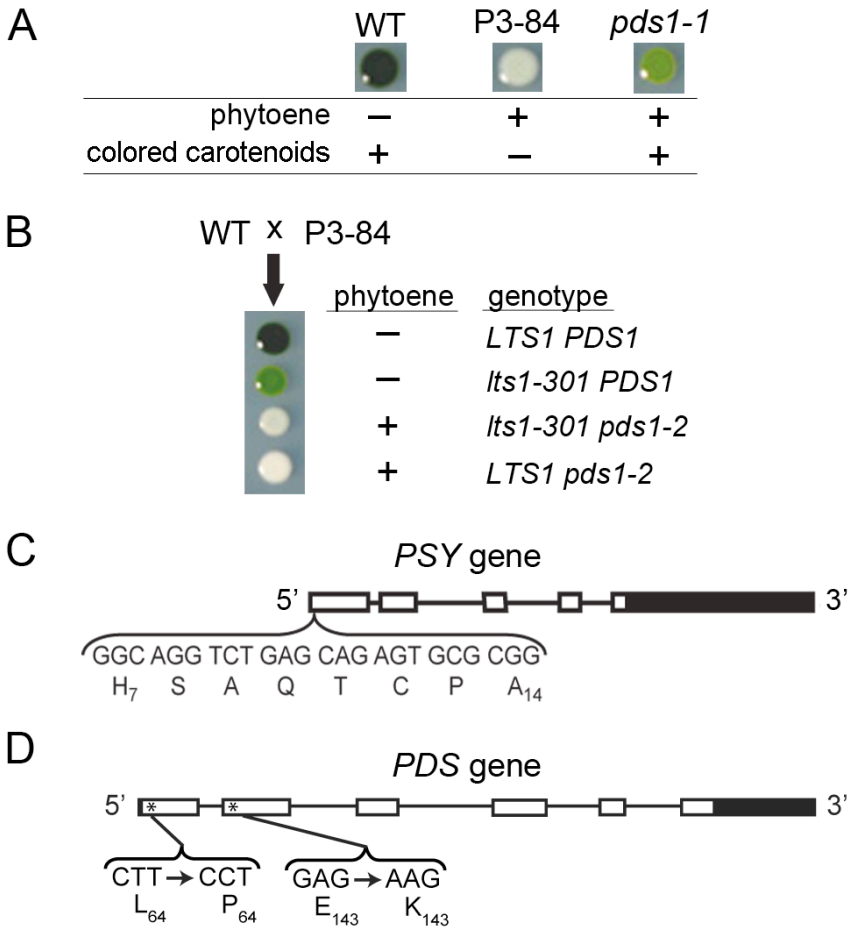

Figure 2.7. Analysis of enhancer strain P3-84 (*lts 1-301 pds1-2)* and intragenic suppressors of *pds1-2* mutants.
A). Color and pigment phenotype of dark grown wild-type (WT), P3-84, and *pds1-1* mutants. (-) indicates no accumulation while (+) indicates presence of carotenoid. Colored carotenoids include all carotenoids downstream of phytofluene.

B). Tetratype tetrad phenotype from crosses between wild-type and P3-84 cells. The presence (+) or absence (-) of phytoene phenotype is indicated for each progeny along with their corresponding genotype. Wild-type genotype symbolized by (+).
C). Structure of *PSY* gene in *Chlamydomonas*. UTRs are indicated by solid boxes, exons by open boxes and four introns by lines. The bracket highlights the eight amino acids and their corresponding nucleotides deleted from the chloroplast transit peptide in *lts1-301*, P3-84, and in *pds1-2* suppressor mutants. Subscript numbers note position of the amino acid residue in the wild-type PSY protein.
D). Structure of *PDS* gene in *Chlamydomonas*. UTRs are indicated by solid boxes, exons by open boxes and five introns by lines. The brackets highlight the two missense mutations found in P3-84. Subscript numbers note position of the amino acid residue in the wild-type PDS protein.

The *PDS1* and *PSY* sequencing results from P3-84 explained the unexpected tetratype phenotypes recovered in the cross between P3-84 and wild-type. The two parental phenotypes were represented: dark green wild-type and white P3-84 (Figure 2.7A and 2.7B). For the two unexpected phenotypes, the light-green, no phytoene accumulating phenotype belonged to progeny with reduced PSY activity (Figure 2.7B). Sequencing of *PSY* and *PDS1* genes from this progeny (*lts1-301*) revealed that it has the eight amino acid chloroplast transit peptide deletion in *PSY* and no mutations in *PDS1* (Figure 2.7C). The *lts1-301* strain synthesizes wild-type carotenoids, but at reduced levels, indicating that PSY function is reduced or "leaky" (Table 2.2) most likely because of inefficient transport of the PSY protein into the chloroplast. The second unexpected phenotype, white plus phytoene accumulation, belonged to progeny with wild-type *PSY* and the two mutations in *PDS* (L64P and E143K) (Figure 2.7B). This second white progeny, *pds1-2*, is an intragenic enhancer mutant for *pds1-1* since the only carotenoid detected was phytoene (Table 2.2). Both P3-84 (*lts1-301 pds1-2*) and *pds1-2* survive only in the dark. Like *lts1-201* and *pds1-1* mutants, they do not survive when cultured under very low light. In contrast, *lts1-301* is very light tolerant, growing almost as well as wild-type cells in HL (Figure 2.3).

Table 2.2. Quantification of chlorophyll, carotenoid, and α-tocopherol content of *lts1* and *pds1* mutants

	total chl (fmol/cell)	chl *a/b* ratio	α-tocopherol (fmol/cell)	total colored carotenoids (fmol/cell)	total xanthophylls (fmol/cell)	lutein (fmol/cell)	zeaxanthin (fmol/cell)	phytoene (total peak area)
Wild-type	0.5201 ± 0.0404	2.17 ± 0.23	0.0041 ± 0.0044	0.1616 ± 0.0307	0.1079 ± 0.0208	0.0377 ± 0.0291	0.0069 ± 0.0030	0
lts1-301 **(leaky *psy*)**	0.2297 ± 0.0243	2.24 ± 0.51	0.0134± 0.0044	0.0391 ± 0.0056	0.0306 ± 0.0051	0.0111 ± 0.0032	0.0099 ± 0.0016	0
lts1-210 **(null *psy*)**	0.0128 ± 0.0041	39.24 ± 1.09	0.0275 ± 0.0042	0	0	0	0	0
pds1-1 **(leaky *pds*)**	0.0655 ± 0.0076	2.67 ± 0.15	0.0102 ± 0.0001	0.0075 ± 0.0006	0.0061 ± 0.0006	0.0025 ± 0.0006	0.0031 ± 0.0	3,605 ± 177
pds1-2 **(null pds)**	0.0113 ± 0.0020	13.84 ± 0.27	0.0064 ± 0.0009	0	0	0	0	2,642 ± 232
pds1-3 **(null *pds*)**	0.0177 ± 0.0084	13.84 ± 0.27	0.0569 ± 0.0159	0	0	0	0	4,048 ± 907
lts1-301 pds1-2	0.0096 ± 0.0031	14.44 ± 0.42	0.0090 ± 0.0011	0	0	0	0	167 ± 34
suppressor *pds1-4*	0.1726 ± 0.0643	2.08 ± 0.12	0.0067 ± 0.0015	0.0313 ± 0.0107	0.0247 ± 0.0076	0.0088 ± 0.0023	0.0059 ± 0.0019	0

suppressor *pds1-5*	0.2464 ± 0.0917	2.12 ± 0.32	0.0081 ± 0.0033	0.0363 ± 0.0075	0.0283 ± 0.0055	0.0102 ± 0.0022	0.0070 ± 0.0029	24 ± 11
suppressor *pds1-6*	0.2297 ± 0.0744	2.32 ± 0.27	0.0080 ± 0.0027	0.0298 ± 0.0072	0.0236 ± 0.0074	0.0088 ± 0.0022	0.0066 ± 0.0029	8 ± 0.68

Chlorophyll (Chl), carotenoid, and α-tocopherol quantities (represented as fmol/ml) were extracted from a total of $1x10^8$ cells for each sample with 200 μl of acetone. Colored carotenoids detected in *C. reinhardtii* include α-carotene, β-carotene, lutein, violaxanthin, antheraxanthin, neoxanthin, loroxanthin, zeaxanthin. Total xanthophylls include lutein, loroxanthin, violaxanthin, antheraxanthin, neoxanthin, and zeaxanthin. Averages and standard deviations are from three independent cultures.

pds1-3 is a null allele derived from DNA insertional mutagenesis

An additional white, phytoene accumulating mutant, *pds1-3*, was isolated from a DNA insertional mutagenesis screen based on its sensitivity to light and white color. Similar to *pds1-1* mutants, *pds1-3* bleached and died at vLL intensities (Figure 2.3) and it also accumulated phytoene (Figure 2.4B). Unlike *pds1-1*, however, it does not synthesize any colored carotenoids (Figure 2.4A).

Tetrads from crosses with wild-type segregated 2:2 for the *pds1-3* and wild-type phenotypes (Table 2.1), indicating that the *pds1-3* mutant phenotype is controlled by a single gene. Co-segregation of the mutant phenotype with paromomycin-resistance also indicates that the mutation is tagged by the transforming pBC1 plasmid (Table 2.1).

To identify the mutation responsible for the white, phytoene-accumulating phenotype of the *pds1-3* mutant, RESDA-PCR was used to recover a flanking sequence tag for one end of the pBC1 vector insert in *pds1-3*. The flanking sequence was used as a query in a BLAST search for homologous sequences [23] against the *Chlamydomonas* genome draft version 4 (http://genome.jgi-psf.org/Chlre4/Chlre4.home.html) and found to have significant identity to a 331 bp sequence on Chromosome 12. Flanking sequence analysis indicated that the insertion interrupts an intron in *PDS1* (Figure 2.8A). A primer was designed within the *Chlamydomonas* genomic DNA flanking the putative insert location obtained from RESDA-PCR for *pds1-3*, and PCR with this primer and three nested primers within the vector was performed (Figure 2.8A). Successful amplification confirmed the location of the plasmid vector in *pds1-3* genomic DNA (Figure 2.8B). Recovery of flanking sequence at the second end of the insert was unsuccessful, however. One reason may be because the insertion of foreign DNA into *Chlamydomonas* genomic DNA is often accompanied by a deletion [8]. With this in mind, PCR primers were designed within the *PDS1* genomic DNA on the side of the insertion for which no flanking sequence could be recovered. MS031A and MS031B primers amplified a 498 bp product from *pds1-3* genomic DNA, 500 bp distant from insertion point while primers MS041A and MS041B amplified a 200 bp fragment 2.5 kb distant from the site of insertion. Successfully amplification and DNA sequencing of PCR products with MS031 and MS041 primers indicated that a large deletion did not accompanied the insertion of pBC1 (Figure 2.8C).

No *PDS1* transcript was detectable by quantitative PCR in *pds1-3*, in contrast to the hypomorphic allele *pds1-1* (Figure. 2.8D). QPCR expression analysis indicates that the *PDS1* transcript is present, although at a reduced level in *pds1-1,* ~13% the level found in wild-type (Figure 2.8D).

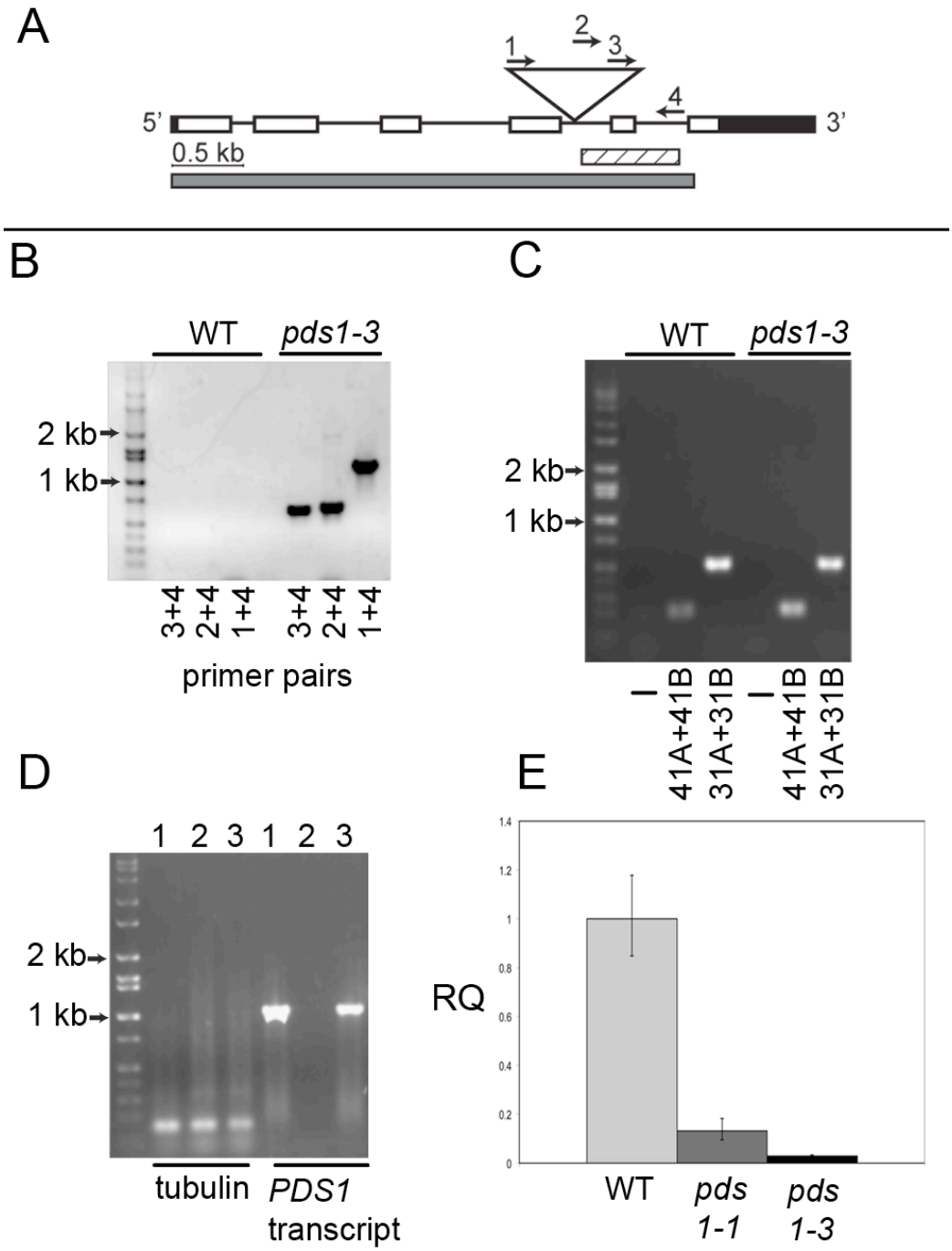

Figure 2.8. Analysis of *pds1*-3 DNA insertional mutant.
A). Schematic of *C. reinhardtii PDS1* gene showing DNA insertion location (triangle), region amplified in flanking sequence tag (striped bar), and region of transcript not detectable by RT-PCR in *pds1-3* (gray bar). UTRs are indicated by black bars and exons by open bars. Genomic DNA spanning the 5' UTR to the 4th exon could be amplified by PCR in *pds1-3*. B). No amplification in wild-type (WT) and amplification in *pds1-3* with three vector-specific primers (1, 2, 3) and one primer in *PDS1* genomic DNA (4), indicated by arrows in panel A, confirming insert location in *pds1-3*.

C). Successful amplification and DNA sequencing of *PDS* on the opposite side of insertion from flanking sequence tag from genomic DNA in wild-type and *pds1-3* revealed that a large deletion did not accompany the vector insert. Amplification products were obtained from genomic DNA 500 bp (primers MS031A and MS031B, in exon 1) and 2.5 kb (primers MS041A and MS041B, in exon 4) distant from insertion site.
D). Amplification of *PDS1* transcript (gray bar in panel A) from total RNA in wild-type (1), *pds1-3* (2), and *pds1-1* (3), with the amplification of tubulin as a positive control
E). Relative *PDS1* transcript levels in wild-type cells (light gray bar), *pds1-1* (dark gray bar), and *pds1-3* (black bar). Relative quantification fold change (RQ) values to the calibrator (WT *PDS1* transcript levels) is shown.

Growth defects of *pds1* mutants

Multiple independent alleles of *lts1* but no *pds1* mutants were isolated in a previous screen for white mutants of *C. reinhardtii* [6]. To understand why, the growth rates of *pds1* mutants were compared to *lts1-201* and wild-type cells. Comparison of growth rates in liquid TAP in the dark indicated that *pds1-1* and *pds1-3* mutants grew more slowly than either *lts1-201* or wild-type cells (Figure 2.9A). Differences in growth between *pds1* mutants and white *lts1-201* or wild-type cells were even more pronounced in plating assays. First, the plating efficiency of *pds1*, *lts1*, and wild-type strains was measured as colony-forming units (CFU). After 3 weeks growth in the dark, the plating efficiency of *pds1-1* was 53.50% ± 2.83; *pds1-3* was 48.35% ± 2.90; *lts1-201* was 86.70% ± 10.18; and wild type was 83.27% ± 3.48 (Figure 2.9B). Wild-type and *lts1-201* cells formed similarly sized colonies, whereas both types of *pds1* mutants formed smaller colonies (Figure 2.9B).

The second plating experiment determined how visible *pds1* mutants were in a background of wild-type cells when grown in a 1:1 ratio. Plating efficiency was accounted for in this experiment but was underestimated by 100 CFUs/plate for *pds1* mutants. The actual number of cells inoculated was 2500 for *pds1* strains and 1650 for wild-type and *lts1-201* strains per plate. With ~50% and ~80% plating efficiencies for *pds1* strains and wild-type/*lts1-201* strains, respectively, the expected CFU for *pds1* mutants was 1250 and 1320 CFU/plate for wild-type/*lts1-201* strains. In both fitness tests, wild-type and *lts1-201* cells formed similarly sized colonies after 12 days of growth in the dark while both types of *pds1* mutants formed colonies that were smaller than wild-type and *lts1-201* colonies (Figure 10B, 10C). *Pds1-3* mutants formed the smallest colonies—some of which were barely detectable with the naked eye at 12 days (Figure 2.9B). *Pds1-1* and *pds1-3* mutants also did not survive the plating procedure as well as null *psy* and wild-type cells. After 3 weeks growth in the dark, the percent of CFU observed from the expected 1000 CFU for *pds1-1* was 53.50% ± 2.83; *pds1-3*, 48.35% ± 2.90; *lts1-201*, 86.70% ± 10.18; and wild-type, 83.27% ± 3.48 (Figure 2.9B). For the visibility test light green *pds1-1* and white *pds1-3* mutants were each dark grown in a 1:1 ratio with dark green wild-type cells, after adjusting for percent survival after plating with glass beads, to determine how distinguishable they were in a background of dark green cells (Figure10C). For a comparison white *psy* mutants were also grown with wild-type cells. On TAP-agar plates with a 1:1 ratio of *lts1-201* to wild-type cells, white *lts1-201* colonies were easily identified; they were as densely populated and equal in diameter to wild-type colonies (Figure 2.9C). In contrast, it was difficult to identify light green *pds1-1* and white *pds1-3* mutants among wild-type colonies because their colonies were frequently half the diameter or smaller than wild-type colonies and

fewer in number (Figure 2.9C). Of the carotenoid mutants tested, *pds1-3* colonies were the smallest and the least dense of the carotenoid mutants. Because of their extremely small size, it was difficult to determine the color of some *pds1* colonies and as a result, they could have been mistaken for extremely small wild-type colonies or not been detected at all.

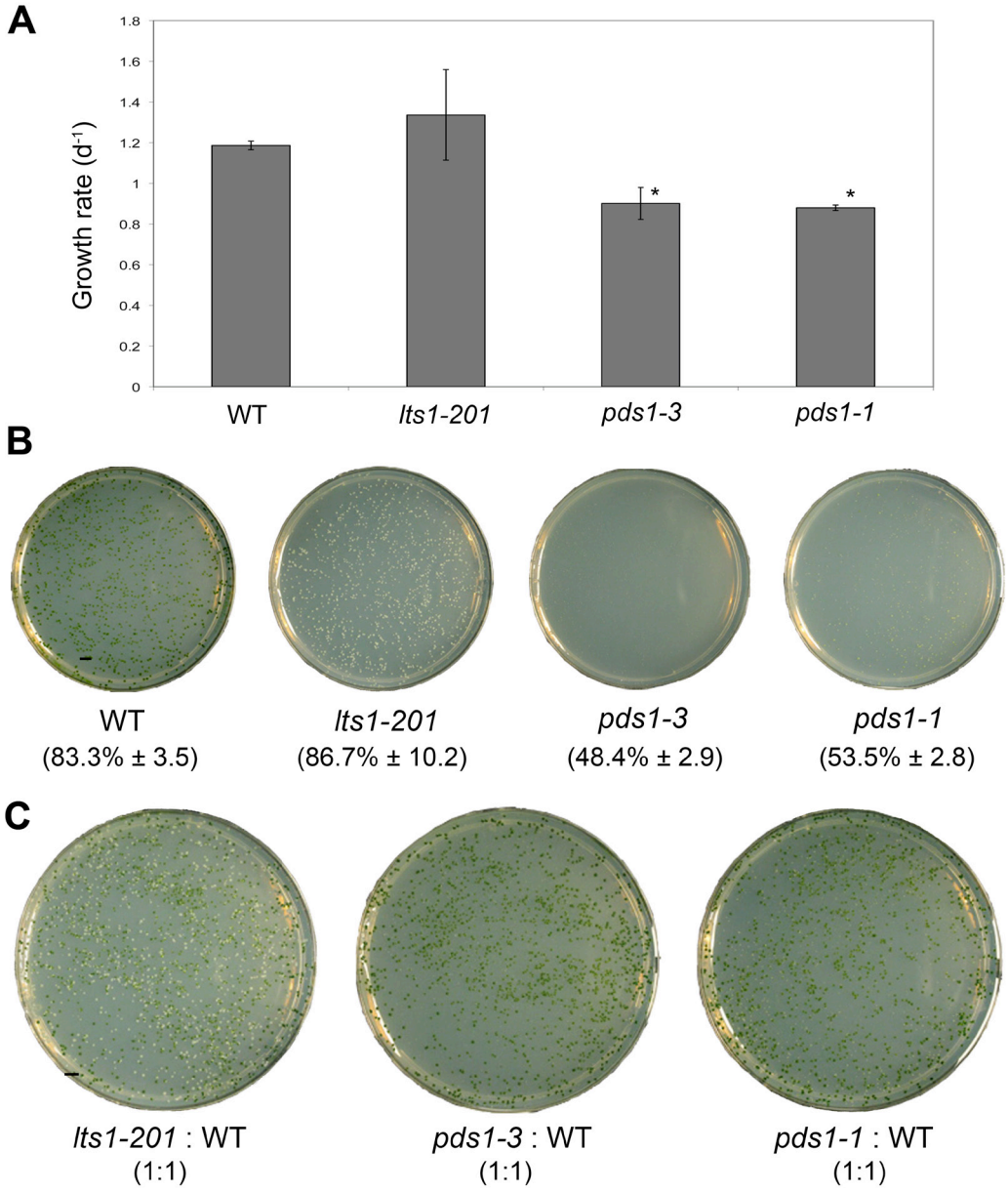

Figure 2.9. Results of plating assays of wild-type, *lts1-201*, *pds1-3*, and *pds1-1*.
A). Growth rate per day for wild-type, *lts1-201* (null *psy)*, *pds1-3*, and *pds1-1*. Biological triplicates of each strain were grown in the dark in liquid TAP on a shaker. *Significantly differently from *lts1-201* and wild-type values under the same conditions using a two-tailed t test ($P<0.05$).
B). Percent of cells that survived plating with glass beads (% survival ± standard deviation) after 12 days of growth in the dark. Scale bar represents 5 mm.

C). ~1:1 ratio of carotenoid mutant to wild-type cells after 12 days of growth in the dark. Because plating efficiency was underestimated for *pds1* mutants the expected CFU/plate for *pds1* was actually 1250 CFU/plate and 1320 CFU/plate for wild-type and *lts1-201* strains. Scale bar represents 5 mm.

Intragenic *pds1-2* suppressor mutants

To gain further insight into amino acid residues important for PDS structure and function, suppressor mutants of *pds1-2* were isolated. 16 light green *pds1-2* suppressor mutants falling into three allelic classes were isolated from UV mutagenesis of white P3-84 mutants.

PSY and *PDS1* genes were both sequenced from *pds1-2* suppressor mutants to identify any revertants and/or additional mutations. All 16 suppressor mutants retained the chloroplast transit peptide mutation in the *PSY* gene (*lts1-301*) from strain P3-84 (Figure 2.7C). Four of these strains, csp6, csp10, csp14, and csp15, had a reversion of the *pds1-1* mutation: a transition from "A/T" (Lys143) back to wild-type "G/C" (Glu143) (Figure 2.6, 2.10A). These suppressors retained the L64P mutation, which was named *pds1-4*. The second class of intragenic *pds1-2* suppressor mutants, *pds1-5*, had the original *pds1-1* mutation (E143K) plus a new *pds1* mutation, which converted the *pds1-2* mutation (L64P) in exon one to L64F (Figure 2.7, 2.10A). Seven *pds1-5* strains were isolated: csp3, csp4, csp5, csp9, csp11, csp16 and csp17 (Figure 2.3). The third class of intragenic *pds1-2* suppressor mutants had three mutations in *PDS1*: E143K from *pds1-1*, L64P from *pds1-2* and a new mutation, K90M. The methionine at position 90 resulted from a transversion mutation that changed the wild-type "A" to a "T (Figure 2.6, 2.10A). In this third allelic class, *pds1-6*, five strains were isolated: csp1, csp7, csp8, csp12, and csp13 (Figure 2.3, csp8 not shown).

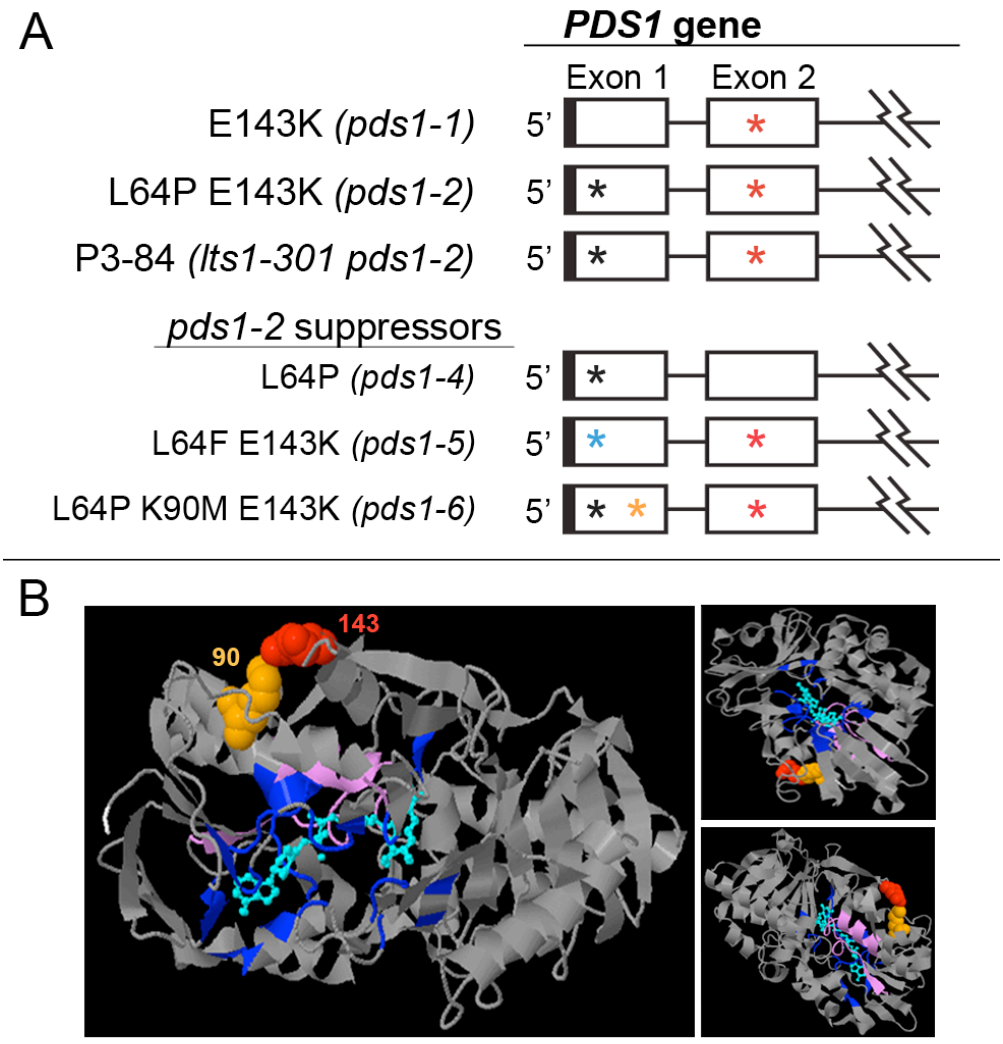

Figure 2.10. Analysis of intragenic suppressors of *pds1-2* mutants.
A). Schematic depiction of *pds1-1*, *P3-84*, *pds1-2*, and *pds1-2* suppressors (*pds1-4*, *pds1-5*, and *pds1-6)*. Cartoon of the *Chlamydomonas PDS1* gene showing only exons one and two. Jagged lines indicate only a partial depiction of the *PDS1* gene. UTRs are indicated by solid boxes, exons by open boxes and introns by lines. Asterisks mark positions of mutations in *pds1-1*, *pds1-2*, P3-84 and *pds1-2* suppressor mutants. Black and blue asterisks represent mutations L64P and L64F, respectively. Orange asterisk in exon 1 signifies location of the K90M mutation, and red asterisks in exon 2 signify the E143K mutation.
B). 3DLigandSite structural prediction of the *Chlamydomonas* PDS protein showing positions of amino acid residues mutated in *pds1-1* and *pds1-6* mutants, E143K and K90M, respectively. L64P and L64F were not mapped because the first 71 amino acids of the N-terminus had no structural prediction. Amino acid residue 72 on the N-terminus of the predicted PDS protein structure is colored in white as a point of reference. Ligand and wild-type amino acids corresponding to mutated residues were colored as follows: position 90 (spacefilling, orange); position 143 (spacefilling, red); ligand [NAD(P)/FAD] (cyan); predicted ligand binding sites (indigo); start of predicted N-terminus (amino acid residue 72, white); and carotenoid binding site proposed by Armstrong *et al.* (amino acid residues 492-517, lavender). Three different perspectives of the predicted structure are shown.

Light green intragenic suppressor mutants of *pds1-2* were more light tolerant than light green *pds1-1* and white *pds1* mutants but less light tolerant than medium green *lts1-301* single mutants (Figure 2.3). All suppressor mutants grew well under vLL, but only *pds1-4* mutants could survive in LL. The *pds1-5* and *pds1-6* mutants bleached and died in LL (Figure 2.3). No suppressor mutant survived in HL. Pigment analysis of *pds1-2* suppressor mutants showed that all three classes synthesize the full spectrum of wild-type colored carotenoids, but at 20% the levels found in wild-type cells (Table 2.2). Similar to suppressor mutants, *lts1-301* had 24% of the total colored carotenoids of wild-type cells. Comparison of total xanthophylls, known for their photoprotective properties [24,25], did not reveal any significant differences between suppressor mutants and *lts1-301*. Zeaxanthin, a xanthophyll particularly important for photoprotection [25,26,27], was elevated 1.6 fold in *lts1-301* compared to suppressor mutants and 1.4 fold higher than in wild-type cells. The levels of lutein were significantly lower than in wild-type cells but not significantly different among suppressor mutants or *lts1-301* mutants. Two of the three *pds1-2* suppressor mutant classes still accumulated phytoene. The *pds1-5* and *pds1-6* strains accumulated phytoene ~17% and ~6% the phytoene levels present in the starting strain P3-84, respectively (Table 2.2). Like wild-type cells, *pds1-4* mutants did not accumulate any phytoene (Table 2.2).

Structural prediction

The 3DLigandSite web server predicted that the *C. reinhardtii* PDS protein has a structure most similar to a human monoamine oxidase, C2c70B. Both C2c70B and the *C. reinhardtii* PDS proteins were classified as oxidoreductases and had 12% identity to each other. 3DLigandSite predicted the presence of a dinucleotide-binding motif [NAD(P) or FAD] in the center of the PDS protein (cyan blue, Figure 2.10B) and potential ligand binding sites (indigo, Figure 2.10B) [28,29]. No structural prediction was found for the first 71 amino acid residues on the N-terminus or the last 22 residues on the C-terminus end of the PDS protein. The C-terminus of bacterial carotenoid dehydrogenases was proposed by Armstrong *et al*. to contain a hydrophobic carotenoid-binding pocket which Pecker *et al.* also found conserved among cyanobacteria, algae, and plants [30,31]. In *C. reinhardtii* this region spans amino acid residues 492-517 (Figure 2.10B, lavender).

In the predicted PDS protein structure, amino acid residue 143 (mutated in both *pds1-1* and in *pds1-2* suppressor mutants) and amino acid residue 90 (mutated in *pds1-6*), were adjacent to one another and in spacefilling mode in physical contact (Figure 2.10B, Glu143, red and Lys90, orange). In the wild-type PDS protein these amino acids are Glu143 and Lys90. Amino acid residue 64 affected in both P3-84 and Type II *pds1-2* suppressor mutants could not be visualized because no structure was predicted for the first 71 amino acids of the N-terminus of *C. reinhardtii* PDS.

DISCUSSION

In order to conserve resources and control accumulation of possibly harmful intermediates, metabolic pathways are commonly regulated at their early steps. Studies in other organisms indicate that the first two steps of carotenoid biosynthesis, catalyzed by PSY and PDS, are likely points of regulation for the whole pathway. *PSY* was reported to be regulated in tomato [32], pepper [33], mustard [34,35], corn [36,37,38], sunflower [39] and algae [40,41] by light and/or carotenoid content. *PDS* was found to be regulated or rate-limiting in algae [41,42,43,44], potato [45], pepper [33], and tomato [31,32].

Previous studies have identified many *C. reinhardtii lts1* mutants affecting *PSY*, but no *C. reinhardtii pds1* mutants had been isolated until this study. A phytoene-accumulating *C. reinhardtii* mutant was previously reported in a study by Stolbova [46], who observed that the light-sensitive *lts4* mutant accumulated phytoene, but without any significant change in pigment composition [46]. The *lts4* mutation was mapped to chromosome 11, indicating that it was not a *pds* mutant since the only copy of the *C. reinhardtii PDS* gene is on chromosome 12 [47]. The *lts4* mutation may be linked to a plastid terminal oxidase (PTOX) or to plastoquinone biosynthesis, both of which are necessary for phytoene desaturation [3,48,49]}.

Similar to *lts1* mutants, *pds1* mutants are extremely light sensitive and pale in color. Mutants lacking PSY (*lst1-201*) or PDS activity (*pds1-2* and *pds1-3*) accumulate no colored carotenoids (Figure 2.4) and die when exposed to even very low light intensities (Figure 2.3). Surprisingly, the leaky *pds1-1* mutant was as light sensitive as *lts1* and *pds1* null mutants even though it was able to accumulate colored carotenoids. The phenotype of *pds1-1* indicates that the amount of colored carotenoids present in *pds1-1* provides insufficient protection from even very low light.

The major difference between the white *lts1* and *pds1* mutants is the accumulation of phytoene in *pds1*. In addition to the lack of colored carotenoids, the accumulation of phytoene might contribute to the cell's susceptibility to photo-oxidative stress. Even in complete darkness, phytoene-accumulating *pds1* mutants grew more slowly and had a lower plating efficiency than wild-type or *lts1* cells (Figure 2.9). Together, these phenotypes could explain the difficulty in isolating *pds1* mutants in previous screens [6]. α-Tocopherol, known for protecting membrane lipids from oxidative damage [50], did not account for the higher growth rate and plating efficiency of *lts1* mutants, because white *pds1-3* mutants contain 2-fold more α-tocopherol (Table 2.2) than white *lts1* mutants [6].

Light sensitivity assays of *pds1-2* suppressor mutants also suggest that phytoene accumulation could enhance photo-oxidative stress. All three classes of suppressor mutants accumulated significant amounts of colored carotenoids, but only *pds1-5* and *pds1-6* mutants accumulated phytoene and were also more light sensitive that *pds1-4* mutants. The *pds1-4* mutants did not have any detectable levels of phytoene and in general did not have more photoprotective carotenoids than either *pds1-5* and *pds1-6* mutants, so their ability to survive in higher light intensities cannot be attributed to the presence of higher levels of total colored carotenoids or to a particular photoprotective carotenoid such as lutein or zeaxanthin.

A deleterious effect of phytoene accumulation might explain the occurrence of the *lts1-301* mutation in the *pds1-1* enhancer mutant, P3-84 (*lts1-301 pds1-2*). The mutation in *PSY* might have arisen secondarily, as a way to mitigate the phytoene accumulation conferred by the the loss of PDS function in the *pds1-2* allele. The *lts1-301* mutation decreases the flux of

metabolites entering carotenoid biosynthesis and therefore reduces the amount of phytoene that accumulates in the cell (Figure 2.4).

In *pds* mutants of plants, the possible effects of phytoene accumulation are difficult to assess. Generally, studies have shown that impairment of PDS activity result in phytoene accumulation and pleiotropic defects in plants. *Arabidopsis* [2,3,51], maize [4,52], rice [1,52,53], and tobacco plants [5] with impaired PDS activity accumulate phytoene, are lethal at the seedling stage, have stunted growth, exhibit albinism, and in the case of maize and rice, seeds experience vivipary. Light-exposed norflurazon-treated plants also accumulate phytoene and produce albino seedlings or white leaf sectors [20,32,54,55]. However, these morphological defects are not exclusive to plants with reduced PDS activity and phytoene accumulation. Mutants in other steps of the carotenoid pathway and in metabolic pathways that feed substrates directly into carotenoid biosynthesis also produce mutants with albinism, vivipary, and stunted growth. These mutants include *psy* mutants [5], *zds* mutants [1,56], GGPP synthase mutants [57] and mutants of the plastidic methylerythritol 4-phosphate (MEP) pathway [58]. Carotenoid and abscisic acid deficiency is probably the primary cause of the adverse phenotypes in plant *pds* mutants.

Amino acid residues affected in *pds1-1, pds1-2,* and intragenic suppressors of *pds1-2* mutants must play an important role in PDS structure and/or function. Phyre prediction of the PDS protein structure placed amino acid residues affected in *pds1-1* and *pds1-6* mutants in close proximity with one another. In wild-type PDS, these amino acids are negatively charged Glu143 and positively charged Lys90, respectively. 3DLigandSite did not identify them as residues required for FAD/NAD(P) binding. Because of their physical proximity to each other, it is possible that these residues form an ion pair that is important for proper folding of PDS. In *pds1-1*, Glu143(-) is converted to Lys143(+). This results in two positively charged residues, Lys143(+) and Lys90(+), in direct contact, which would presumably introduce electrostatic repulsion and possibly promote protein destabilization. Electrostatic repulsion might be alleviated in *pds1-6*, which substitutes Lys90(+) with an uncharged methionine. The *pds1-6* mutants carrying this amino acid change were light green in color, not dark green like wild-type cells, indicating that full PDS activity was not recovered. Accumulation of different mutant PDS proteins could be addressed by immunoblot analysis.

P3-84, *pds1-2*, and all intragenic suppressor mutants have mutations that affect amino acid residue 64, but no structure was predicted for first 71 amino acid residues of the PDS N-terminus. In wild-type cells, this residue is hydrophobic leucine, whereas in P3-84 and *pds1-2* this residue was converted to cyclic proline, which in conjunction with the *pds1-1* mutation severely impaired PDS activity. The *pds1-5* suppressor mutants partially recovered PDS activity by changing the activity-impairing proline to a different hydrophobic amino acid, phenylalanine. The first 70-80 residues of the N-terminus of PDS is not present in the cyanobacterium *Synechocystis* indicating that this region is not critical for PDS activity (Figure 2.6). Instead, it may be involved in chloroplast targeting or perhaps insertion into the thylakoid membrane. Several studies using protein blotting and immunogold labeling have localized PDS proteins in the thylakoid membranes [4,59].

In summary, I have isolated and characterized six alleles of *pds1* in Chlamydomonas. Comparisons of *lts1* and *pds1* mutants suggest that phytoene accumulation is deleterious and that PDS may be an important control point in understanding engineering carotenoid biosynthesis. Homology modeling and structural analysis of the *pds1* mutations have also provided insight into the PDS protein structure and function.

REFERENCES

1. Fang J, Chai C, Qian Q, Li C, Tang J, et al. (2008) Mutations of genes in synthesis of the carotenoid precursors of ABA lead to pre-harvest sprouting and photo-oxidation in rice. The Plant Journal 54: 177-189.
2. Qin G, Gu H, Ma L, Peng Y, Deng XW, et al. (2007) Disruption of phytoene desaturase gene results in albino and dwarf phenotypes in *Arabidopsis* by impairing chlorophyll, carotenoid, and gibberellin biosynthesis. Cell Research 17: 471-482.
3. Norris SR, Barrette TR, DellaPenna D (1995) Genetic dissection of carotenoid synthesis in *Arabidopsis* defines plastoquinone as an essential component of phytoene desaturation. Plant Cell 7: 2139-2149.
4. Hable WE, Oishi KK, Schumaker KS (1998) *Viviparous -5* encodes phytoene desaturase, an enzyme essential for abscisic acid (ABA) accumulation and seed development in maize. Molecular and General Genetics MGG 257: 167-176.
5. Busch M, Seuter A, Hain R (2002) Functional analysis of the early steps of carotenoid biosynthesis in tobacco. Plant Physiology 128: 439-453.
6. McCarthy SS, Kobayashi MC, Niyogi KK (2004) White mutants of *Chlamydomonas reinhardtii* are defective in phytoene synthase. Genetics 168: 1249-1257.
7. Vila M, Couso I, León R (2008) Carotenoid content in mutants of the chlorophyte Chlamydomonas reinhardtii with low expression levels of phytoene desaturase. Metabolic Engineering 43: 1147-1152.
8. Dent RM, Haglund CM, Chin BL, Kobayashi MC, Niyogi KK (2005) Functional Genomics of Eukaryotic Photosynthesis Using Insertional Mutagenesis of Chlamydomonas reinhardtii. Plant Physiology 137: 545-556.
9. Gross CH, Ranum LPW, Lefebvre PA (1988) Extensive restriction fragment length polymorphisms in a new isolate of Chlamydomonas reinhardtii. Current Genetics 13: 503-508.
10. Harris EH (1989) The *Chlamydomonas* Sourcebook: A Comprehensive Guide to Biology and Labortory Use: Academic Press, San Diego.
11. Werner R, Mergenhagen D (1998) Mating type determination of *Chlamydomonas reinhardtii* by PCR. Plant Molecular Biology Reporter 16: 295-299.
12. Davies JP, Weeks DP, Grossman AR (1992) Expression of the arylsulfatase gene from the β2-tubulin promoter in *Chlamydomonas reinhardtii*. Nucleic Acids Research 20: 2959-2965.
13. Rozen S, Skaletsky H (1999) Primer3 on the WWW for General Users and for Biologist Programmers. In: Misener S, Krawetz SA, editors. Bioinformatics Methods and Protocols: Humana Press. pp. 365-386.
14. González-Ballester D, Montaigu Ad, Galván A, Fernández E (2005) Restriction enzyme site-directed amplification PCR: A tool to identify regions flanking a marker DNA. Analytical Biochemistry 340: 330-335.
15. Emanuelsson O, Nielsen H, Heijne Gv (1999) ChloroP, a neural network-based method for predicting chloroplast transit peptides and their cleavage sites. Protein Science 8: 978-984.
16. Pruitt KD, Tatusova T, Maglott DR (2007) NCBI reference sequences (RefSeq): a curated non-redundant sequence database of genomes, transcripts and proteins. Nucleic Acids Research 35: D61-65.

17. Thompson JD, Higgins DG, Gibson T (1994) CLUSTAL W: improving the sensitivity of progressive multiple sequence alignmet through sequence weighting position-specific gap penalties and weight matric choice. Nucleic Acids Research 22: 4673-4680.
18. Wass MN, Sternberg MJE (2009) Prediction of ligand binding sites using homologous structures and conservation at CASP8. Proteins: Structure, Function, and Bioinformatics 77: 147-151.
19. Breitenbach J, Zhu C, Sandmann G (2001) Bleaching herbicide norflurazon Inhibits phytoene desaturase by competition with the cofactors. Journal of Agricultural and Food Chemistry 49: 5270-5272.
20. Simkin AJ, Breitenbach J, Kuntz M, Sandmann G (2000) In vitro and in situ Inhibition of carotenoid biosynthesis in *Capsicum annuum* by bleaching herbicides. Journal of Agricultural and Food Chemistry 48: 4676-4680.
21. Sandmann G, Böger P (1989) Target Sites of Herbicide Action; Sandmann G, Linden H, Böger P, editors. Boca Raton: CRC Press.
22. Mayer M, Barlet D, Beyer P, Kleinig H (1989) The *in vitro* mode of action of bleaching herbicides on the desaturation of 15-cis-phytoene and cis- ζ-carotene in isolated daffodil chromoplasts. Pesticide Biochemistry and Physiology 34: 111-117.
23. Altschul SF, Madden TL, Schäffer AA, al. ae (1997) Gapped BLAST and PSI-BLAST: a new generation of protein database search programs. Nucleic Acids Research 25: 3389-3402.
24. Niyogi KK (1999) Photoprotection revisited: genetic and molecular approaches. Annual Review of Plant Physiology and Plant Molecular Biology 50: 333-359.
25. Niyogi KK, Björkman O, Grossman AR (1997) The roles of specific xanthophylls in photoprotection. Proceedings of the National Academy of Sciences 94: 14162-14167.
26. Baroli I, Do AD, Yamane T, Niyogi KK (2003) Zeaxanthin accumulation in the absence of a functional xanthophyll cycle protects *Chlamydomonas reinhardtii* from photooxidative stress. Plant Cell 15: 992-1008.
27. Holt NE, Zigmantas D, Valkunas L, Li X-P, Niyogi KK, et al. (2005) Carotenoid cation formation and the regulation of photosynthetic light harvesting. Science 307: 433-436.
28. Fraser PD, Linden H, Sandmann G (1993) Purification and reactivation of recombinant *Synechococcus* phytoene desaturase from an overexpressing strain of *Escherichia coli*. Biochemical Journal 291: 687-692.
29. Al-Babili S, von Lintig J, Haubruck H, Beyer P (1996) A novel, soluble form of phytoene desaturase from *Narcissus pseudonarcissus* chromoplasts is Hsp70-complexed and competent for flavinylation, membrane association and enzymatic activation. The Plant Journal 9: 601-612.
30. Armstrong GA, Alberti M, Leach F, Hearst JE (1989) Nucleotide sequence, organization, and nature of the protein products of the carotenoid biosynthesis gene cluster of *Rhodobacter capsulatus*. Molecular and General Genetics MGG 216: 254-268.
31. Pecker I, Chamovitz D, Linden H, Sandmann G, Hirschberg J (1992) A single polypeptide catalyzing the conversion of phytoene to zeta-carotene is transcriptionally regulated during tomato fruit ripening. Proceedings of the National Academy of Sciences of the United States of America 89: 4962-4966.
32. Giuliano G, Bartley GE, Scolnik PA (1993) Regulation of carotenoid Biosynthesis during tomato development. Plant Cell 5: 379-387.

33. Simkin AJ, Zhu C, Kuntz M, Sandmann G (2003) Light-dark regulation of carotenoid biosynthesis in pepper (*Capsicum annuum*) leaves. Journal of Plant Physiology 160: 439-443.
34. Welsch R, Beyer P, Hugueney P, Kleinig H, von Lintig J (2000) Regulation and activation of phytoene synthase, a key enzyme in carotenoid biosynthesis, during photomorphogenesis. Planta 211: 846-854.
35. von Lintig J, Welsch R, Bonk M, Giuliano G, Batschauer A, et al. (1997) Light-dependent regulation of carotenoid biosynthesis occurs at the level of phytoene synthase expression and is mediated by phytochrome in *Sinapis alba* and *Arabidopsis thaliana* seedlings. The Plant Journal 12: 625-634.
36. Li F, Vallabhaneni R, Wurtzel ET (2008) *PSY3*, a new member of the phytoene synthase gene family conserved in the poaceae and regulator of abiotic stress-induced root carotenogenesis. Plant Physiology 146: 1333-1345.
37. Li F, Vallabhaneni R, Yu J, Rocheford T, Wurtzel ET (2008) The maize phytoene synthase gene family: overlapping roles for carotenogenesis in endosperm, photomorphogenesis, and thermal stress tolerance. Plant Physiology 147: 1334-1346.
38. Li F, Tsfadia O, Wurtzel ET (2009) The phytoene synthase gene family in the grasses. Plant Signaling & Behavior 4: 208-211.
39. Campisi L, Fambrini M, Michelotti V, Salvini M, Giuntini D, et al. (2006) Phytoene accumulation in sunflower decreases the transcript levels of the phytoene synthase gene. Plant Growth Regulation 48: 79-87.
40. Schäfer L, Sandmann M, Woitsch S, Sandmann G (2006) Coordinate up-regulation of carotenoid biosynthesis as a response to light stress in *Synechococcus* PCC7942. Plant, Cell & Environment 29: 1349-1356.
41. Bohne F, Linden H (2002) Regulation of carotenoid biosynthesis genes in response to light in *Chlamydomonas reinhardtii*. Biochimica et Biophysica Acta (BBA) 1579: 26-34.
42. Chamovitz D, Sandmann G, Hirschberg J (1993) Molecular and biochemical characterization of herbicide-resistant mutants of cyanobacterial reveals that phytoene desaturation is a rate-limiting step in carotenoid biosynthesis. The Journal of Biological Chemistry 268: 17348-17353.
43. Grünewald K, Eckert M, Hirschberg J, Hagen C (2000) Phytoene desaturase is localized exclusively in the chloroplast and up-regulated at the mRNA level during accumulation of secondary carotenoids in *Haematococcus pluvialis* (Volvocales, Chlorophyceae). Plant Physiology 122: 1261-1268.
44. Steinbrenner J, Sandmann G (2006) Transformation of the green alga *Haematococcus pluvialis* with a phytoene desaturase for accelerated astaxanthin biosynthesis. Applied Environmental Microbiology 72: 7477-7484.
45. Diretto G, Al-Babili S, Tavazza R, Papacchioli V, Beyer P, et al. (2007) Metabolic engineering of potato carotenoid content through tuber-specific overexpression of a bacterial mini-pathway. PLoS ONE 2: e350.
46. Stolbova AV (1999) The *lts4* photosensitive mutation maps to the short arm of *Chlamydomonas reinhardtii* Dangeard Chromosome XI. Genetika 35: 111-113.
47. Merchant SS, Prochnik SE, Vallon O, Harris EH, Karpowicz SJ, et al. (2007) The *Chlamydomonas* genome reveals the evolution of key animal and plant functions. Science 318: 245-250.

48. Carol P, Stevenson D, Bisanz C, Breitenbach J, Sandmann G, et al. (1999) Mutations in the *Arabidopsis* gene *IMMUTANS* cause a variegated phenotype by inactivating a chloroplast terminal oxidase associated with phytoene desaturation. Plant Cell 11: 57-68.
49. Carol P, Kuntz M (2001) A plastid terminal oxidase comes to light: implications for carotenoid biosynthesis and chlororespiration. Trends in Plant Science 6: 31-36.
50. DellaPenna D, Pogson BJ (2006) Vitamin synthesis in plants: tocopherols and carotenoids. Annual Review of Plant Biology 57: 711-738.
51. Wang T, Iyer LM, Pancholy R, Shi X, Hall TC (2005) Assessment of penetrance and expressivity of RNAi-mediated silencing of the *Arabidopsis phytoene desaturase* gene. New Phytologist 167: 751-760.
52. Wurtzel ET, Luo R, Yatou O (2001) A simple approach to identify the first rice mutants blocked in carotenoid biosynthesis. Journal of Experimental Botany 52: 161-166.
53. Miki D, Shimamoto K (2004) Simple RNAi vectors for stable and transient suppression of gene function in rice. Plant Cell Physiology 45: 490-495.
54. Wetzel CM, Rodermel SR (1998) Regulation of phytoene desaturase expression is independent of leaf pigment content in *Arabidopsis thaliana*. Plant Molecular Biology 37: 1045-1053.
55. Aluru MR, Zola J, Foudree A, Rodermel SR (2009) Chloroplast photooxidation-induced transcriptome reprogramming in *Arabidopsis immutans* white leaf sectors. Plant Physiology 150: 904-923.
56. Conti A, Pancaldi S, Fambrini M, Michelotti V, Bonora A, et al. (2004) A deficiency at the gene coding for ζ-carotene desaturase characterizes the sunflower *non dormant-1* mutant. Plant Cell Physiology 45: 445-455.
57. Maluf MP, Saab IN, Wurtzel ET, Sachs MM (1997) The *viviparous12* maize mutant is deficient in abscisic acid, carotenoids, and chlorophyll synthesis. Journal of Experimental Botany 48: 1259-1268.
58. Page JE, Hause G, Raschke M, Gao W, Schmidt J, et al. (2004) Functional analysis of the final steps of the 1-deoxy-D-xylulose 5-phosphate (DXP) pathway to isoprenoids in plants using virus-induced gene silencing. Plant Physiology 134: 1401-1413.
59. Linden H, Lucas M, de Felipe MR, Sandmann G (1993) Immunogold localization of phytoene desaturase in higher plant chloroplasts. Physiologia Plantarum 88: 229-236.

CHAPTER 3

Light conditional mutants affecting conversion of zeta-carotene to lycopene in *Chlamydomonas reinhardtii*

SUMMARY

To characterize carotenoid biosynthesis in the green alga *Chlamydomonas reinhardtii,* carotenoid-deficient mutants were generated using UV and DNA insertional mutagenesis and screened for pigment accumulation via HPLC analysis. Mutants that accumulated zeta-carotene (ζ-carotene) or prolycopene were isolated and found to be genetically linked to the predicted zeta-carotene desaturase (*ZDS1*) and carotene isomerase (*CRTISO1*) genes, respectively. Grown in the dark, *zds1* mutants are pale yellow-green and accumulate zeta-carotene and low levels of xanthophylls, but in low light they turn green, have reduced levels of zeta-carotene and accumulate downstream carotenoids (alpha- and beta-carotenes and xanthophylls), indicating that light can partially bypass *zds1* mutations. The *crtiso1* mutants are yellow-in-the-dark and accumulate prolycopene, but they green in the light due to photoisomerization of prolycopene. Null mutants for *ZDS1* and *CRTISO1* still accumulate cyclic carotenes and xanthophylls in the dark, indicating incomplete inhibition of carotenoid biosynthesis and suggesting that a third carotene desaturase exists besides ZDS and PDS in *C. reinhardtii*.

PREFACE

Past and current members of the Niyogi Lab who have contributed to the work in this chapter include: Sarah McCarthy who isolated and completed genetic and molecular analyses on *crtiso1-2*, *crtiso1-3*, and *zds1-3*; Rachel Dent who isolated and identified flanking sequences from DNA insertional mutants *zds1-1* and *crtiso1-1*; and Marilyn Kobayashi who isolated *zds1-2*.

INTRODUCTION

Early carotenoid biosynthesis in oxygenic photosynthetic organisms (plants, eukaryotic algae, and cyanobacteria) is catalyzed by five enzymes: phytoene synthase (PSY), phytoene desaturase (PDS), 15-cis-ζ-carotene isomerase (Z-ISO), ζ-carotene desaturase (ZDS), and carotenoid isomerase (CRTISO). The first C_{40} carotenoid compound, colorless 15-*cis*-phytoene, is formed then desaturated and isomerized to red-colored all-*trans*-lycopene. Fungi, archaea, and heterotrophic and anoxygenic bacteria require only two enzymes, PSY (CrtB) and the CrtI-type PDS, to convert 15-*cis*-phytoene to all-*trans*-lycopene [1,2]. Organisms with CrtI-type desaturases accumulate all-*trans* isomers of phytofluene, ζ-carotenes, neurosporene, and lycopene [1,2,3]. In contrast, plant-type phytoene desaturation is distinguished by the *cis*-configured intermediates accumulated by mutants with blocks in each step of phytoene desaturation. Plant-type phytoene desaturation or poly-*cis*-carotene pathway results in 7,9,7',9'-*tetracis*-lycopene (prolycopene) via *cis*-isomers of phytofluene, ζ-carotenes, neurosporene [4,5,6]. Because poly-*cis* lycopene is formed, plant-type desaturases require an isomerase, CRTISO, to transform prolycopene to all-*trans*-lycopene [7,8,9]. A second carotene isomerase, Z-ISO [10], is also necessary for *cis*-to-*trans* isomerization of the central 15-*cis* double bond of PDS product 9,15,9-*tricis*-ζ-carotene to 9,9-*dicis*-ζ-carotene, which is the primary substrate for ZDS [5,11,12,13] (Figure3.1). Z-ISO and CRTISO are essential for carotenoid biosynthesis in dark-grown and non-photosynthetic cells; however, in photosythetically active cells light can stimulate, to a certain extent, the same *cis*-to-*trans* isomerizations reactions [6,7,8,14].

Chlamydomonas reinhardtii mutants with blocks in the first and second steps of carotenoid biosynthesis, PSY and PDS, exhibit extreme light sensitivity and accumulate colorless compounds, geranylgerany diphophosphate and 15-*cis*-phytoene, respectively [15]. In contrast, I show here that *C. reinhardtii* mutants with blocks in ZDS and CRTISO activity are less light sensitive than mutants affecting PSY and PDS. Light can partially rescue the yellow to pale yellow-green color exhibited by *zds1* and *crtiso1* mutants that accumulate *cis*-ζ-carotenes and prolycopene, respectively, in the dark, turning the mutants to a green color in low light.

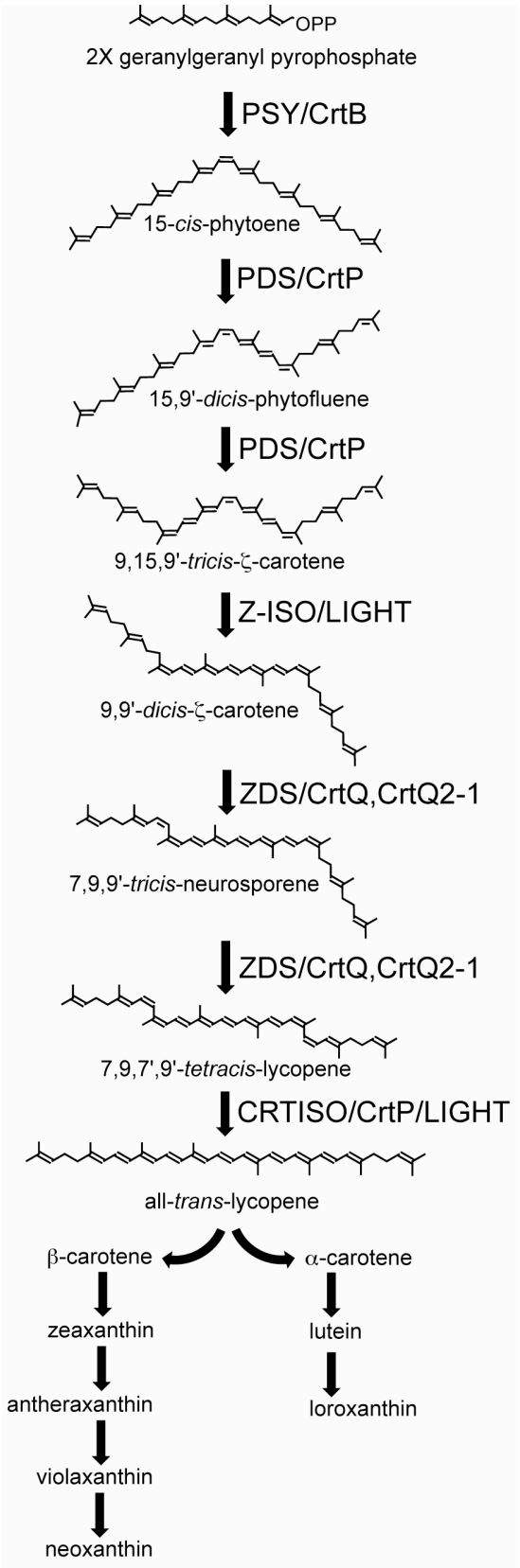

Figure 3.1. The poly-*cis* carotene desaturation pathway found in plants

MATERIALS AND METHODS

Strains and growth conditions

Strains: The wild-type *C. reinhardtii* strains used in this work, 4A+ (*mt*+), 4ax5.2- (*mt*-), and 17D- (*mt*-), are in the 137c genetic background [16]. CC-517 (*ac5 mt*-) and CC-1677 (*ac5 mt*+) were obtained from the Chlamy Center (http://www.chlamy.org/info.html). Genetic linkage tests were completed using the polymorphic wild-type strain, S1D2 (*mt*-) [17]. All strains were maintained on Tris-acetate-phosphate (TAP) agar medium [18] at 25°C in complete darkness.

Growth phenotype in response to increasing light intensities or "greening" assay: To observe growth in response to light, a loopful each of 4A+, *zds1-1* (Cal025.02.09), *zds1-2* (mk38-4), *zds1-3* (sm1-41), *crtiso1-1* (CAL007.01.09), *crtiso1-2* (sm3-42), *crtiso1-3* (sm6-34) were individually used to inoculate 1 ml of TAP. The cultures were then incubated at 25ºC overnight in the dark. The 1 ml culture was then used to inoculate 50 ml of TAP and allowed to grow with shaking at 125 rpm in the dark at 25ºC until cell densities reached approximately $3x10^6$ cells/ml. Cell densities were measured with a Multisizer3 Coulter Counter (Beckman Coulter, Fullerton, CA) and diluted to desired concentrations. 5 µl of each concentration was then spotted onto 50 ml of TAP-agar and grown for 2 days in the dark. After 4 days of dark growth, all cells except dark-only ones were gradually shifted into the light. On day 5, cells were shaded with 2 layers of window screen for 24 hours (S2vLL, 4 µmol photons m^{-2} sec^{-1}) followed by 1 layer of window screen for 24 hours (S1vLL, 8 µmol photons m^{-2} sec^{-1}). On Day 7, all window screens were removed and cells were exposed to 12 µmol photons m^{-2} sec^{-1} (vLL). On Day 8, low light (LL) and high light (HL) treatments were shifted to 20 µmol photons m^{-2} sec^{-1} (S2LL), followed by 30 µmol photons m^{-2} sec^{-1} (S1LL), and finally 60 µmol photons m^{-2} sec^{-1} (LL) every 24 hours. On day 11, HL treatments were shifted further to higher light intensities: 133 µmol photons m^{-2} sec^{-1} (S2HL), to 236 µmol photons m^{-2} sec^{-1} (S1HL), and lastly to 400 µmol photons m^{-2} sec^{-1} (HL) (Table 3.1). All cells were grown for a total of 16 days.

Table 3.1. Timeline of gradually increasing light intensities used in "greening" assay.

	Day 1	Day 2	Day 3	Day 4	Day 5	Day 6	Day 7	Day 8	Day 9	Day 10	Day 11	Day 12	Day 13	Day 14	Day 15	Day 16
vLL	Dark	Dark	Dark	Dark	S2 vLL	S1 vLL	vLL	vLL	vLL	vLL	vLL	vLL	vLL	vLL	vLL	vLL
LL	Dark	Dark	Dark	Dark	S2 vLL	S1 vLL	vLL	S2LL	S1LL	LL	LL	LL	LL	LL	LL	LL
HL	Dark	Dark	Dark	Dark	S2 vLL	S1 vLL	vLL	S2LL	S1LL	LL	S2HL	S1HL	HL	HL	HL	HL

Mutagenesis

DNA insertional mutagenesis: The *zds1-1* and *crtiso1-1* mutants were generated by transforming 4A+ cells with the plasmid pSP124S (4138 bp) [19] as described by Dent et al [16]. pSP124S carries a copy of the *ble* gene which confers resistance to the antibiotic zeocin (bleomycin). Yellow, yellow-green, and very pale green mutants that grew on zeocin were picked for further analysis.

UV and EMS mutagenesis: UV or ethyl methanesulfonate (EMS) mutagenesis of the 4A+ strain was used to isolate the pigment-deficient mutants *zds1-2*, *zds1-3*, *zds1-4* and *crtiso1-*

2, *crtiso1-3*, *crtiso1-4*. Mutageneses were carried out as described previously [15]. Yellow, yellow-green, and pale green colored mutants were also picked in these screens.

All light colored mutants were screened further for carotenoid deficiency using high performance liquid chromatography (HPLC).

HPLC analysis

Carotenoid, chlorophyll, and tocopherol extraction and analysis: Mutants were grown in the dark on TAP-agar, then scraped from the plates and analyzed for pigment accumulation. For more detailed pigment analysis, each strain was first started in 3.0 ml TAP, grown for 24 hours in 8 μmol photons m^{-2} sec^{-1}, then 0.5 ml of this culture was used to inoculate six 50 ml batches of TAP media in 125 ml Erlenmeyer flasks. Three replicates were wrapped in foil for "dark" treatments while three cultures were grown at 20 μmol photons m^{-2} sec^{-1} for "light" treatments. All treatments were grown with shaking at 125 rpm until cell densities reached approximately $2x10^6$ cells/ml. Pigments were extracted from a total of $7x10^7$ cells for each replicate with 200 μl of acetone in the presence of a green safelight (Eastman Kodak Company, Rochester, NY) and analyzed via HPLC as previously described [15]. A 100% acetone sample was run in between each light treatment and strain type during HPLC analysis. Prolycopene and ζ-carotene isomers were identified according to their spectral properties and retention times (RT).

Genetic analysis

Crosses and genetic linkage tests: Crosses were carried out according to standard procedures [18]. Progeny of crosses involving *zds1-1* and *crtiso1-1* were tested for zeocin-resistance by growing the cells on TAP-agar supplemented with 5 μg/ml zeocin (Invitrogen, Carlsbad, CA) for 2 weeks in the dark.

For genetic linkage analyses, *crtiso1-2* and *zds1-2* mutants were each crossed to S1D2 and the resulting progeny were analyzed using single nucleotide polymorphism (SNP) markers in *CRTISO1* and *ZDS1*. Primers for linkage analysis to *CRTISO1* were CISNP2_f (5'-GGCGCAAGTACGAGGAGT-3') and CISNP_r2 (5'-GTGGAGAGTTGGGGAGGTG-3'). CISNP2_f and CISNP2_r primers amplified a 195-bp Cleaved Amplified Polymorphic Sequence (CAPS) product that was digested with *BssHII* overnight. *ZDS1* primers, ZdsF8 (5'-CATAGTCGGGCAAGACCAAT-3') and ZdsR8.1 (5'- ACCTCTGTGGCAGCTTCTGT-3') amplified a 566 bp CAPS product that was digested with *BglI*. The *CRTISO1* CAPS marker was run on a 3% Metaphor agarose gel (Cambrex, East Rutherford, NJ), and the *ZDS1* CAPS marker was run on a 2% agarose gel.

Vegetative diploids were constructed to test dominance of the *zds1* mutation. Each *zds1* mutant was first crossed to *arg7-8,* an arginine-deficient strain [20]. The *zds1 arg7-8* (*mt*-) double mutants were selected by their yellow-green color and their requirement for L-arginine, and then they were crossed to a *ZDS1 arg7-1* (*mt*+) mutant and plated directly on TAP-agar without L-arginine in LL at 25°C. After 10 days in the light, surviving colonies were picked and tested for their ploidy using mating-type PCR [20].

Molecular analyses

DNA isolation and sequencing methods were the same as those used for characterizing *pds1* mutants (Chapter 2). TAIL-PCR [21] was used to identify genomic DNA flanking the insertion site of the pBC1 transforming plasmid [16] for mutants *zds1-1* and *crtiso1-1*. The pSP124S insertion site was further inspected using primers designed specifically from isolated genomic DNA flanking sequences and with pSP124S-specific primers RMD223L (5'-CTGCGCTCCTTCTGGCAT TTAA-3'), and RMD230 (5'-8CCGTATTACCGCCTTTGAGTG-3'). Primers specific to *ZDS1* were ZdsF17 (5'-GCGACCTGAGCGAAGTGG-3') and ZdsR17 (5'-GGACTGTGTCTACC-3') while primers specific to *CRTISO1* were Crtiso3A (5'-CACGCGTCGCTCTATAATGA-3') and Crtiso1627R (5'-CGACGTGACCCAGTCAATTA-3').

DNA gel-blot analysis: 5 μg genomic DNA for each sample was digested with *NcoI* and eletrophoresed in an 0.8% agarose gel in TBE buffer (45 mM Tris-borate, 1 mM EDTA pH 8), transferred to nitrocellulose, and hybridized with a probe for *ZDS1* and for pSP124S [22]. The *ZDS1* probe was a 1181 bp fragment amplified from 4A+ genomic DNA using primers ZdsF3 (5'-ACACGTTCTGCAACAACGAC-3') and ZdsR3 (5'-GTTGCGCCTCCTGTCAT-3') while the pSP124S probe consisted of a 968 bp *BamHI-XbaI* fragment containing the *ble* gene. Probes were labeled using Amersham Gene Images AlkPhos Direct Labelling and Detection System with CDP-Star (GE Healthcare Bio-Sciences Corp., Piscataway, NJ).

Multiple sequence alignment of ZDS1 and CRTISO1 proteins

Protein sequences for CRTI, PDS, ZDS, and CRTISO were retrieved from the National Center for Biotechnology Information (NCBI) (www.ncbi.nlm.nih.gov) or from the Department of Energy (DOE) Joint Genome Institute (JGI) *Chlamydomonas reinhardtii* v4 genome (www.jgi.doe.gov/chlamy) and *Ostreococcus tauri* genome (JGI, http://genome.jgi-psf.org/Ostta4/Ostta4.home.html). The protein sequences were aligned using ClustalW version 1.83 [23] at http://www.ch.embnet.org/software/ClustalW.html and shaded according to Blosum 62 matrix. Percent protein identity was determined by aligning protein sequences with NCBI's Blast 2 Sequences (bl2seq).

RESULTS

In screens for light-sensitive mutants, six yellow to pale yellow-green colored mutants were isolated. All six mutants exhibited moderate to high light sensitivity. When cells were not slowly introduced to light, particularly when they were grown directly in LL or HL on TAP medium, they bleached or turned white and died. Even a direct shift from dark conditions to vLL, resulted in cells bleaching and growing poorly (data not shown). Cells, however, could grow well in light if they were first grown in the dark and then gradually shifted to higher light intensities (Table 3.1). They survived well in vLL even at low cell densities and maintained some growth in LL (Figure 3.2). Pale yellow-green-in-the-dark *zds1-1*, *zds1-2*, and *zds1-3* mutants turned light-green under vLL, but exhibited bleached centers under LL and died under HL. Compared to *zds1* mutants, *crtiso1-1*, *crtiso1-2*, and *crtiso1-3* grew readily in LL and, depending on the cell density, even in HL. Dark-grown *crtiso1-1*, *crtiso1-2*, and *crtiso1-3* mutants were yellow but turned medium-green in vLL, dark-green in LL, and medium-green in

HL (Figure 3.2). Wild-type cells in comparison were dark-green in the dark, vLL, and LL and medium-green in HL.

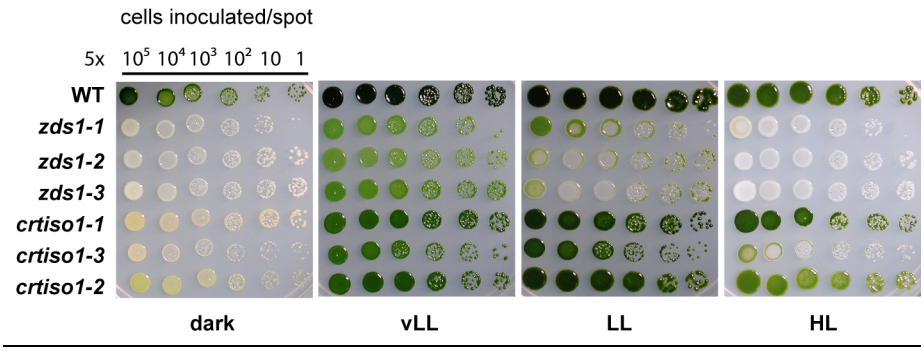

Figure 3.2. Light sensitivity and "greening" phenotype of *zds1* and *crtiso1* mutants.
Cells were spotted onto TAP-agar and grown for 4 days in the dark before being gradually exposed to increasing light intensities. All cells were grown for a total of 16 days. Light intensities: Dk (dark), vLL (12 µmol photons m^{-2} sec^{-1}), LL (60 µmol photons m^{-2} sec^{-1}), HL (400 µmol photons m^{-2} sec^{-1}). WT (wild-type)

zds1 mutants accumulate ζ-carotene while *crtiso1* mutants accumulate prolycopene.

Pigment analyses of *zds1* and *crtiso1* mutants showed a disturbance in the carotenoid biosynthetic pathway. Dark-grown *zds1* and *crtiso1* mutants have significant reductions in chlorophyll and xanthophyll levels compared to wild-type (Table 3.2 and Figure 3.3A). Dark-grown *zds1-1* and *crtiso1-1* mutants had abnormal chlorophyll *a* to chlorophyll *b* ratios (chl *a/b*) of 3.7 and 1.5, respectively, and total chlorophyll levels that were 10-fold lower wild-type cells. Total xanthophyll levels were 100-fold lower in *zds1-1* mutants and 22-fold lower in *crtiso1-1* than wild-type cells. The antioxidant, α-tocopherol (α-toc), was 3-fold higher in *zds1-1* and *crtiso1-1* than in wild-type cells. Based on published absorbance spectra [11,24], the major carotenoids (peaks ζ1 and ζ2, Figure 3.3B) accumulated in *zds1-1*, *zds1-2*, and *zds1-3* were identified as ζ-carotene isomers—more specifically 9,15,9'-tricis-ζ-carotene (ζ1: RT=13.77 min, λ_{max} =378 398 422 nm, λ_{max} III/II=0.72, cis peak at 294 nm) and 9,9'-dicis-ζ-carotene (ζ2: RT=13.99 min, λ_{max} =382 402 426 nm, λ_{max} III/II=1.10). Similarly, the major carotenoid accumulated (peak pL, Figure 3.3B) in *crtiso1-1*, *crtiso1-2*, and *crtiso1-3* mutants was identified as prolycopene or 7,9,7',9'-tetracis-lycopene (pL: RT=12.94 min, λ_{max} = (416) 440 (469) nm, λ_{max} III/II=0.00). In contrast, the major carotenes accumulated by wild-type cells in the dark and in the light were β-carotene isomers: *all-trans*-β-carotene (β1: RT=13.79 min, λ_{max} =430 454 480 nm, λ_{max} III/II=0.20), 9-*cis*-β-carotene (β2: RT=14.11 min, λ_{max} =424 448 474 nm, λ_{max} III/II=0.26), and 13-*cis*-β-carotene (β3: RT=14.56 min, λ_{max} =424 448 472 nm, λ_{max} III/II=0.07).

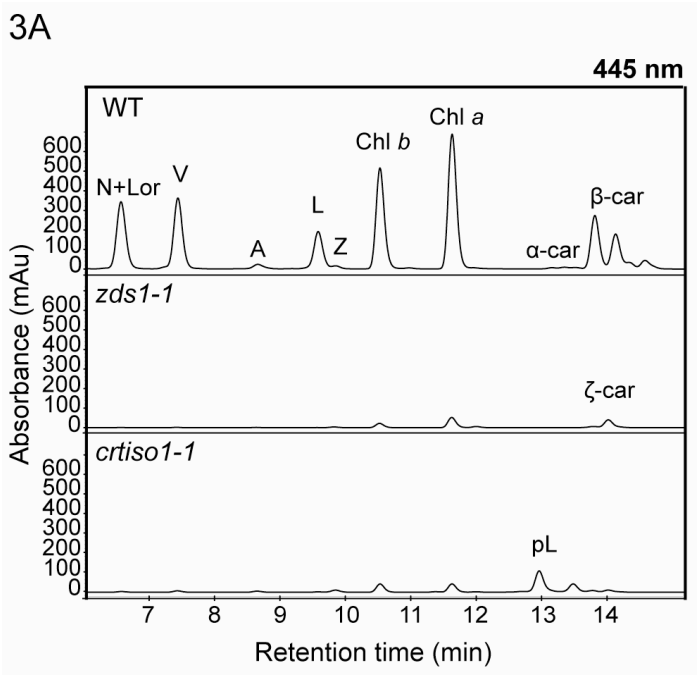
3A
445 nm
WT
Chl a
Chl b
N+Lor
V
L
A
Z
α-car
β-car
zds1-1
ζ-car
crtiso1-1
pL
Absorbance (mAu)
Retention time (min)

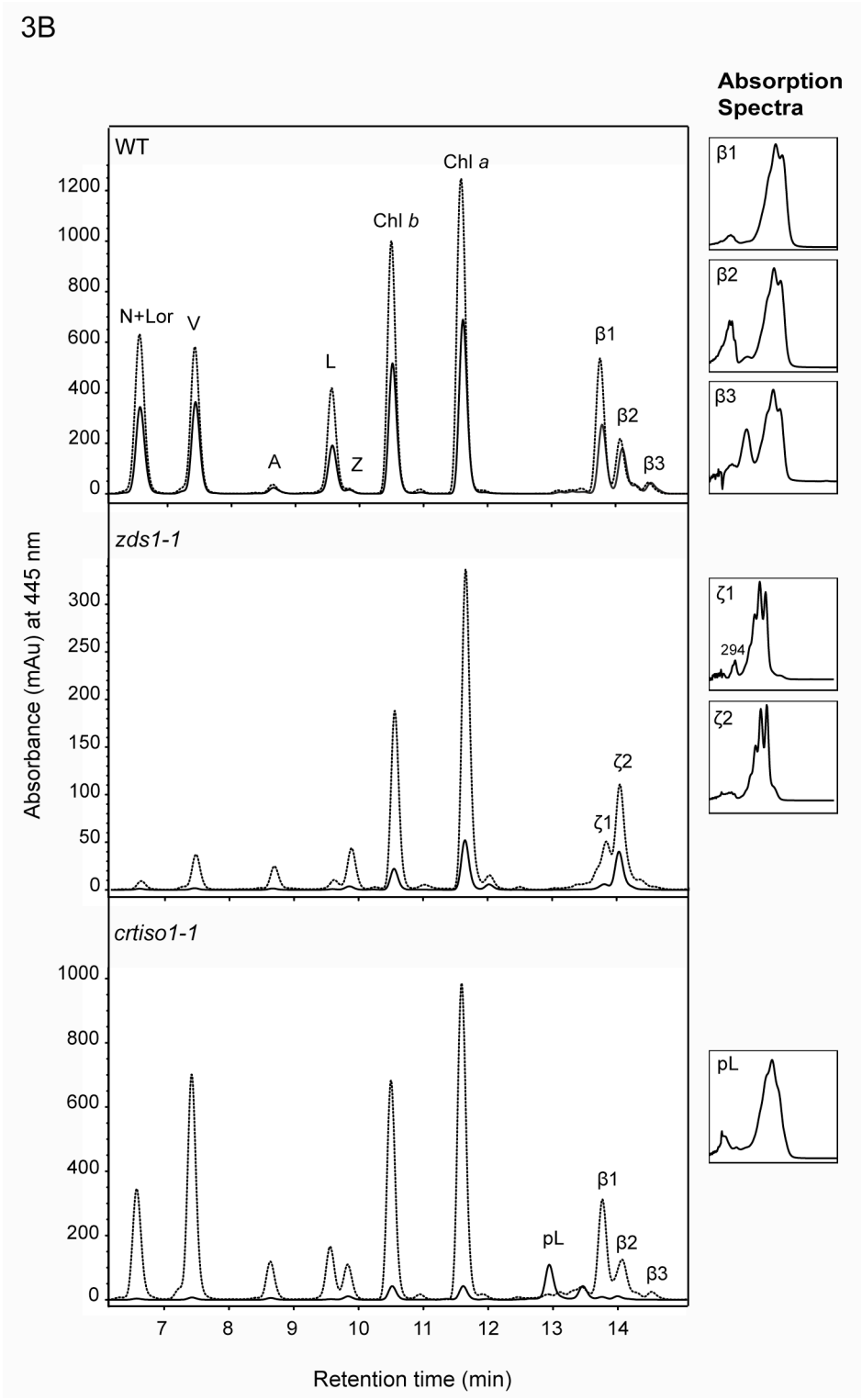

Figure 3.3. Chlorophyll and carotenoid profiles of *zds1-1* and *crtiso1-1* mutants under dark and light conditions

Chlorophylls and carotenoids were detected at 445 nm. Pigments were extracted from a total of $7x10^7$ cells for each sample and analyzed via HPLC coupled with a diode array detector. N+Lor (neoxanthin + loroxanthin); V (violaxanthin); A (antheraxanthin); L

(lutein); Z (zeaxanthin); Chl *a* and Chl *b* (chlorophyll *a* and *b*); α-car, β-car (α- and β-carotenes); ζ-car (ζ-carotenes); pL (prolycopene). Specific isomers were ζ1 (9,15,9'-*tricis*-ζ-carotene); ζ2 (9,9'-*dicis*-ζ-carotene); β1 (*all-trans*-β-carotene); β2 (9-*cis*-β-carotene); and β3 (13-*cis*-β-carotene).
3A). Pigment levels in dark-grown *zds1-1* and *crtiso1-1* mutants relative to wild-type cells.
3B). Pigment levels of dark and light-grown cultures overlayed on top of each other. Solid lines depict pigments present dark-grown cells while dotted lines represent light-grown cells (20 µmol photons m^{-2} sec^{-1}). Right panels depict absorption spectra of specific carotene isomers present in wild-type*, zds1-1* and *crtisos1-1*. 294 indicates wavelength of *cis* peak.

Both *zds1-1* and *crtiso1-1* mutants exhibited dramatic increases in chlorophyll and xanthophyll levels when grown in moderate low light (20 µmol photons m^{-2} sec^{-1}) reflecting the green color phenotype of both types of mutants under light conditions (Figure 3.2). Comparing light growth versus dark growth, total chlorophyll levels increased 6-fold in *zds1-1* and 20-fold in *crtiso1-1* mutants. Chlorophyll *a/b* ratios, total xanthophylls, and α-tocopherol levels approached wild-type values (chl *a/b*= 2.108, xanthophylls= 0.4345 fmol/cell, α-toc= 0.0061 fmol/cell) in light-grown *crtiso1-1* mutants (Chl *a/b*= 2.409, xanthophylls= 0.3454 fmol/cell, α-toc= 0.0067 fmol/cell), but remained abnormal for light-grown *zds1-1* mutants (chl a/b= 2.912, xanthophylls= 0.0298 fmol/cell, α-toc= 0.0095 fmol/cell). For light-grown *zds1-1* and *crtiso1-1* mutants, lutein levels were 48-fold and 2.6-fold less, respectively, than wild-type levels, whereas zeaxanthin levels were 2-fold and 6.5-fold higher, respectively (Table 3.2). Dark-grown *zds1-1* and *crtiso1-1* mutants had highly reduced lutein levels, but only slightly reduced zeaxanthin levels compared to wild-type cells. Zeaxanthin levels in *crtiso1-1* mutants were equivalent to wild-type levels. In *crtiso1-1* mutants ,light resulted in the accumulation of β-carotenes and a reduction in prolycopene (Figure 3.3B).

Table 3.2. Quantification of chlorophyll, xanthophyll, and α-tocopherol levels in *zds1-1* and *crtiso1-1* mutants

	total cholorophyll (fmol/cell)	chlorophyll *a/b* ratio	α-tocopherol (fmol/cell)	total xanthophyll (fmol/cell)	lutein (fmol/cell)	zeaxanthin (fmol/cell)
Wild-type dark	0.8505 ± 0.2356	2.088 ± 0.029	0.0030 ± 0.0007	0.1973 ± 0.0542	0.0357 ± 0.0154	0.0028 ± 0.0007
Wild-type light	1.9264 ± 0.2427	2.108 ± 0.058	0.0061 ± 0.0020	0.4345 ± 0.0502	0.0964 ± 0.0145	0.0044 ± 0.0008
***zds1-1* dark**	0.0610± 0.0066	3.703 ± 0.226	0.0103 ± 0.0008	0.0019 ± 0.0004	0.0001 ± 0.0000	0.0008 ± 0.0001
***zds1-1* light**	0.3975 ± 0.0847	2.912 ± 0.067	0.0095 ± 0.0030	0.0298 ± 0.0048	0.0020 ± 0.0003	0.0093 ± 0.0010
***crtiso1-1* dark**	0.0728 ± 0.0112	1.518 ± 0.061	0.0088 ± 0.0013	0.0086 ± 0.0018	0.0004 ± 0.0001	0.0028 ± 0.0004
***crtiso1-1* light**	1.5222 ± 0.1285	2.409 ± 0.105	0.0067 ± 0.0003	0.3454 ± 0.0511	0.0364 ± 0.0063	0.0288 ± 0.0036

Pigment and α-tocopherol concentrations extracted from an equal number of cells for each replicate. Cells were grown for 2 days either in the dark or in the light (20 mol photons m^{-2} sec^{-1}). Averages and standard deviations are for 3 independent cultures.

Molecular genetic analysis of *zds1* mutants

Genetic analysis was carried out to determine if ζ-carotene accumulation and the pale yellow-green-in-the-dark color phenotype of *zds1* mutants were due to defects in ZDS activity. Crosses to wild-type produced tetrad progeny segregating 2:2 for the mutant phenotype (ζ-carotene accumulation, pale yellow-green-in-the-dark color) and wild-type phenotype (β-carotene accumulation, dark-green color) for each of the three ζ-carotene accumulating mutants (Table 3.3A). The 2:2 segregation pattern indicated that only one nuclear gene was responsible for the mutant phenotype of each *zds1* mutant. Zeocin resistance also displayed a 2:2 segregation pattern for the DNA insertional mutant *zds1-1*. When progeny from crosses of *zds1-1* and the wild-type strain 4ax5.2- were grown in the dark on TAP-agar plus zeocin, only pale yellow-green-in-the-dark mutants could grow on zeocin, whereas all dark green colonies died (Table 3.3A). The cosegregation of the yellow-green-in-the-dark color phenotype with zeocin resistance revealed that the pSP124S vector was closely linked to the mutant phenotype. Furthermore, reciprocal crosses of independently isolated ζ-carotene accumulating mutants to one another produced only pale yellow-green-in-the-dark progeny and no dark-green wild-type recombinants (Table 3.3B). This result showed that *zds1* mutants were alleles of the same gene.

Heterozygous diploids of *zds1-1*, *zds1-2*, and *zds1-3* were generated to determine dominance of the mutations The phenotype of each heterozygote diploid (*zds1-1/ZDS1*, *zds1-2/ZDS1*, and *zds1-3/ZDS1*) was dark green with no detectable ζ-carotene, demonstrating that the ζ-carotene accumulating mutations are recessive.

Crosses of *zds1-2* to the polymorphic wild-type strain, S1D2, showed that ζ-carotene accumulation and the pale yellow-green-in-the-dark color phenotype of cells were linked to the *ZDS1* gene (gene model C_440086 [25] or Joint Genome Institute (JGI) *Chlamydomonas reinhardtii* v4. Protein ID 182457). A CAPS marker located within the 3'UTR of the *ZDS1* locus cosegregated with the pale yellow-green-in-the-dark mutant phenotype (Figure 3.4). The CAPS marker consisted of a 566 bp amplified fragment containing a *BglI* site in S1D2 but not in the 137c genetic background. Restriction digests with *BglI* resulted in 332 bp and 234 bp fragments in S1D2 and a 566 bp fragment in the 137c background. All pale yellow-green-in-the-dark progeny from crosses of S1D2 to *zds1-2* produced one fragment (566 bp) when digested with *BglI*, whereas all dark-green progeny produced two fragments (332 bp and 234 bp) (Figure 3.4). This result showed that the pale yellow-green-in-the-dark phenotype is linked to the *ZDS1* locus and that a mutation in *ZDS1* is likely responsible for the pale yellow-green-in-the-dark and ζ-carotene accumulation in *zds1-2*.

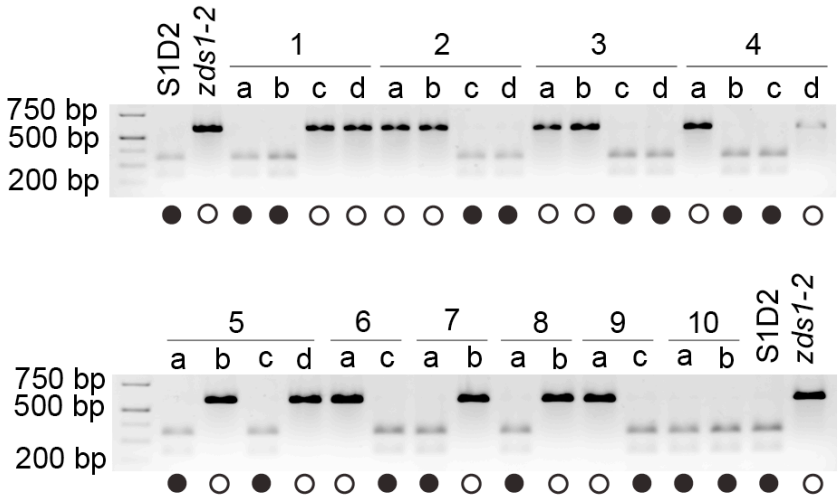

Figure 3.4. Genetic linkage analyses of *zds1* mutants
A marker located within the *ZDS1* locus cosegregated with the pale yellow-green, ζ-carotene accumulating mutant phenotype of *zds1-2*. Amplification and *BglI* digestion of a 566 bp fragment of the *ZDS1* gene containing the single nucleotide polymorphism in the 3'UTR was used to score progeny from crosses between *zds1-2* and polymorphic wild-type strain (S1D2). Five complete and five partial tetrads were scored: individual progeny within tetrads are labeled "a, b, c, d". Solid circles indicate dark green progeny with wild-type carotenoid composition while open circles indicate pale yellow-green progeny with ζ-carotene accumulation.

The *C. reinhardtii ZDS1* gene encodes a putative protein of 582 amino acids. The gene itself is on chromosome 7 and is predicted to be 6345 bp with 14 exons. Sequencing *ZDS1* from ζ-carotene-accumulating mutants uncovered a frameshift mutation in *zds1-3* and a nonsense mutation *zds1-2*. The *zds1-2* mutation consisted of cytosine being exchanged for a thymine in exon 6, resulting in the conversion of glutamine at amino acid position 200 into a stop codon (Figure 3.5). In *zds1-3* a "CA" insert into exon 5 shifted the open reading frame beginning with phenylalanine 164 (Figure 3.5).

A.

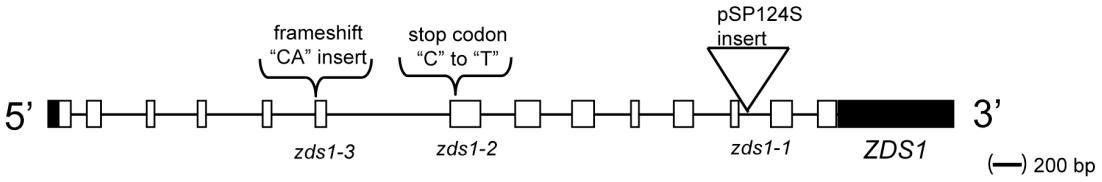

B.

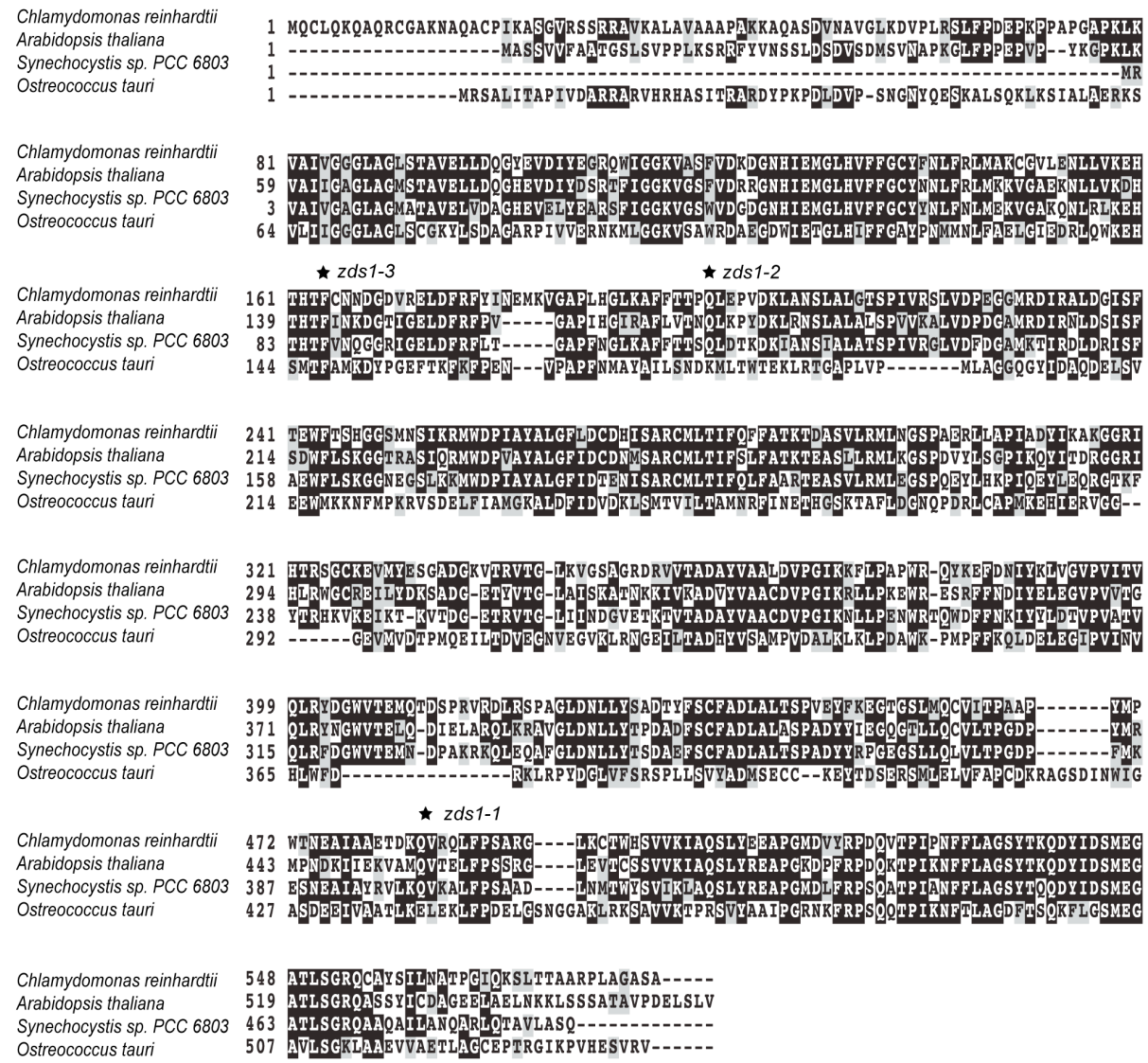

Figure 3.5. Mutations identified in *zds1* mutants.
A). Schematic of the *ZDS1* gene in *Chlamydomonas*. UTRs are indicated by solid boxes, exons by open boxes and introns by lines. The brace highlights the specific molecular changes in *zds1-2* and *zds1-3*. The triangle depicts location of mutagenizing vector in *zds1-1*.
B). Multiple sequence alignment of ZDS1 protein sequences.

Alignment of ZDS amino acid sequences from eukaryotic algae, *Chlamydomonas* (JGI protein ID 182457) and *Ostreococcus* (JGI protein ID 21852); a plant, *Arabidopsis* (GenBank ID Q38893)*;* and a cyanobacterium, *Synechocystis sp.* PCC6803 (GenBank ID P74306). Conserved residues were scored using Blosum 62 matrix, with darker shading indicating higher conservation and no shading indicating low or no conservation. Asterisks mark position of mutations in *zds1* alleles.

Because zeocin resistance cosegregated with the ζ-carotene accumulating mutant phenotype of *zds1-1*, the mutation was tagged by the plasmid pSP124S. *C. reinhardtii* genomic sequences flanking the pSP124S insert were recovered using TAIL-PCR [16]; resulting in the identification of the insertion site as the *ZDS1* locus. DNA gel blot analysis confirmed this result. Restriction digestion with *NcoI* cuts within the *ZDS1* locus twice. This resulted in three fragments of sizes 1450 bp, 3995 bp, and 3483 bp containing *ZDS1* sequences from wild-type cells. pSP124S had only one *NcoI* restriction site. The pSP124S specific DNA hybridization probe consisted of the entire *ble* gene (968 bp), which was excised from the pSP124S plasmid using *XbaI* and *BamHI*. Two *ZDS1* specific DNA hybridization probes were made: Zds probe F1-R1 (1114 bp) was specific to the 1450 bp fragment which contained 25% of the *ZDS1* gene sequences and Zds probe F3-R3 (1223 bp) specific to the 3995 bp fragment which contained 60% of the *ZDS1* gene sequences. No probes were tested against the 3483 bp *ZDS1 NcoI* fragment as it contained only 900 bp of the *ZDS1* sequence. During DNA gel blot analyses, the probe specific to the *ble* gene did not hybridize to any DNA fragment from wild-type cells but it did hybridize to a 6 kb DNA fragment from *zds1-1* cells (Figure 3.6B). Because one band was detected by the *ble* probe, the *ble* insertion locus did not disrupt multiple loci in the *zds1-1* mutant. DNA gel blot analysis using the Zds F1-R1 probe did not show any difference in DNA hybridization patterns between wild-type and *zds1-1* cells (data not shown). When Zds F3-R3 probe was used, there was a clear difference in DNA hybridization patterns in wild-type cells compared to *zds1-1* cells. Zds F3-R3 probe hybridized to a ~4 kb fragment in wild-type cells, which is consistent with the 3995 bp *ZDS1* fragment, and a 6 kb fragment in *zds1-1* cells, which is the same fragment size that hybridized to the *ble* gene probe (Figure 3.6B). DNA gel-blot analysis showed that the *zds1-1* mutation could be tagged by the pSP124S plasmid.

To confirm the DNA gel blot analysis and to identify the precise location of the pSP124S insert in the *ZDS1* gene, PCR analysis was performed. *ZDS1* specific primers, ZdsF17 and ZdsR17, were able to amplify a 733 bp fragment from wild-type cells but not from *zds1-1* cells (Figure 3.6A). When either ZdsF17 or ZdsR17 were paired with vector specific primers, RMD230 or RMD223L, DNA fragments were amplified from *zds1-1* but no fragments were amplified from wild-type cells. ZdsF17 paired with RMD 223L amplified a 1400 bp product from *zds1-1* while ZdsR17 paired with RMD230 produced a fragment size of about 750 bp (Figure 3.6A). Sequencing of the region spanned by ZdsF17 and ZdsR17 in *zds1-1* mutants found that entire pSP124S plasmid had inserted into the intron between exons 12 and 13; no deletion of the *ZDS1* accompanied the insertion of pSP124S.

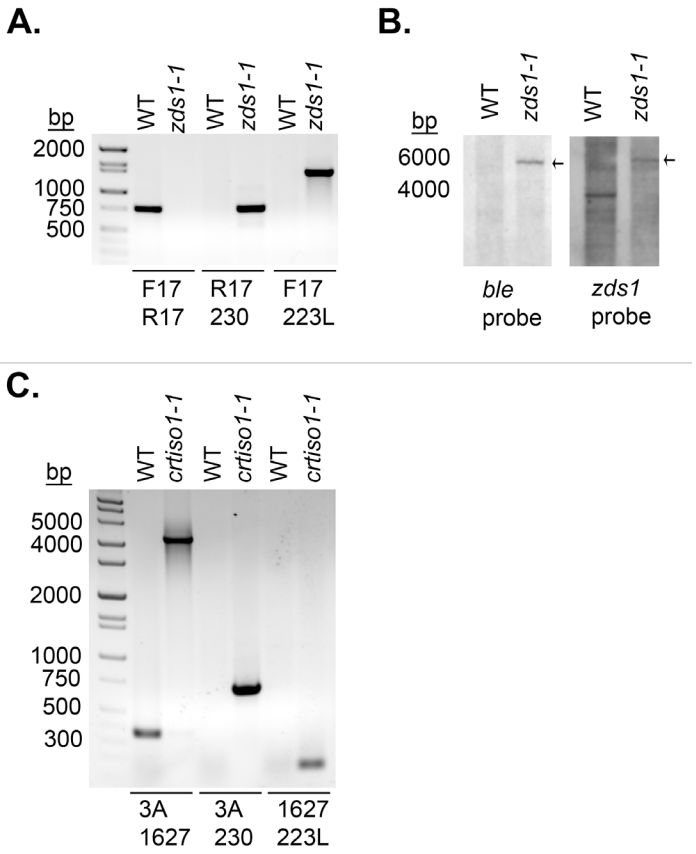

Figure 3.6. Molecular analysis of *zds1-1* and *crtiso1-1* DNA insertional mutants.
A). Genomic DNA amplification in wild-type (WT) and no amplication in *zds1-1* with *ZDS1* specific primers F17 (ZdsF17) and R17 (ZdsR17). No amplification in WT and amplification in *zds1-1* with vector-specific primers 230 (RMD230) and 223L (RMD223L).
B). DNA gel blot of *zds1-1* and wild-type (WT) genomic DNA digested with *NcoI*. The *ble* probe was a *XbaI/BamHI* fragment from pSP124S and the *ZDS1* probe was amplified from wild-type genomic DNA using primers ZdsF3 and ZdsR3. On the same DNA blot, the *ble* probe and the *ZDS1* probe hybridization to a 6kb fragment in *zds1-1* mutants while from wild-type DNA the *ZDS1* probe hybridized to a 4 kb fragment and no fragments using the *ble* probe.
C). Genomic DNA amplification in wild-type (WT) and no amplication in *crtiso1-1* with CRTISO*1* specific primers 3A (Crtiso3A) and 1627 (Crtiso1627R). No amplification in WT and amplification in *crtiso1-1* with vector-specific primers 230 (RMD230) and 223L (RMD223L).

C. reinhardtii mutants that accumulate ζ-carotenes in the dark were previously characterized by Nikulina *et al.* in 1999 [26]. Nikulina *et al.* reported that the ζ-carotene accumulating mutants, called *ac5* mutants, were pale-green in the light and yellow-white in the dark, and accumulated high ζ-carotenes levels along with low levels of β-carotenes and other colored carotenoids. When *ac5* strains (CC-1677 and CC-517) were obtained from the Chlamy Center, the strains had lost their yellow-white-in-the-dark phenotype. Both strains CC-1677 and CC-517 had gained the wild-type color phenotype—dark green in the light and in the dark.

Backcrosses to wild-type strains 4A+ and 4ax5.2- were carried out with both *ac5* strains. Crosses with CC-1677 produced very few zygospores and after many attempts only 5 progeny, from incomplete tetrads, were isolated. The 5 progeny were all medium to dark green except one, which was yellow (data not shown). HPLC analysis showed wild-type carotenoid composition for the dark and medium green progeny and an abnormal carotenoid composition for yellow progeny. The yellow progeny accumulated more than one type of carotenoid in the retention time characteristic of β-carotenes and ζ-carotenes. Typically, most carotenoids have spectra with 3 more-or-less distinct peaks or shoulders. The peak obtained from the yellow progeny had 5 shoulders suggesting that the spectra of more than one carotenoid had been combined (data not shown). Because no distinct ζ-carotene peaks could be detected and because many attempts at crossing the yellow progeny back to wild-type have failed, experiments to determine if CC-1677 is allelic to any of the *zds1* mutants were not conducted.

Similar to CC-1677, isolation of ζ-carotene accumulating progeny from CC-517 were unsuccessful. Unlike CC-1677, CC-517 in crosses to 4A+ produced many viable progeny—producing tetrads that contained both light green and dark green progeny. HPLC analysis of the resulting progeny showed that both dark and light green colored progenies had wild-type carotenoid composition with normal levels of chlorophylls for dark green progeny and reduced levels in light green progeny (data not shown). However, further crosses with light green CC-517 progeny to wild-type 4A+ did not produce any progeny that accumulated ζ-carotenes.

Molecular genetic analysis of *crtiso1* mutants

As with *zds1* mutants, genetic analyses showed that the *crtiso1-1*, *crtiso1-2*, and *crtiso1-3* mutant phenotypes were due to a single nuclear gene and that the three mutants were alleles of a single gene. Tetrad analyses showed that the *crtiso1* mutant phenotypes, prolycopene accumulation and yellow-in-the-dark color, cosegregated 2:2 in progeny from crosses with wild-type (Table 3A). Reciprocal crosses to other yellow-in-the-dark and prolycopene accumulating mutants did not yield any recombinant dark green wild-type progeny—demonstrating allelism of the *crtiso1* mutants (Table 3.3B). For the DNA insertional mutant, *crtiso1-1*, zeocin resistance also cosegregated with the yellow-in-the-dark and prolycopene accumulating mutant phenotype, which indicated that the pSP124S vector tagged the *crtiso1-1* mutation. Dominance tests were not carried out for *crtiso1* mutants.

Genetic linkage analysis showed that the *crtiso1* mutant phenotype cosegregated with a CAPS marker located with in the *C. reinhardtii CRTISO1* gene (gene model C_1180035 [25] or JGI *Chlamydomonas reinhardtii* v4. protein ID 196597). The *CRTISO1* CAPS marker consisted of a 195 bp amplification product that has a *BssHII* restriction site in the 137c genetic background but not in the S1D2 genetic background. Restriction digests of the 195 bp amplification product with *BssHII* from the 137c background produced two fragments with sizes of 77 bp and 119 bp and only one product from S1D2. Linkage analysis showed that the yellow-in-the-dark mutant phenotype was linked to the *CRTISO1* marker: all yellow-in-the-dark progeny carried the *BssHII* restriction site, producing two fragments while all dark-green progeny did not carry the *BssHII* restriction site (data not shown).

The *C. reinhardtii CRTISO1* gene is 6138 bp and has 15 exons. It is located on chromosome 16 and encodes for a putative protein with 568 amino acids. *Chlamydomonas* CRTISO1 shows high identity to *Arabidopsis* and *Synechocystis* sp. PCC6803 CRTISO1 proteins (Figure 6B). Sequencing of *CRTISO1* from *crtiso1-2*, and *crtiso1-3* uncovered

molecular changes in both mutants compared to wild-type cells. The molecular basis of the *crtiso1-2* mutant phenotype consisted of a 9 bp deletion in exon 8, resulting in the deletion of highly conserved amino acids valine, glycine, and arginine at positions 298 to 300 (Figure 3.7). In *crtiso1-3* the mutant phenotype was due to removal of the 3' splice site of the intron between exon 6 and exon 7 when a guanine was changed to adenine (Figure 3.7A).

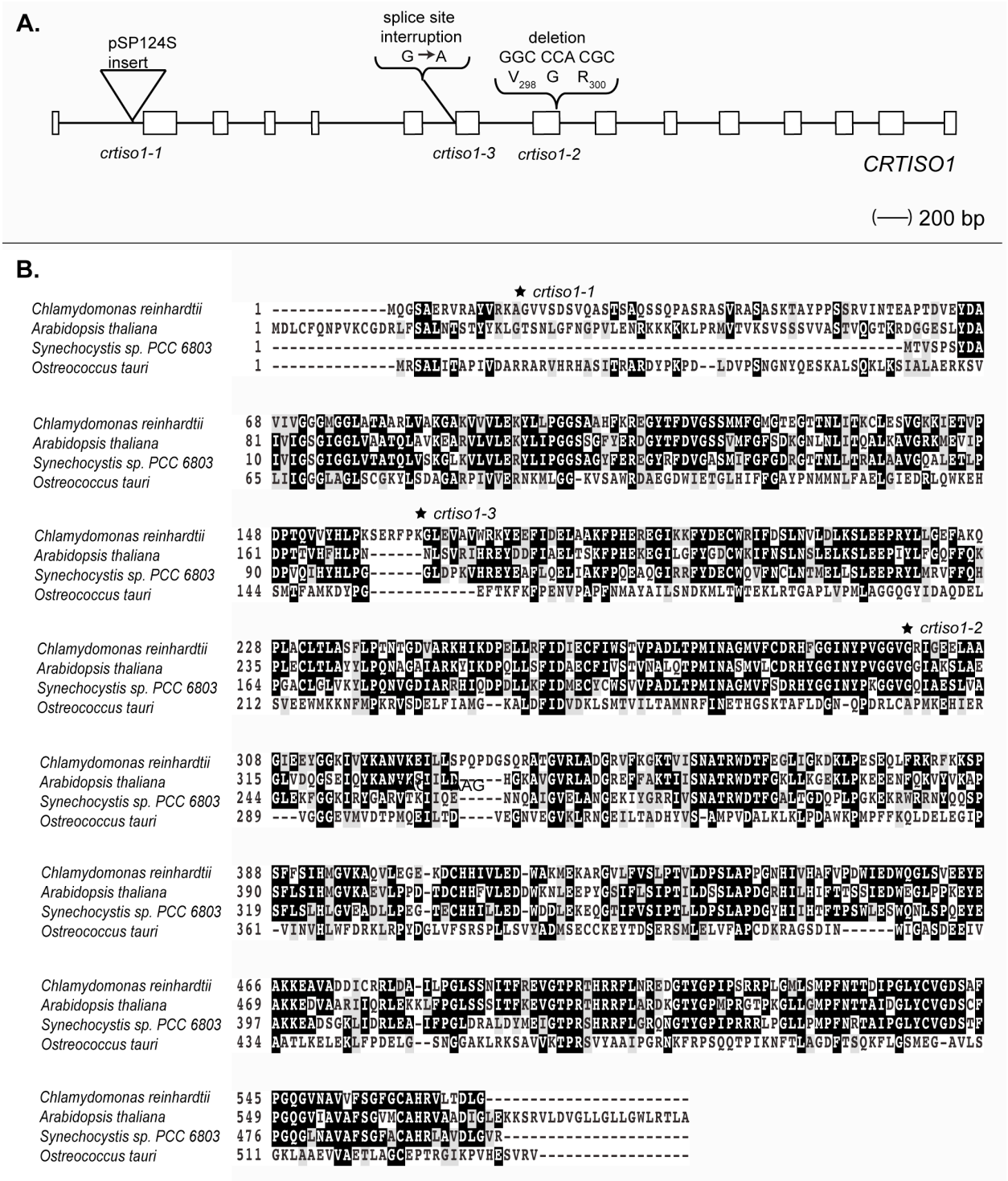

Figure 3.7. Mutations identified in *crtiso1* mutants

A). Schematic of the *CRTISO1* gene in *Chlamydomonas*. Exons are indicated by open boxes and four introns by lines. The brace highlights the specific molecular changes in *crtiso1-2* and crtiso*1-3*. Subscript numbers note position of the amino acid residue in the wild-type CRTISO1 protein. The triangle depicts location of mutagenizing vector in *crtios1-1*.
B). Multiple sequence alignment of CRTISO1 protein sequences.
Alignment of CRTISO amino acid sequences from eukaryotic algae, *Chlamydomonas* (JGI protein ID 196597) and *Ostreococcus* (JGI protein ID 21852); a plant, *Arabidopsis* (GenBank ID NP_172167.2)*;* and a cyanobacterium, *Synechocystis sp.* PCC6803 (GenBank ID BAA10798.1). Conserved residues were scored using Blosum 62 matrix, with darker shading indicating higher conservation and no shading low or no conservation. Asterisks mark position of mutations in *crtiso1* alleles.

Dent *et al.* reported the presence of two *ble* insertions in the *CRTISO1* locus in the *crtiso1-1* mutant [16]. The insertion occurred in the intron between the first and second exons and was not accompanied by any deletion of the *CRTISO1* gene. Amplification of the region flanking the insertion site using *CRTISO1* specific primers produced a 347 bp fragment in wild-type cells and an approximately 4200 bp fragment in *crtiso1-1* mutant (Figure 3.6C). The presence of the pSP124S vector was further confirmed when vector-specific primers were paired with *CRTISO1* flanking sequence primers. Vector-specific primers RMD230 and RMD223L amplified fragments approximately 650 bps and 100 bps when paired with Crtiso3A and Crtiso1627R, respectively, from *crtiso1-1* but no amplification products from wild-type genomic DNA (Figure 3.6C).

Table 3.3. Genetic analyses of *crtiso1* and *zds1* mutants.

A. Tetrad analysis of *zds1* and *crtiso1* mutants crossed to wild-type (4ax5.2 or 4A+)

	Total Progeny	WT progeny	Mutant progeny	Mutant progeny recombinant for zeocin marker
zds1-1 (*mt+)* x WT (*mt-*)	27	14	13	0
zds1-2 (*mt+*) x WT (*mt-*)	48	24	24	N/A
zds1-3 (*mt+*) x WT (*mt-*)	46	22	24	N/A
crtiso1-1 (*mt-*) x WT (*mt+*)	60	29	31	0
crtiso1-2 (*mt+*) x WT (*mt-*)	77	38	39	N/A
crtiso1-3 (*mt+*) x WT (*mt-*)	55	26	29	N/A

B. Reciprocal crosses of *zds1* and *crtiso1* mutants to demonstrate allelism

	Total Progeny	WT recombinant progeny (dark-green phenotype)	Nonrecombinant progeny (pale yellow green or yellow color)
zds1-1 (*mt+)* x *zds1-2* (*mt-*)	39	0	39
zds1-2 (*mt+*) x *zds1-3* (*mt-*)	55	0	55
zds1-3 (*mt+*) x *zds1-1* (*mt-*)	41	0	41
crtiso1-1 (mt-) x *crtiso1-2* (mt+)	37	0	37
crtiso1-2 (mt+) x *crtiso1-3* (mt-)	20	0	20

WT = wild-type.

DISCUSSION

In this study, *C. reinhardtii* mutants that accumulated *cis* carotenes, ζ-carotene and prolycopene, were isolated and found to be genetically linked to the *ZDS1* and *CRTISO1* genes, respectively. Lesions were identified in three alleles each for the *ZDS1* and *CRTISO1* loci. The *zds1-2* and *zds1-3* mutations result in reading frame shifts and introduction of premature stop codons in the first third of the putative ZDS protein, whereas *zds1-1* has a large vector insert in an intron near the 3'UTR. The three alleles in *ZDS1* resulted in very similar carotenoid profiles in the dark and in the light; consequently, the *zds1-1*, *zds1-2*, and *zds1-3* alleles are most likely null mutations. By the same reasoning, *crtiso1-1*, *crtiso1-2*, and *crtiso1-3* alleles are probably null mutations. The *CRTISO1* gene in c*rtiso1-1* was interrupted by an insert in the first intron, and *crtiso1-3* has a splice site eliminated in the first quarter of the gene. The *crtiso1-2* allele results in deletion of three codons in a highly conserved region of the predicted CRTISO1 polypeptide. Because *crtiso1-2* accumulated similar levels of carotenoids in the dark as *crtiso1-1* and *crtiso1-3*, it was deemed to have a complete block in CRTISO1 activity in the dark even though mutants were slightly greener in color than the deep yellow of *crtiso1-1* and *crtiso1-2*. This greener color in the dark is due to higher levels of chlorophylls found in the cell. Surprisingly, all six *zds1* and *crtiso1* mutants continued to synthesize very low levels of cyclic carotenes and xanthophylls in the dark, suggesting the possibility of another carotene desaturase pathway in *C. reinhardtii* that can partially bypass ZDS1 and CRTISO1.

C. reinhardtii ZDS1 protein is highly similar to plant-type ZDS proteins. Amino acid sequence identity between *C. reinhardtii* ZDS1 is 61% to *Arabidopsis thaliana* ZDS and 59% to *Synechocystis* PCC6803 CrtQ. This protein similarity to plant-type ZDS enzymes is also reflected functionally in *zds* mutants of different species. *C. reinhardtii zds1* mutants had a pale yellow-green-in-the-dark phenotype that could turn a light-green in very low light. Maize [27], *Arabidopsis* [28], and sunflower [29] plants with defects in ZDS activity produced white to yellow cotyledons or leaves that in dim light and/or in later developmental stages would turn a very light green. ζ-carotenes and no xanthophylls were accumulated in etiolated or yellow tissues from these plants [29,30]. Unlike plant *zds* mutants, *C. reinhardtii zds1* mutants under light conditions had significant increases in chlorophyll and xanthophyll, as well as ζ-carotenes levels. Wild-type *C. reinhardtii* cells also exhibited increases in carotenoid levels when grown in the light, which shows that carotenogenesis in *C. reinhardtii* is promoted by light.

Two isomers of ζ-carotenes (9,15,9'-*tricis*-ζ-carotene and 9,9'-*dicis*-ζ-carotene) were detected in *C. reinhardtii zds1* mutants in the light and in the dark. *In vitro* and *in vivo* experiments have demonstrated that plant-type ZDS has stereoselectivity for the 9,9-dicis-ζ-carotene and not for 9,15,9'-*tricis*-ζ-carotene because of the *cis*-configuration of the central C-15 double bond [5,11,13]. Light or a carotene isomerase, Z-ISO, could promote isomerization of the product of plant-type PDS, 9,15,9'-*tricis*-ζ-carotene, to 9,9'-*dicis*-ζ-carotene [5,30,31]. In dark- and light-grown *C. reinhardtii zds1* mutants, 9,9'-*dicis*-ζ-carotene was the major carotene found in cells with much lower levels of 9,15,9'-*tricis*-ζ-carotene, suggesting the existence Z-ISO activity. A *C. reinhardtii* homolog (JGI protein ID 293635) of Z-ISO was identified using the *A. thaliana* Z-ISO [13] protein sequence as a query in BLAST searches. However, genetic linkage analysis and the accumulation of 9,9'-*dicis*-ζ-carotene as the primary carotene in the dark indicate that none of the *zds1* mutants has primary defects in Z-ISO activity. Other ζ-carotene accumulating mutants have been isolated in *C. reinhardtii,* in addition to the three reported here, but none have 9,15,9'-*tricis*-ζ-carotene as the primary carotene in the dark.

Because light can compensate for lack of Z-ISO activity, a hypothetical *C. reinhardtii z-iso* mutant should have the predicted phenotypes of yellow colored colonies with 9,15,9'-*tricis*-ζ-carotene accumulation only in the dark and green-in-the-light colonies with wild-type carotenoids, similar to *crtiso1* mutant phenotypes. However, no such mutants were found in my screens for ζ-carotene-accumulating mutants.

Light-induced "greening" of *crtiso1* mutants and photoisomerization of prolycopene

Dark-grown *crtiso1* mutants primarily accumulate prolycopene and trace amounts of xanthophylls. With light growth, xanthophylls and cyclic carotenes accumulated to almost wild-type levels and prolycopene was no longer detected. This same phenotype was observed in another green alga *Scenedesmus obliquus* C-6D, also with defects in CRTISO/CrtH activity [6]. The dark-grown *S. obliquus* C-6D accumulated prolycopene and acyclic carotenes 9,9'-*dicis*-ζ-carotenes, phytofluene, 9,15,9'-*tricis*-ζ-carotene, and cis-neurosporenes [6,11,12]. In the light, the mutant phenotype of *S. obliquus* C-6D was reversed and wild-type cyclic carotenes and xanthophylls were synthesized [6]. ζ-carotene-accumulation in *S. obliquus* C-6D was reminiscent of ζ-carotene accumulation in *zds1* mutants with 9,9'-*dicis*-ζ-carotenes as the dominating carotene accumulated (44% of total carotenoids) accompanied by lower levels of 9,15,9'-*tricis*-ζ-carotene (12%), prolycopene (10%), and other *cis*-carotenes [6]. Arabidopsis *ccr2* [8], rice *zebra2* [14], and tomato *tangerine* [4,7] mutants all have disrupted CRTISO activity and like *C. reinhardtii crtiso1* mutants accumulate prolycopene as the dominant caroteneoid in the dark. Light also has a "greening" effect on plant *crtiso* mutants: yellow to orange-colored seedlings and newly formed leaves turn green and accumulate chlorophyll in the light, though at a delayed rate compared to wild-type plants [7,8,14]. In the light, plant *crtiso* mutants accumulated xanthophylls and cyclic carotenoids and prolycopene was undetectable [7,8,14].

Carotenoid biosynthesis mutants that accumulate 9,15,9'-tricis-ζ-carotenes [13] or prolycopene (7,9,7'9'-tetracis-lycopene) in the dark can bypass blocks in the *cis*-carotene desaturation pathway if grown in the light. In vitro experiments with extracts of ζ-cartoene substrates and *E. coli* functional complementation systems expressing PDS, which produces the 9,15,9'-tricis-ζ-carotene, showed that the isomer 9,15,9'-*tricis*-ζ-carotene is very efficiently isomerized to 9,9-*dicis*-carotene in the light [5,11,13,31]. Prolycopene, in contrast, seems to be less efficiently photoisomerized. In an *E. coli* functional complementation system expressing genes for *A. thaliana* PDS and ZDS, dark-cultured cells accumulated mainly 9,15,9'-*tricis*-ζ-carotenes and lower amounts of other *cis*-carotenes such as prolycopene, 9,9-*dicis*-ζ-carotenes, and 7,9,9'-*cis*-neurosporenes. When the *E. coli* cells expressing PDS and ZDS were grown in the light, prolycopene was the main carotene detected with very little all-*trans*-lycopene in the mixture. Light was shown to convert the prolycopene substrate itself to all-*trans*-lycopene plus numerous *cis*-isomers of lycopene over several hours of light exposure [32]. In the same study, *cis*-isomers of lycopene treated with iodine and light were transformed into all-*trans*-lycopene. Prolycopene accumulated in *crtiso* mutants of plants and algae can be efficiently photoisomerized to all-*trans*-lycopene. Experiments with a *Synechocystis* PCC6803 *crtH* mutant showed that 20 minutes of light was enough to convert significant levels of *cis*-carotenes to all-*trans*-lycopene [9]. Efficient photoisomerization of prolycopene to all-trans-lycopene may require a photosynthetic cell [33]. Issacson *et al.* [7] observed that the outer pericarp of green

fruit from the tomato tangerine mutant accumulated wild-type carotenoids while orange-colored inner pericarp and placental tissues accumulated prolycopene.

Photo-oxidation

C. reinhardtii or plant mutants lacking ZDS activity exhibit more severe phenotypes than mutants with defects in CRTISO activity. *C. reinhardtii zds1* mutants formed light green colonies under very low light but at higher light intensities bleached and died, whereas *crtiso1* mutants could form dark green colonies even under high light intensities. Plants with mutations that completely block ZDS activity are seedling lethal and albino [27,28,29] while plants with blocks in CRTISO activity are fully viable [7,8,14]. In photosynthetic cells, light can rescue the *crtiso/crtH* mutant phenotype by allowing the formation of all-*trans*-lycopene, which is the substrate for α- and β-carotene and xanthophyll production. In plant *zds* mutants, ζ-carotene desaturation cannot be completed and photoprotective xanthophylls do not form. *C. reinhardtii zds1* mutants, however, were viable in vLL conditions possibly due to an unknown carotene desaturase operating in the cell that permits the formation of low levels of cyclic carotenes and xanthophylls.

Reduced levels of photoprotective carotenoids in photosynthetically active cells frequently lead to insufficient dissipation of excess light energy which in turn often results in photo-oxidative damage to the cells. Xanthophylls have multiple photoprotective roles. They can dissipate excess light energy as heat by de-exciting singlet excited chlorophyll (^{1}Chl*) in a process often referred to as non-photochemical quenching of Chl fluorescence (NPQ) [34]. Xanthophylls also act as quenchers of triplet excited chlorophylls (^{3}Chl*) and singlet oxygen ($^1O_2$*) and have roles in preventing lipid peroxidation [34]. Arabidopsis *ccr2*, tomato *tangerine*, and rice *zebra2* mutants all accumulated much less lutein than wild-type plants while xanthophyll cycle carotenoids zeaxanthin, antheraxanthin, and violaxanthin increased to at least wild-type levels or higher [7,8,14]. Quantification of lutein and xanthophyll levels in *C. reinhardtii zds1-1* and *crtiso1-1* mutants revealed a similar pattern to plant *crtiso* mutants. The *zds1* mutants had extremely reduced levels of lutein in the dark and light, whereas lutein levels in *crtiso1* mutants were very low in the dark but only slightly reduced in the light. The extent of photo-oxidative bleaching visible in light-cultured *C. reinhardtii* colonies follows this pattern of lutein accumulation; in LL *zds1* colonies almost completely bleach except for areas of higher cells density where cells can shade each other while *crtiso1* mutants are very green and exhibit bleaching only under HL conditions. Chai *et al.* attributed the striping phenotype (green and white variegated leaves) of *zebra2* mutants to highly reduced levels of lutein observed in the mutant plants grown in the light [14]. While lutein levels were very low in *zds1* and *crtiso1* mutants, zeaxanthin levels in light-grown cells were accumulated in higher levels than wild-type cells. Studies of *A. thaliana* and *C. reinhardtii* mutants that did not accumulate zeaxanthin or lutein or both demonstrated that lutein and zeaxanthin had complementary photoprotective roles [35,36]. An *A. thaliana* mutant lacking zeaxanthin but with higher than wild-type levels of lutein displayed higher NPQ than mutants lacking zeaxanthin only [37]. Additionally, α-tocopherol, a scavenger of reactive oxygen species was increased in *zds1* and *crtiso1* mutants.

Characterization of *pds1* (Chapter 2), *zds1*, and *crtiso1* mutants clearly demonstrate that the plant-type poly-*cis*-carotene desaturation pathway is responsible for the majority of carotenoid biosynthesis in *C. reinhardtii.* However, the accumulation of low levels of xanthophylls in all three *zds1* mutants and all three *crtiso1* mutants suggest that an alternative carotene desaturation pathway is active in dark-grown cells and may be photo-activated.

REFERENCES

1. Misawa N, Nakagawa M, Kobayashi K, Yamano S, Izawa Y, et al. (1990) Elucidation of the *Erwinia uredovora* carotenoid biosynthetic pathway by functional analysis of gene products expressed in *Escherichia coli*. Journal of Bacteriology 172: 6704-6712.
2. Sandmann G (1994) Carotenoid biosynthesis in microorganisms and plants. European Journal of Biochemistry 223: 7-24.
3. Sandmann G (2009) Evolution of carotene desaturation: the complication of a simple pathway. Archives of Biochemistry and Biophysics 483: 169-174.
4. Clough JM, Pattenden G (1983) Stereochemical assignment of prolycopene and other poly-Z-isomeric carotenoids in fruits of the tangerine tomato *Lycopersicon esculentum* var. 'Tangella'. Journal of the Chemical Society, Perkin Transactions 1: 3011-3018.
5. Bartley GE, Scolnik PA, Beyer P (1999) Two *Arabidopsis thaliana* carotene desaturases, phytoene desaturase and & z-carotene desaturase, expressed in *Escherichia coli,* catalyze a poly-*cis* pathway to yield pro-lycopene. European Journal of Biochemistry 259: 396-403.
6. Ernst S, Sandmann G (1988) Poly-*cis* carotene pathway in the *Scenedesmus* mutant C-6D. Archives of Microbiology 150: 590-594.
7. Isaacson T, Ronen G, Zamir D, Hirschberg J (2002) Cloning of *tangerine* from tomato reveals a carotenoid isomerase essential for the production of β-carotene and xanthophylls in plants. Plant Cell 14: 333-342.
8. Park H, Kreunen SS, Cuttriss AJ, DellaPenna D, Pogson BJ (2002) Identification of the carotenoid isomerase provides insight into carotenoid biosynthesis, prolamellar body formation, and photomorphogenesis. Plant Cell 14: 321-332.
9. Masamoto K, Wada H, Kaneko T, Takaichi S (2001) Identification of a gene required for cis-to-trans carotene isomerization in carotenogenesis of the cyanobacterium *Synechocystis sp.* PCC 6803. Plant and Cell Physiology 42: 1398-1402.
10. Li Q, Farre G, Naqvi S, Breitenbach J, Sanahuja G, et al. (2010) Cloning and functional characterization of the maize carotenoid isomerase and β-carotene hydroxylase genes and their regulation during endosperm maturation. Transgenic Research 19: 1053-1068.
11. Breitenbach J, Sandmann G (2005) ζ-Carotene cis isomers as products and substrates in the plant poly-cis carotenoid biosynthetic pathway to lycopene. Planta 220: 785-793.
12. Sandmann G (1991) Light-dependent switch from formation of poly-cis carotenes to all-trans carotenoids in the *Scenedesmus mutant* C-6D. Archives of Microbiology 155: 229-233.
13. Chen Y, Li F, Wurtzel ET (2010) Isolation and characterization of the *Z-ISO* gene encoding a missing component of carotenoid biosynthesis in plants. Plant Physiology 153: 66-79.
14. Chai C, Fang J, Liu Y, Tong H, Gong Y, et al. (2011) *ZEBRA2*, encoding a carotenoid isomerase, is involved in photoprotection in rice. Plant Molecular Biology 75: 211-221.
15. McCarthy SS, Kobayashi MC, Niyogi KK (2004) White mutants of *Chlamydomonas reinhardtii* are defective in phytoene synthase. Genetics 168: 1249-1257.
16. Dent RM, Haglund CM, Chin BL, Kobayashi MC, Niyogi KK (2005) Functional Genomics of Eukaryotic Photosynthesis Using Insertional Mutagenesis of Chlamydomonas reinhardtii. Plant Physiology 137: 545-556.
17. Gross CH, Ranum LPW, Lefebvre PA (1988) Extensive restriction fragment length polymorphisms in a new isolate of Chlamydomonas reinhardtii. Current Genetics 13: 503-508.

18. Harris EH (1989) The *Chlamydomonas* Sourcebook: A Comprehensive Guide to Biology and Labortory Use: Academic Press, San Diego.
19. Lumbreras V, Stevens DR, Purton S (1998) Efficient foreign gene expression in *Chlamydomonas reinhardtii* mediated by an endogenous intron. Plant Journal 14: 441-447.
20. Werner R, Mergenhagen D (1998) Mating type determination of *Chlamydomonas reinhardtii* by PCR. Plant Molecular Biology Reporter 16: 295-299.
21. Liu Y-G, Mitsukawa N, Oosumi T, Whittier RF (1995) Efficient isolation and mapping of *Arabidopsis thaliana* T-DNA insert junctions by thermal asymmetric interlaced PCR. Plant Journal 8: 457-463.
22. Sambrook J, Fritsch EF, Maniatis T (1989) Molecular Cloning: a laboratory manual. Cold Spring Harbor: Cold Springs Harbor Press.
23. Thompson JD, Higgins DG, Gibson T (1994) CLUSTAL W: improving the sensitivity of progressive multiple sequence alignmet through sequence weighting position-specific gap penalties and weight matric choice. Nucleic Acids Research 22: 4673-4680.
24. Isaacson T, Ohad I, Beyer P, Hirschberg J (2004) Analysis in vitro of the enzyme CRTISO establishes a poly-cis-carotenoid biosynthesis pathway in plants. Plant Physiology 136: 4246-4255.
25. Lohr M, Im C-S, Grossman AR (2005) Genome-Based Examination of Chlorophyll and Carotenoid Biosynthesis in *Chlamydomonas reinhardtii*. Plant Physiology 138: 490-515.
26. Nikulina K, Chunaev AS, Boschetti A (1999) Accumulation of ζ-carotene in Chlamydomonas reinhardtii under control of the *ac5* nuclear gene. Plant Cell Reports 19: 37-42.
27. Matthews PD, Luo R, Wurtzel ET (2003) Maize phytoene desaturase and {zeta}-carotene desaturase catalyse a poly-Z desaturation pathway: implications for genetic engineering of carotenoid content among cereal crops. Journal of Experimental Botany 54: 2215-2230.
28. Dong H, Deng Y, Mu J, Lu Q, Wang Y, et al. (2007) The *Arabidopsis Spontaneous Cell Death1* gene, encoding a [zeta]-carotene desaturase essential for carotenoid biosynthesis, is involved in chloroplast development, photoprotection and retrograde signalling. Cell Research 17: 458-470.
29. Conti A, Pancaldi S, Fambrini M, Michelotti V, Bonora A, et al. (2004) A deficiency at the gene coding for ζ-carotene desaturase characterizes the sunflower *non dormant-1* mutant. Plant Cell Physiology 45: 445-455.
30. Li F, Murillo C, Wurtzel ET (2007) Maize *Y9* encodes a product essential for 15-cis-{zeta}-carotene isomerization. Plant Physiology 144: 1181-1189.
31. Beyer P, Mayer M, Kleinig H (1989) Molecular oxygen and the state of geometric isomerism of intermediates are essential in the carotene desaturation and cyclization reactions in daffodil chromoplasts. European Journal of Biochemistry 184: 141-150.
32. Magoon EF, Zechmeister L (1957) Stepwise stereoisomerization of prolycopene, a poly*cis* carotenoid, to all-*trans*-lycopene. Archives of Biochemistry and Biophysics 69: 535-547.
33. Giuliano G, Giliberto L, Rosati C (2002) Carotenoid isomerase: a tale of light and isomers. Trends in Plant Science 7: 427-429.
34. Niyogi KK (1999) Photoprotection revisited: genetic and molecular approaches. Annual Review of Plant Physiology and Plant Molecular Biology 50: 333-359.

35. Niyogi KK, Björkman O, Grossman AR (1997) The roles of specific xanthophylls in photoprotection. Proceedings of the National Academy of Sciences 94: 14162-14167.
36. Niyogi KK, Grossman AR, Bj√∂rkman O (1998) *Arabidopsis* mutants define a central role for the xanthophyll cycle in the regulation of photosynthetic energy conversion. Plant Cell 10: 1121-1134.
37. Li Z, Ahn TK, Avenson TJ, Ballottari M, Cruz JA, et al. (2009) Lutein accumulation in the absence of zeaxanthin restores nonphotochemical quenching in the *Arabidopsis thaliana npq1* mutant. Plant Cell 21: 1798-1812.

CHAPTER 4

A mutant that improves the greening phenotype of *zds1* identifies a light-induced, CRTISO-like protein as a possible second ζ-carotene desaturase in *Chlamydomonas reinhardtii*

SUMMARY

Null mutants affecting the plant-type ζ-carotene desaturase gene, *ZDS1,* in *Chlamydomonas reinhardtii* are able to synthesize low levels of downstream colored carotenoids in the dark. Even higher levels of cyclic carotenes and xanthophyll accumulate in *zds1* in the light, and partial greening of the cells occurs. This implies the occurrence of a putative second ζ-carotene desaturase, ZDS2, that can bypass the lack of ZDS1 and convert ζ-carotene to lycopene. Cycloheximide treatment of *zds1* in the dark and light did not block formation of downstream cyclic carotenes, suggesting that expression of ZDS2 in dark-grown *zds1* cells is sufficient. Because carotenoid isomerase (CRTISO) is evolutionarily related to bacterial CrtI-type carotene desaturases, the phenotype of a *zds1 crtiso1* double mutant was investigated. The *zds1 crtiso1* double mutant still accumulated downstream carotenoids, indicating that CRTISO is not ZDS2. To isolate mutant strains affected in the function of ZDS2, a *zds1* strain were mutagenized and screened for two types of phenotypes: (1) yellow-green-in-the-dark mutants that no longer turned light-green in the light and accumulated only ζ-carotenes and (2) gain-of-function mutants that allow *zds1* to turn very green in the light. Mutants that could not turn green in the light were isolated, but carotenoids downstream of ζ-carotene were still detected in the dark. Finally, three dominant mutants that were greener in the light were isolated. One such mutant, zSup63, showed increased expression of a gene encoding a CRTISO-like protein, JGI protein ID 516552, which is likely to be ZDS2. A DNA insertional mutant in the putative *ZDS2* gene encoding 516552 is available, and isolation of a *zds1 zds2* double mutant is in progress.

PREFACE

I would like to acknowledge contributions to this work by Rachel Dent who created and identified DNA insertional mutant CAL.028.02.09.

INTRODUCTION

The early steps in carotenoid biosynthesis involve synthesis of phytoene from GGPP and then desaturation/isomerization to produce lycopene. The first committed step to carotenoid biosynthesis is catalyzed by phytoene synthase (PSY), whose product is 15-*cis*-phytoene. The desaturation or addition of double bonds and isomerization of *cis*-phytoene to all-*trans*-lycopene can be catalyzed by a single protein, the CrtI-type phytoene desaturase, or through the cooperation of four different enzymes: PDS/CrtP, Z-ISO, ZDS/CrtQ/CrtQb/CrtQ-1, and CRTISO/CrtH (Figure 4.1). CrtP, CrtQ, CrtQb, CrtQ-1, and CrtH refer to prokaryotic carotenoid biosynthesis proteins. CrtI-type desaturases generates all-*trans*-lycopene via intermediates with *trans*-configuration [1,2,3]. Plant-type desaturases, PDS and ZDS, uses *cis*-isomers as substrates and require isomerases, Z-ISO and CRTISO, to synthesize all-*trans*-lycopene [2,4,5,6,7,8,9,10].

Generally, CrtI-type phytoene desaturases are found in archaea, anoxygenic photosynthetic bacteria, some heterotrophic bacteria, and fungi, whereas PDS/Z-ISO/ZDS/CRTISO and their cyanobacterial counterparts are active in oxygenic photosynthetic organisms (plants and algae, which includes cyanobacteria). Exceptions to this include the cyanobacteria *Gloeobacter violaceus* and *Nostoc* PCC7120 (formerly *Anabaena* PCC7120), which have carotene desaturases more related to CrtI-type desaturases than to plant-type desaturases. Transformation of the *G. violaceus* gene *glr0867* (encoding a CrtI-like protein) into a phytoene-producing *Escherichia coli* strain resulted in lycopene production, indicating that *glr0867* encodes a four-step desaturase [11,12]. CrtQa/CrtQ-1 from *Nostoc* PCC7120 is a ζ-carotene desaturase that is structurally more related to the CrtI-type desaturases than to the plant-type ZDS, and it was able to use *cis* and *trans* isomers as substrates [13,14]. Although CRTISO/CrtH functions in the plant-type phytoene desaturation pathway, like CrtQa, it is more closely related to bacterial CrtI-type phytoene desaturases than to either PDS or ZDS [15].

Chlamydomonas reinhardtii zds1 null mutants continue to synthesize downstream carotenoids like xanthophylls in the dark and in the light despite having a block early in carotenoid biosynthesis. The *zds1* mutant phenotype suggests the existence of a second ζ-carotene desaturase in *C. reinhardtii*. To identify the enzyme responsible for the accumulation of xanthophylls in dark-grown *zds1* null mutants, attempts were made to isolate (1) loss-of-function mutations that block accumulation of xanthophylls in the dark and greening of *zds1* in low light and (2) gain-of-function mutations that enable *zds1* to turn very green in the light and tolerate higher light intensities.

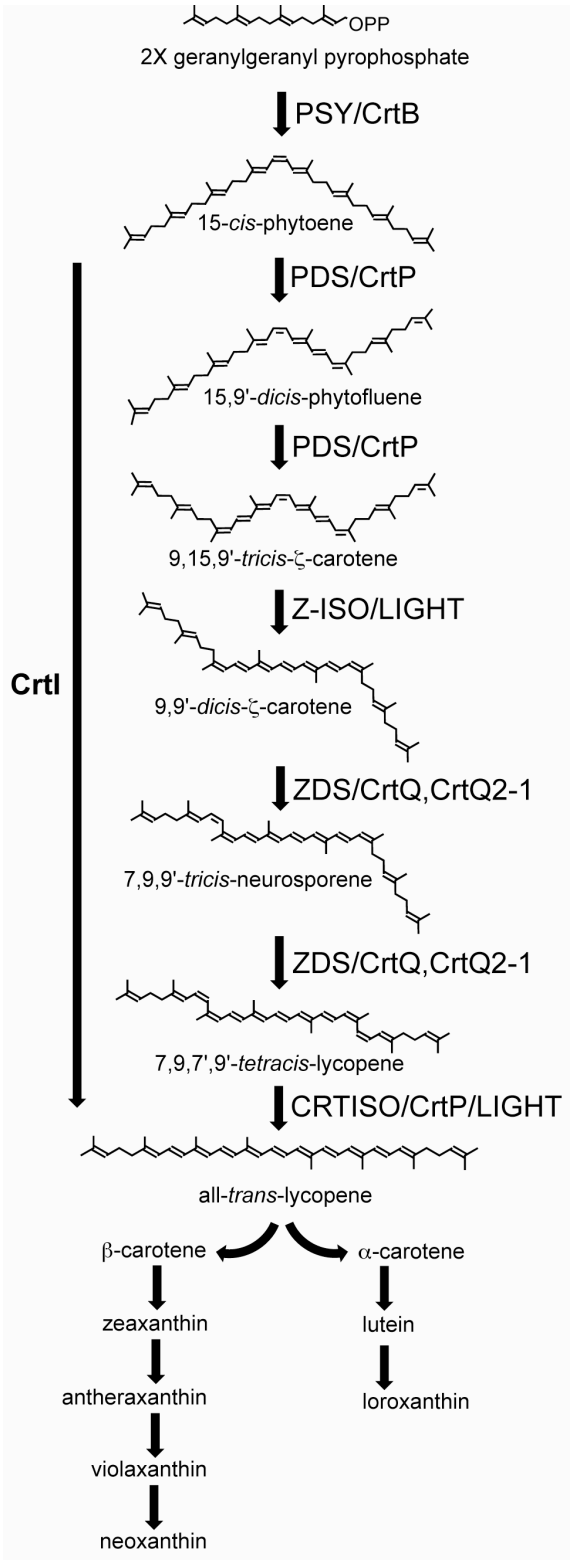

Figure 4.1. Desaturation of 15-*cis*-phytoene to all-*trans*-lycopene by PDS/ZDS-type and CrtI-type phytoene desaturases

MATERIALS AND METHODS

Strains and growth conditions

The wild-type *C. reinhardtii* strains used in this work, 4A+ (*mt+*) and 4ax5.2- (*mt-*), are in the 137c genetic background [16]. The *crtiso1-1* (Cal007.01.09) and *zds1-1* (Cal025.02.09) mutants were derived from DNA insertional mutagenesis [16]. All strains were maintained on Tris-acetate-phosphate (TAP) agar medium [17] at 25°C in complete darkness.

Light sensitivity assays

Dark-grown cells were shifted to the light to reveal any color changes induced by light or photosensitivity. The "greening" phenotype of *zds1-1* and *zds1-1 crtiso1-1* mutants was assayed after slowly introducing them to increasing light intensities as previously described in Chapter 3.

Light sensitivity of haploid and diploid strains was tested in four light conditions with four different growth media. The four light treatments were dark, very low light (vLL, 12 μmol photons m^{-2} sec^{-1}), low light (LL, 60 μmol photons m^{-2} sec^{-1}), and high light (HL, 400 μmol photons m^{-2} sec^{-1}). The four types of growth media were TAP-agar only, TAP-agar plus 50 μg/ml L-arginine (TAP+Arg), TAP-agar plus 5 μg/ml zeocin (TAP+Zeo), and TAP-agar +50 μg/ml L-arginine plus 5 μg/ml zeocin (Arg+Zeo). Cultures were grown in 25 ml of liquid TAP+Arg in the dark until cell densities reached ~$3x10^6$ cells/ml. Cultures were then serially diluted, spotted onto agar media, and grown in the dark for a week before they were shifted into the four light conditions for 2 weeks. For LL and HL treatments, cells were shaded with one layer of window screen for the first 12 hours before they were fully exposed to the specified light intensity.

Cycloheximide treatment

For cycloheximide experiments, wild-type strain 4A+ and *zds1-1* were scraped from TAP-agar and used to inoculate 3 ml TAP liquid medium. The 3 ml cultures were allowed to grow overnight without shaking in the dark and then used to inoculate three 125 ml TAP cultures in 500 ml Erlenmeyer flasks. The 125 ml cultures were allowed to grow for 6 days in the dark with shaking at 125 rpm at 25ºC; cell densities reached ~$4x10^6$ cells/ml by day 6. The 125 ml cultures were combined into one 475 ml culture, which was then divided into six treatments with three replicates per treatment for each strain. The six treatments were (1) dark for 6 hrs with no cycloheximide (cyc-); (2) dark for 6 hrs with cycloheximide (cyc+); (3) 6 hours of low light with no cycloheximide (6 hrs LL, cyc-); (4) 6 hours of low light with cycloheximide (6 hrs LL, cyc+); (5) 24 hours of low light with no cycloheximide (24 hrs LL, cyc-); and (6) 24 hours of low light with cycloheximide (24 hrs LL, cyc+). Each replicate consisted of 20 ml of cells grown horizontally in 50 ml BD Falcon tubes (Becton Dickinson and Company, Franklin Lakes, NJ) with shaking at 125 rpm at 25°C. Dark treatments were wrapped in aluminum foil while low light treatments were exposed to 50 μmol photons m^{-2} sec^{-1} of white light for 6 hours or 24 hours. Cycloheximide treatments were incubated with 10 μg/ml of cycloheximide (Sigma, St. Louis, MO) dissolved in methanol. A total of 100 μl of methanol was added to cyc+ and cyc- treatments. Cells were harvested by centrifugation at 3000 rpm, 25°C for 10 minutes; decanting the supernatant; resuspending the cell pellet in 500 μl of TAP media; centrifuging at 13,000 rpm

for 10 minutes; and removing all liquid. Pigments were extracted from the cell pellet with 200 μl of acetone and analyzed via HPLC as previously described [18]. All treatments were harvested and extracted for pigments in the dark with a very dim green safe light (Eastman Kodak Company, Rochester, NY).

Generation of mutants

***zds1-1crtiso1-1* and *zds1-1 arg7* double mutants:** *zds1-1 crtiso1-1* double mutants were generated by crossing *zds1-1* (*mt+*) to *crtiso1-1* (*mt-*). The *zds1-1 arg7-8* (*mt-*) and *zds1-1 arg7-1* (*mt+*) double mutants were generated by crossing *zds1-1* (*mt-*) to *arg7-8* (*mt+*) and *zds1-1* (*mt+*) to *arg7-1* (*mt-*) using established methods [17]. Progeny from all crosses were grown on TAP-agar or TAP-agar with 50 μg/ml of L-arginine in the dark at 25°C. The *zds1-1 arg7* double mutants were identified by their pale-yellow-green-in-the-dark color and their requirement for arginine. The *zds1-1 crtiso1-1* mutants were identified using *ZDS1* (ZdsF17, 5'-GCGACCTGAGCGAAGTGG-3') and *CRTISO1* (crtiso3A, 5'-CACGCGTCGCTCTATAATGA-3') specific primers and primers specific to pSP124S, the mutagenizing plasmid (RMD223L, 5'-CTGCGCTCCTTCTGGCATTTAA-3' or RMD230, 5'-8CCGTATTACCGCCTTTGAGTG-3').

Screen for *zds1-1* mutants that no longer turned green in the light: Liquid cultures of *zds1-1* in TAP were grown to a density of ~3x106 cells/ml. Cells were mutagenized according to previously described methods [18] using UV light of $5.5x10^4$ μJ cm^{-2}. After two weeks of growth in the dark, 6,030 surviving colonies were picked and inoculated using a toothpick into separate wells containing 150 μl of liquid TAP in 96-well plates. Cells were allowed to grow in the dark for 2 days at 25°C before replica plating. 5 μl of each colony was spotted onto 2 sets of TAP agar plates: one "dark" treated and one "light" treated. Dark-treated cells were grown for 20 days in the dark while light-treated cells were gently introduced to light. Light-treated cells were first grown in the dark for 4 days followed by 2 days under 4 μmol photons m^{-2} sec^{-1} of white light, followed by 2 days at 8 μmol photons m^{-2} sec^{-1}, 4 days at 12 μmol photons m^{-2} sec^{-1}, 2 days at 20 μmol photons m^{-2} sec^{-1}, 2 days at 40 μmol photons m^{-2} sec^{-1}, and finally 4 days at 80 μmol photons m^{-2} sec^{-1}. Colonies that remained yellow or turned white in the light were picked from dark-grown plates. Potential non-greening *zds1-1* mutants were rescreened before pigment analysis via HPLC.

Screen for *zds1-1* mutants that are very green in the light: A *zds1-1 arg7-8* (*mt-*) double mutant for was used as the starting strain. The *zds1-1 arg7-8* cells, started in a 1 ml culture 24 hours earlier, were used to inoculate 300 ml of TAP+Arg. The culture was grown with shaking (125 rpm) in the dark at 25°C until the cell density reached ~$5.0x10^6$ cells/ml. The cells were then centrifuged at 3,000 rpm and the cell pellet gently resuspended in fresh 30 ml of TAP media plus L-arginine. 25 ml of the culture was exposed to $5.0x10^4$ μJ cm^{-2} of UV light and allowed to recover overnight in the dark. 60 plates of TAP-agar+Arg were spread with 10x 10^6 UV-mutagenized cells/plate and allowed to grow for a week in the dark. The mutagenized cells were then selected for growth in low light (LL, 60 μmol photons m^{-2} sec^{-1}) for two weeks. After two weeks any green colonies were picked and rescreened three successive times for their ability to remain green under LL. The first two rescreens were carried out in the following manner. Green mutant colonies were inoculated into 150 μl of TAP+Arg into their own well in a 96-well plate. The cells were allowed to grow for two days in the dark before 5 μl of the culture was spotted onto TAP-agar+Arg. Cells spotted onto TAP-agar+Arg were grown in the dark for

another 2 days before being exposed to LL. Colonies that turned light green or darker under LL were selected and rescreened again in LL. For the third rescreen, potential suppressors were grown in 10 ml TAP+Arg media in 15 ml BD falcon conical centrifuge tubes, laid horizontally with shaking, in the dark at 25°C. Cells were grown in the dark for 4 days before cell concentrations were adjusted to $2x10^6$ cells/ml. Each mutant was then serially diluted 10-fold to a final dilution of 20 cells/ml. The dilution series was spotted onto two plates of TAP-agar+Arg; one plate was grown in the dark for 3 weeks while the second plate was grown for 2 days in the dark then directly shifted to LL for 3 weeks. After 3 weeks, light grown colonies were scored according to their ability to remain green at lower cell densities.

Mutants that remained after three LL screens were crossed to a *zds1-1 arg7-1* (*mt+*) strain to select diploids and to test for dominance of the very-green-in-LL mutant phenotype. Parental strains, *zds1-1 arg7-1* (*mt+*) and *zds1-1arg7-8* suppressors (*mt-*), were individually started in 800 μl TAP-N+Arg, a nitrogen-deficient TAP medium [17] and incubated in 8 μmol photons m^{-2} sec^{-1} overnight to induce gametogenesis. The *zds1-1 arg7-1* (*mt+*) gamete culture was mated to *zds1-1arg7-8* suppressors (*mt-*) overnight in 8 μmol photons m^{-2} sec^{-1}. The mating mixture was divided onto two, TAP-4% agar plates (800 μl/plate) and grown in the dark for a week, after which one set of plates was placed in LL at 25°C for 3 weeks. After 3 weeks, the dark-grown mating mixtures were themselves shifted into LL conditions for another 2 weeks. Medium to dark green colonies that formed after LL growth were picked, and their genomic DNA was tested by mating-type-specific PCR [19] to determine ploidy.

Phylogenetic analysis of carotenoid desaturase-like proteins

Protein sequences for CRTI, PDS, ZDS, and CRTISO were retrieved from the National Center for Biotechnology Information (www.ncbi.nlm.nih.gov) or from the Department of Energy (DOE) Joint Genome Institute (JGI) *Chlamydomonas reinhardtii* v4 genome (www.jgi.doe.gov/chlamy). Candidate carotenoid desaturase protein sequences were obtained by BLAST searches of the JGI *Chlamydomonas reinhardtii* genome [20] using PDS, ZDS, and CRTISO from *C. reinhardtii*, CRTISO2 and CRTISO3 from *A. thaliana* (Barry Pogson, personal communication), and CrtI from *Pantoea ananatis* as query sequences.

A phylogenetic tree of PDS, ZDS, CRTISO, CRTI, and candidate carotenoid desaturase protein sequences from plants, algae, bacteria, and fungi was constructed via the Phylogeny.fr platform (www.phylogeny.fr) [21]. Phylogeny.fr used the PhyML v3.0 aLRT [22,23] program with the maximum likelihood method to build a phylogenetic tree from MUSCLE v3.7 alignment [24] of protein sequences. Multiple sequence alignments (MSA) were used without the GBlock program, which removes poorly aligned regions and divergent regions. Phylogenetic trees were edited and graphically depicted with TreeDyn v198.3 [25].

RNA extraction and quantitative real-time PCR (qPCR) analysis

RNA from dark- and vLL- (8-12 μmol photons m^{-2} sec^{-1}) grown cells were both started in 50 ml of TAP+Arg media in 125 ml Erlenmeyer flasks with shaking at 125 rpm at 25°C until cell densities reached ~$3.0x10^6$ cells/ml. Cell densities were measured with a Multisizer3 Coulter Counter (Beckman Coulter, Fullerton, CA). Three 50 ml cultures were grown for every strained tested. Dark-grown cultures were wrapped in aluminum foil for growth or kept in a dark cabinet during cell counts and RNA extraction. On the day of RNA extraction, cells were counted and

cultures were adjusted to a volume of 25 ml and to a cell density of $1.5x10^6$ cells/ml. The 25 ml cultures were then placed back on the shaker for 4 hours before cells were centrifuged at 3000 rpm for 5 min and RNA extracted from cell pellets using 1 ml of Trizol reagent (Invitrogen, Carlsbad, CA). Total RNA was treated with DNAse I (Invitrogen, Carlsbad, CA) and then quantitated using a NanoDrop 2000 (Thermo Scientific, Wilmington, DE).

First-strand cDNA was synthesized from 1 μg total RNA with random primers (5'-NNNNNNNNN-3') using Omniscript reverse transcriptase (Qiagen, Valencia, CA) according to the manufacturer's protocol. The 20 μl of cDNA reaction was diluted to 70 μl with sterile water and 1 μl was used to determine cDNA concentrations using a NanoDrop 2000. cDNA concentrations were then adjusted to 250 ng/μl with sterile water. qPCR reactions were set up using 5 μl cDNA (250 ng/μl) synthesis reaction as template, 2 μl of each primer at 2.5 μM, and 10 μl 2X Sybr-green master mix (Qiagen, Valencia, CA) in a final volume of 20 μl. qPCR reactions were analyzed on an ABI-7300 qPCR machine, with standard cycling. Transcript levels were quantified using the $\Delta\Delta C_t$ method. *CBLP* was selected as the endogenous control gene, amplified with primers SWQ41 (5'-GAGTCCAACTACGGCTACGC-3') and SWQ42 (5'-GGTGTTCAGGTCCCACAGAC-3'). Primers 130438_133F (5'-AGCCCACCCCTAAACTCACT-3') and 130438_264R (5'-ACTCGCACACAGTCACCTTG-3') spanning exons 1, 2, and 3 of gene model au5.g6551 (encoding for JGI protein ID 516552) produced amplicons of 132 bp. Primer pair C200034_345F (5'-CAGCATACCGCGTGTTCTT-3') in exon 3 and C200034_38B (5'-CCAGCCAGTCCAGGTAGGAG-3') in exon 5, producing an amplicon of approximately 124 bp, was used for expression analysis of the gene model encoding JGI protein ID 513725.

RESULTS

All three previously characterized *C. reinhardtii zds1* mutants accumulated xanthophylls in the dark and even larger quantities in the light (Chapter 3, Figure 3.3B). Light exposure also turned the pale yellow-green-in-the-dark *zds1* mutant phenotype to a light-green color (Figure 4.2). Therefore, I hypothesized that *C. reinhardtii* has a second ζ-carotene desaturase, ZDS2, which might be induced by light.

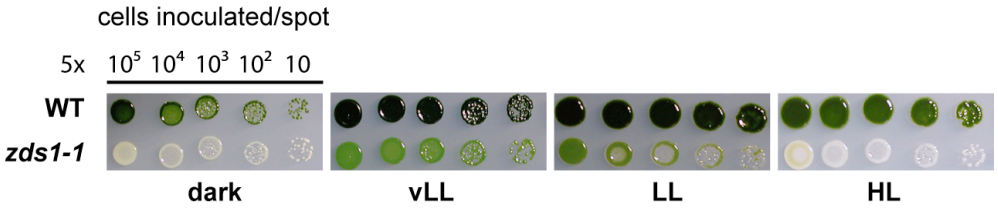

Figure 4.2. Light sensitivity and "greening" phenotype of *zds1-1* mutants. Cells were spotted onto TAP-agar and grown for 4 days in the dark before being gradually exposed to increasing light intensities. All cells were grown for a total of 16 days. Light intensities: Dk (dark), vLL (12 µmol photons m^{-2} sec^{-1}), LL (60 µmol photons m^{-2} sec^{-1}), HL (400 µmol photons m^{-2} sec^{-1}). WT (wild type)

Cycloheximide treatment

To investigate the role that light plays in the greening of *zds1* mutants, *zds1-1* cells were treated with cycloheximide, an inhibitor of cytoplasmic protein synthesis, and either kept in the dark or exposed to light for 6 or 24 hours. Xanthophyll levels (Figure 4.3, blue bars) and carotene levels (Figure 4.3, yellow bars) were the same for *zds1-1* in the dark with or without cycloheximide, with levels of 9,9'-*dicis*-ζ-carotene isomer that were at least five-fold higher than 9-15,9'-*tricis*-ζ-carotenes levels (Table 4.1). The light-induced decrease of ζ-carotene isomers and concomitant increase in α- and β-carotenes (Table 4.1) still occurred in the presence of cycloheximide (Figure 4.3B, orange bars), suggesting that (1) expression of ZDS2 in dark-grown cells is sufficient to allow subsequent conversion of accumulated ζ-carotene isomers to cyclic carotenes in the light and (2) light plays an additional role, perhaps in photoisomerization of a ζ-carotene substrate. Cycloheximide did, however, block the light-induced accumulation of xanthophylls in *zds1-1* (Figure 4.3, blue bars).

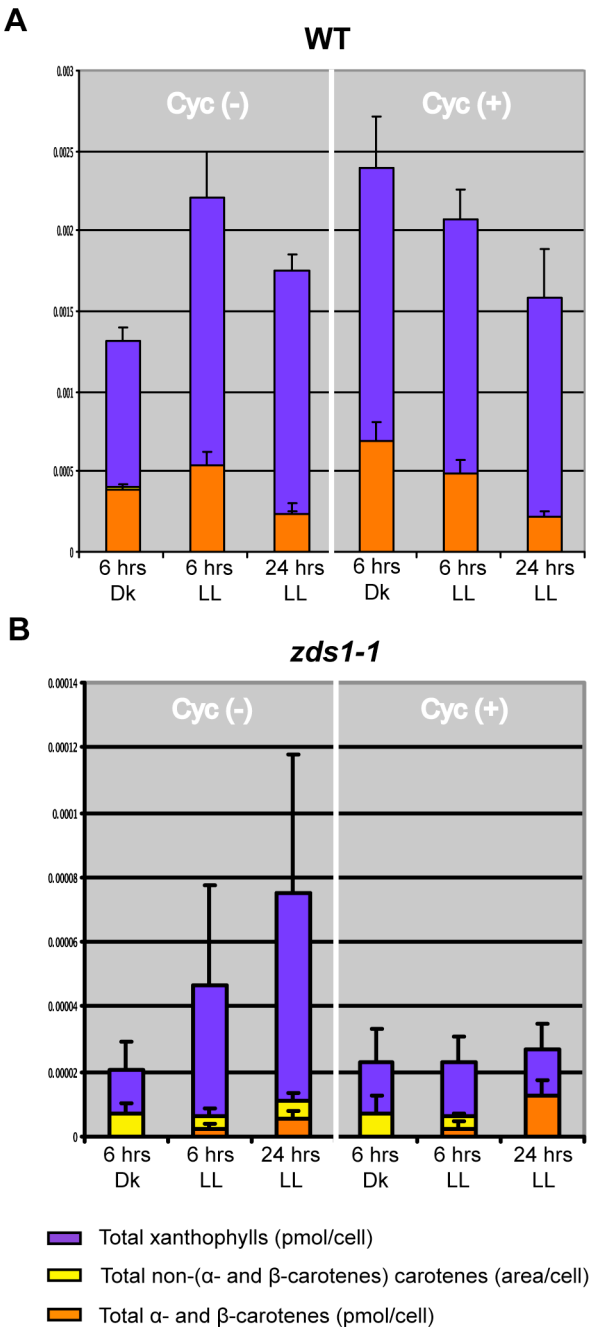

Figure 4.3. Effect of light and cycloheximide on carotenoid accumulation in *zds1-1* mutants.

Blue bars represent total xanthophylls (neoxathin/loroxanthin, violaxanthin, antheraxanthin, lutein, and zeaxanthin); orange bars represent total α-carotenes and β-carotenes; yellow bars represent non-(α- and β-carotenes) carotenes (ζ-carotene isomers, neurosporene, β-zeacarotenes, and phytofluene isomers). β-zeacarotenes are cyclization products of neurosporene. Cells were treated without cycloheximide (Cyc-) or with 10 µg/ml cycloheximide (Cyc+) for 6 hrs in the dark, or 6 or 24 hrs in the light (LL, 50 µmol photons m^{-2} sec^{-1}).

Table 4.1. Levels of ζ-carotene isomers in *zds1-1* mutants treated with cycloheximide and light

	Dark 6 hrs		6 hrs LL		24 hrs LL	
	Cyc-	**Cyc+**	**Cyc-**	**Cyc+**	**Cyc-**	**Cyc+**
9,15,9'-*tricis*-ζ-carotenes	8.55E-07 ±2.38E-07	9.42E-07 ±7.13E-07	0	0	0	0
9,9'-*dicis*-ζ-carotenes	5.38E-06 ±2.0E-06	5.17E-06 ±3.85E-06	1.26E-06 ±8.42E-07	5.42E-07 ±2.4E-07	1.87E-06 ±8.74E-07	0

Mean and standard deviations of three independent cultures. Values are in peak area/cell. Treatments without cycloheximide (Cyc-) and with 10 ug/ml cycloheximide (Cyc+) were incubated with the antibiotic for the same length of time as light exposure (LL, 50 μmol photons m^{-2} sec^{-1}).

Three approaches were undertaken to identify the hypothetical ZDS2: (1) isolation and characterization of *zds1 crtiso1-1* double mutants, (2) mutagenesis of *zds1* to isolate mutants that are no longer able to accumulate carotenoids downstream of ζ-carotenes, and (3) isolation of mutants that enhance the greening of *zds1*.

zds1 crtiso1 double mutants

To facilitate generation of *zds1 crtiso1* double mutants, DNA insertional alleles of *zds1* and *crtiso1* were crossed to each other, and tetratype tetrads were selected for further analyses. Tetratype tetrads had progeny that had the following color phenotypes in the dark: dark green (wild type, recombinant), yellow (*crtiso1-1*, parental), pale yellow-green (*zds1-1*, parental), and pale yellow-green (*zds1-1 crtiso1-1*, recombinant). Three *zds1-1 crtiso1-1* progeny were identified by PCR analysis (data not shown). The double mutants were yellow-green in the dark and light-green in the light, and they had a similar "greening" response to light as the *zds1-1* single mutant (Figure 4.4A). Also like *zds1-1* single mutants, dark grown *zds1-1 crtiso1-1* mutants accumulated large amounts of ζ-carotenes and minor quantities of xanthophylls (Figure 4.4B). Because *zds1-1 crtiso1-1* double mutants still accumulated carotenoids downstream of ζ-carotenes in the dark, I concluded that the *C. reinhardtii* CRTISO protein does not have ZDS activity.

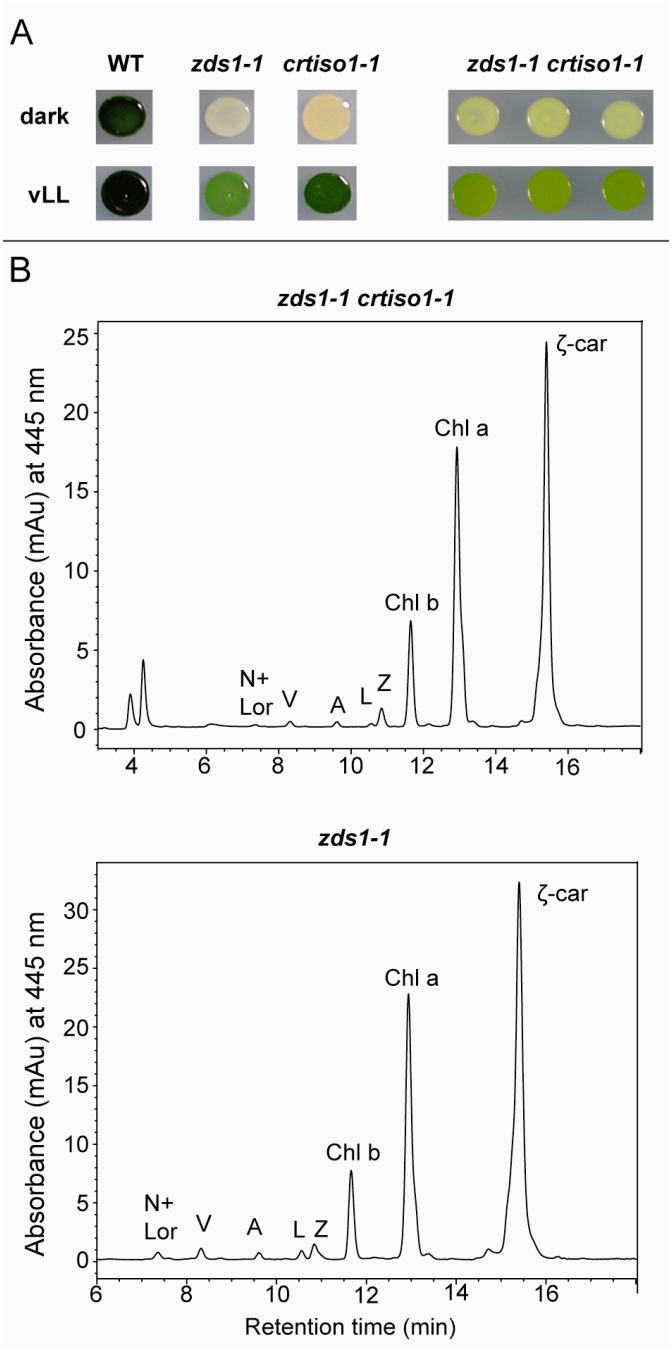

Figure 4.4. Double mutant *zds1-1 crtiso1-1* still accumulates xanthophylls.
A). Wild type, *zds1-1*, *crtiso1-1*, and *zds1-1 crtiso1-1* cells were spotted onto TAP-agar and grown for a week in the dark before being gradually introduced to very low light (vLL, 12 µmol photons m^{-2} sec^{-1}). Cells were grown for 2 weeks in vLL; dark grown cells were grown for a total of 21 days. The *zds1-1 crtiso1-1* double mutants were derived from three independent tetrads.
B). Chlorophyll and carotenoid profiles of dark grown *zds1-1* and *zds1-1 crtiso1-1* mutants. Chlorophylls and carotenoids were detected at 445 nm via HPLC coupled with a diode array detector. N+Lor (neoxanthin + loroxanthin), V (violaxanthin), A (antheraxanthin), L (lutein),

Z (zeaxanthin), Chl *a* and Chl *b* (chlorophyll *a* and *b*), and ζ-car (ζ-carotenes). Pigment levels were not normalized by cell number.

Loss-of-function mutants

In the second approach, pale yellow-green-in-the-dark *zds1-1* mutants that could not "green" in the light were isolated. After UV mutagenesis, 6030 pale yellow-green or yellow-in-the-dark mutants were picked and replica plated in the light. In the primary screen, 321 colonies were picked (Figure 4.5). After rescreening, only 57 mutants remained, and these were divided into two color phenotypic classes: 'zwhite' for cells that were white in the dark and 'zyellow' for cells that were yellow-green in the dark but that bleached and died in the light. HPLC analysis of the 57 potential mutants further reduced this number to 18 mutants that did not appear to accumulate carotenoids downstream of ζ-carotenes. Unfortunately, repeated HPLC analysis, each time using larger quantities of cells for pigment extraction, showed downstream xanthophyll accumulation in dark-grown cells of all 18 remaining mutants.

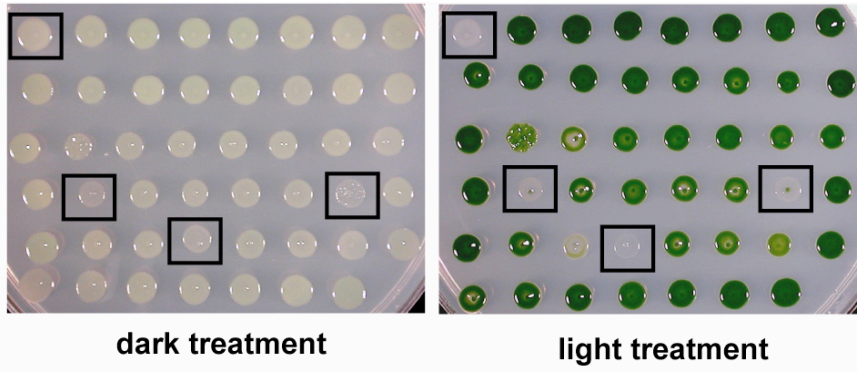

Figure 4.5. Example of color phenotypes of non-greening *zds1-1* mutants. Replica plates of UV-mutagenized cells grown in the dark or in the light. Cells were spotted onto TAP-agar and grown for 20 days in the dark or gradually introduced to the light over a period of 20 days. The final light intensity tested was 80 μmol photons m^{-2} sec^{-1} for 4 days. Colonies that were yellow, pale yellow, or white in color were picked from dark treatments. Boxes highlight "non-greening" mutants selected for rescreening and later for pigment analysis.

Gain-of-function mutants

In the third approach, mutants derived from *zds1-1* that could survive and turn very green in LL were isolated. To facilitate dominance testing of potential mutants, a *zds1-1 arg7-8* (*mt-*) strain was used as the starting strain. UV mutagenesis of *zds1-1 arg7-8* followed by selection in LL led to the isolation of 300 green colonies after two weeks (Figure 4.6B). In the dark, UV mutagenized cells formed a pale yellow lawn, whereas in LL the majority of cells bleached and died (Figure 4.6B). Cells not mutagenized with UV light formed pale yellow-green colonies in the dark and bleached and died under LL conditions (Figure 4.6A). After two rounds of

rescreening, 152 green-in-LL colonies were identified for further analysis. Interestingly, all 152 colonies retained the yellow- to yellow-green-in-the-dark phenotype of the parental strain; no mutants formed green colonies in the dark. The 152 green-in-LL colonies were screened a third time in the light; this time to determine their ability to remain green at even low cell densities. Only 45 of the 152 colonies survived for 3 weeks in LL. The eight best mutants were selected for dominance testing. These eight mutants had a medium-green or darker green color and could form colonies in spots with a 1000 or fewer cells inoculated per spot (Figure 4.6C).

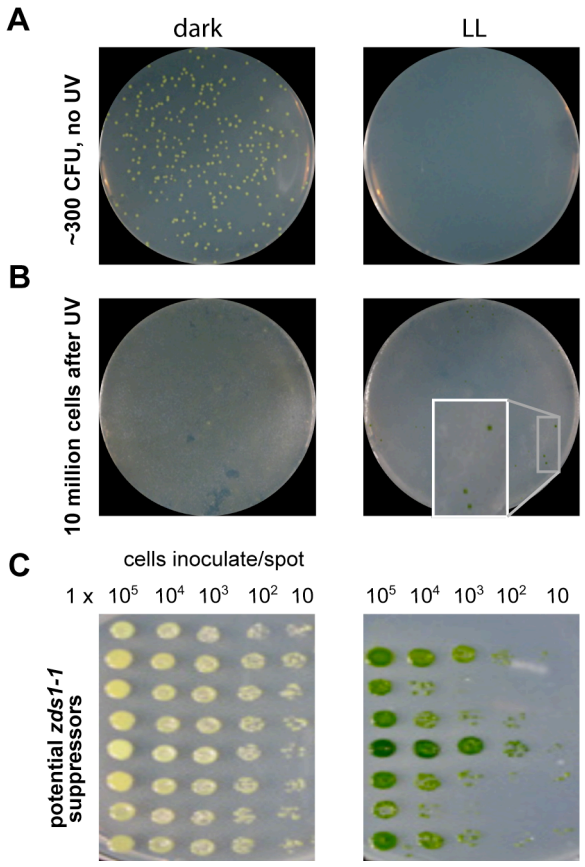

Figure 4.6. Selection/screening for *zds1-1* mutants that are greener in the light.
A). Colony-forming units (CFU) of *zds1-1* cells not exposed to UV light, grown in the dark or in low light (LL).
B). TAP-agar+Arg plates inoculated with 10 million UV mutagenized cells grown in the dark or in the light. Inset in LL plate is a magnification of green colonies that were picked for further characterization.
C). Example of third LL screen used to identify very-green-in-LL *zds1-1* suppressor mutants. Cells were spotted onto 35 ml of TAP-agar and grown for 23 days in the dark or for LL conditions, 2 days first in the dark followed by 21 days in LL.
Dark treatments (left panel) or LL treatments (60 µmol photons m^{-2} $sec^{-1}$of light, right panel)

To test dominance, the eight mutants that exhibited a strong green phenotype were crossed to a *zds1-1 arg7-1* (*mt+*) strain, and vegetative diploids were selected in the dark on TAP

medium without arginine. Yellow-green diploid colonies that grew in the dark were then shifted into LL for 2 weeks. Of the eight potential suppressor mutants tested, three (zSup3, zSup49, and zSup63) produced yellow-green-in-the-dark diploid colonies that turned very green in LL (Figure 4.7A). The ploidy of these colonies was confirmed by mating type PCR (Figure 4.7B). The other five mutants yielded diploids with LL phenotypes like the *zds1-1/zds1-1* diploid control, which bleached and died in LL conditions (Figure 4.7A).

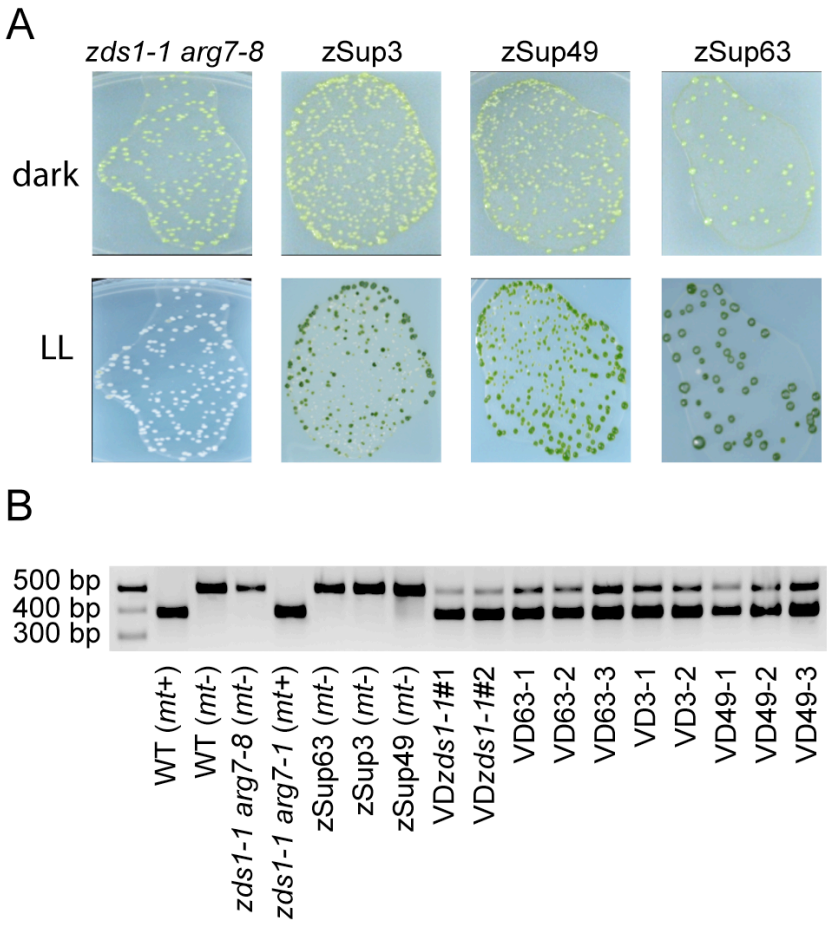

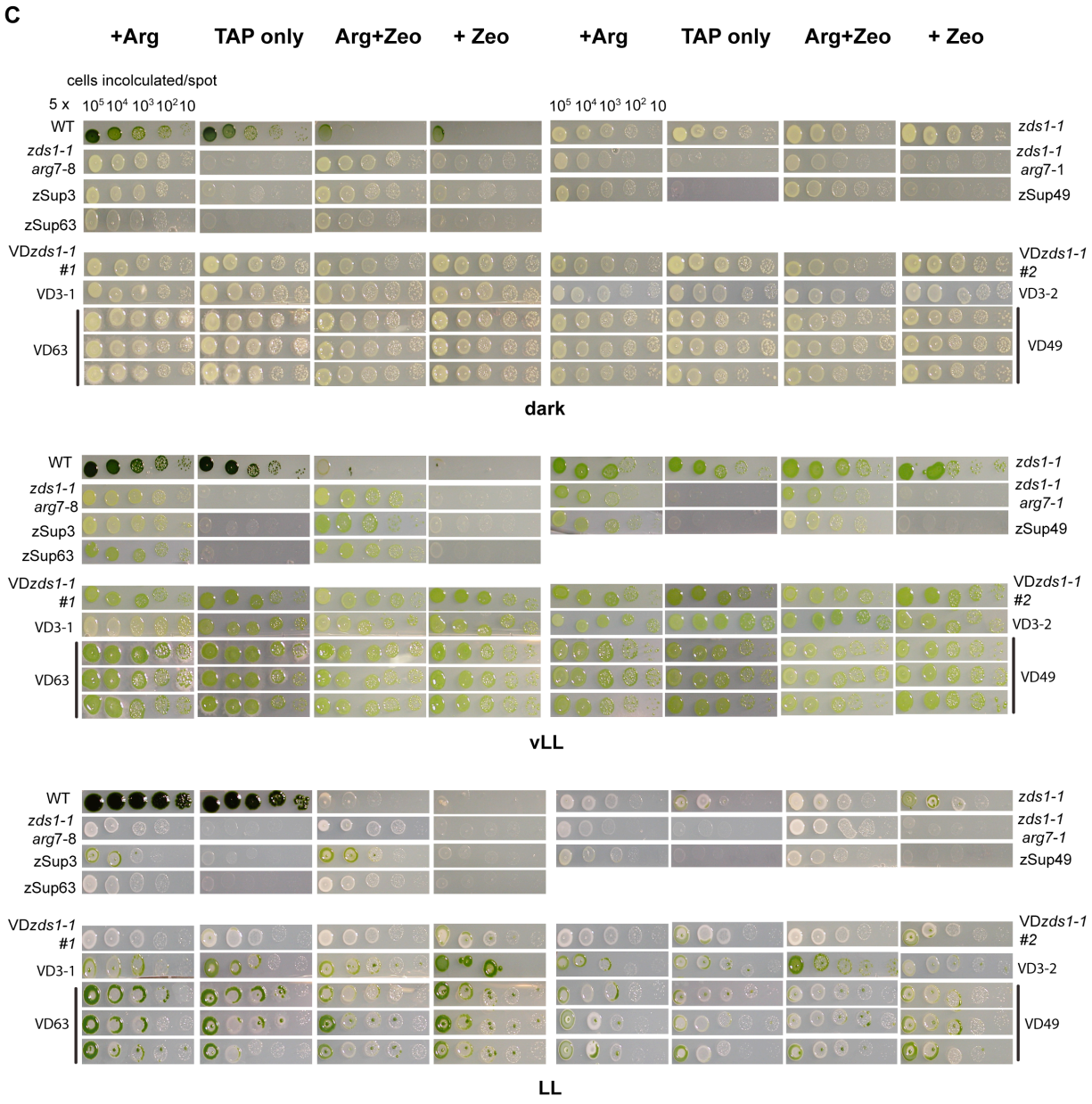

Figure 4.7. Mutants derived from *zds1-1* that have a dominant very-green-in-LL phenotype.

A). *zds1-1 arg7-8* suppressors mutants (zSup3, zSup49, and zSup63) and their parental strain, *zds1-1 arg7-8*, all *mt-*, were mated to a *zds1-1 arg7-1* (*mt+*) strain to isolate vegetative diploids. Vegetative diploids were selected on TAP-agar lacking L-arginine in the dark and then moved to low light conditions (LL, 60 µmol photons m^{-2} sec^{-1}) for 2 weeks. All vegetative diploids had a yellow-green-in-the-dark phenotype. In LL conditions, *zds1-1* suppressor mutants produced vegetative diploids that were green, whereas control vegetative diploids, *zds1-1/zds1-1 arg7-8/arg7-1 mt+/mt-,* had a white and bleached phenotype.

B). Mating-type determination to show that colonies formed in panel A were diploids while parental strains were haploid.

C). Light sensitivity assay of *zds1-1*, *zds1-1* suppressor mutants, and vegetative diploids. Cells were spotted onto TAP-agar alone (TAP only) or TAP-agar supplemented with 50 µg/ml

L-arginine (+Arg), 5 μg/ml zeocin (+Zeo), or both L-arginine and zeocin (Arg+Zeo). Cells were grown in the dark for a week then shifted to the various light conditions for another 2 weeks. Light conditions include dark, vLL (12 μmol photons m^{-2} sec^{-1}), LL (60 μmol photons m^{-2} sec^{-1}), and HL (400 μmol photons m^{-2} sec^{-1}). Genotypes of parental strains were *zds1-1 arg7-8, zds1-1 arg7-1,* and *zds1-1 arg7-8* suppressors mutants (zSup3, zSup49, and zSup63). Wild type strains (WT), 4A+ and 4ax5.2-, with opposite mating types were used as a reference for mating type. "VD" prefix indicates vegetative diploids randomly selected from colonies that grew from crosses depicted in panel A. VD*zds1-1* #1 and VD*zds1-1* #2 have the genotype *zds1-1/zds1-1 arg7-8/arg7-1 mt+/mt-*. Other vegetative diploids have the genotype *zSup mutation/+ zds1-1/zds1-1 arg7-8/arg7-1 mt+/mt-*. Vegetative diploids derived from zSup63 (VD63-1, VD63-2, and VD63-3), from zSup3 (VD3-1 and VD3-2), and from zSup49 (VD49-1, VD49-2, and VD49-3).

Dominance of the *zds1-1 arg7-8* suppressor mutant phenotype was confirmed in an assay that tested the sensitivity of haploid and diploid strains of *zds1-1* and *zds1-1* suppressors to light. This light assay also tested three other phenotypes: (1) the arginine-requiring phenotype of haploid strains, (2) the zeocin-resistant phenotype of mutants carrying the *zds1-1* mutation, and (3) the arginine-independent phenotype of vegetative diploid strains. Light sensitivity was tested using dark, vLL, LL, and HL conditions. Wild type cells produced dark green colonies under all light conditions, and they survived on all media tested except those containing the antibiotic zeocin. All haploid (*zds1-1, zds1-1arg7-8*, *zds1-1arg7-8*, zSup3, zSup49, and zSup49) and diploid (VD*zds1-1,* VD3, VD49, and VD63) strains carrying the *zds1-1* mutation produced yellow-green colonies in the dark and on media containing zeocin (Figure 4.7C). Haploid strains, with the exception of *zds1-1* and wild type, did not produce colonies unless the growth media was supplemented with L-arginine (+Arg and Arg+Zeo treatments). Diploid strains grew on all four media types. In general all strains carrying the *zds1-1* mutation turned a light-green color under vLL conditions. Diploid *zds1-1* mutants strains were only slightly greener in color than their haploid counter parts, *zds1-1 arg7*; however, they were not as green as *zds1-1* without the *arg7* mutation in vLL (Figure 4.7C). In LL conditions, *zds1-1* and *zds1-1 arg7* strains bleached and died. On TAP-agar with zeocin, *zds1-1* mutants did have colonies with some green color in spots inoculated with $5x10^5$ and $5x10^4$cells. Suppressor mutant, zSup3, also had colonies with green color on the edges on TAP+Arg and TAP+Arg+Zeo media. ZSup49 and zSup63 did not produce any green colonies in LL. Diploid strains from *zds1-1* suppressor mutants, VD3, VD63, and VD49, all produced colonies in LL that had green color in spots with the highest cell density (Figure 4.7C, $5x10^5$ cells inoculated/spot). VD63 strain produced the darkest green colonies in LL, not including wild-type cells. Control diploid strains, VDzds1-1#1 and #2, also had slightly green colonies in LL treatments, but unlike VD63 strains which had medium-green-ringed colonies up to cell densities of $5x10^3$ cells inoculated/spot, VDzds1-1 had lighter green-ringed colonies in spots containing $5x10^5$ cells inoculated/spot with a little greening observed in spots inoculated with $5x10^4$ cells. In HL, all strains except wild type, completely bleached and died (data not shown). This light assay showed that the *zds1-1* green-in-the-light and *zds1-1* suppressor very-green-in-the-light mutant phenotypes are dependent on higher cell densities and confirmed that the *zds1-1 arg7-8* suppressor mutant phenotypes of zSup3, zSup49, and zSup63 are dominant.

Candidate genes for ZDS2

A candidate gene approach was undertaken to identify the gene responsible for the accumulation of carotenoids downstream of ζ-carotenes in dark-grown *zds1* mutants. To date, desaturases and/or isomerases responsible for the conversion of *cis*-phytoene to all-*trans*-lycopene have fallen into two main classes—the plant-type or PDS/ZDS/CRTISO pathway or the bacterial-type or CrtI-type desaturases. Plant, algal, bacterial, and fungal protein sequences of PDS, ZDS, CRTISO, and CrtI were used as a query in BLAST homology searches against the *C. reinhardtii* genome (www.jgi.doe.gov/chlamy) to identify candidate *C. reinhardtii* proteins with carotenoid desaturase activity. Candidate proteins were chosen based on strong expressed sequence tags (EST) support and if homologs existed in plants or other algae. Four potential *C. reinhardtii* carotenoid desaturase-like proteins were selected along with protein sequences of PDS, ZDS, CRTISO, and CrtI from published sources to build a phylogenetic tree. A phylogenetic tree was constructed using four candidate protein sequences from *C. reinhardtii* that are similar to known early carotenoid desaturases and isomerases from *C. reinhardtii*, two plants, three cyanobacteria, two bacteria, and one fungus (Figure 4.8). As expected, the phylogenetic tree showed two major groups, one composed of PDS and ZDS sequences and another of mostly CRTISO and CrtI sequences. The exception was CrtQa from the cyanobacteria *Nostoc sp*. PCC7120, which clustered with CrtI-type desaturases even though it is functionally a ζ-carotene desaturase [13,14]. Two *C. reinhardtii* candidate carotenoid proteins, JGI 516552 and JGI 513725, were most closely related to CRTISO and CrtI proteins, respectively. The other candidate proteins, JGI 205488 and JGI 188867, were less similar and grouped outside of the four main branches (CRTISO/CrtH, CRTI, ZDS/CrtQ, and PDS/CrtP).

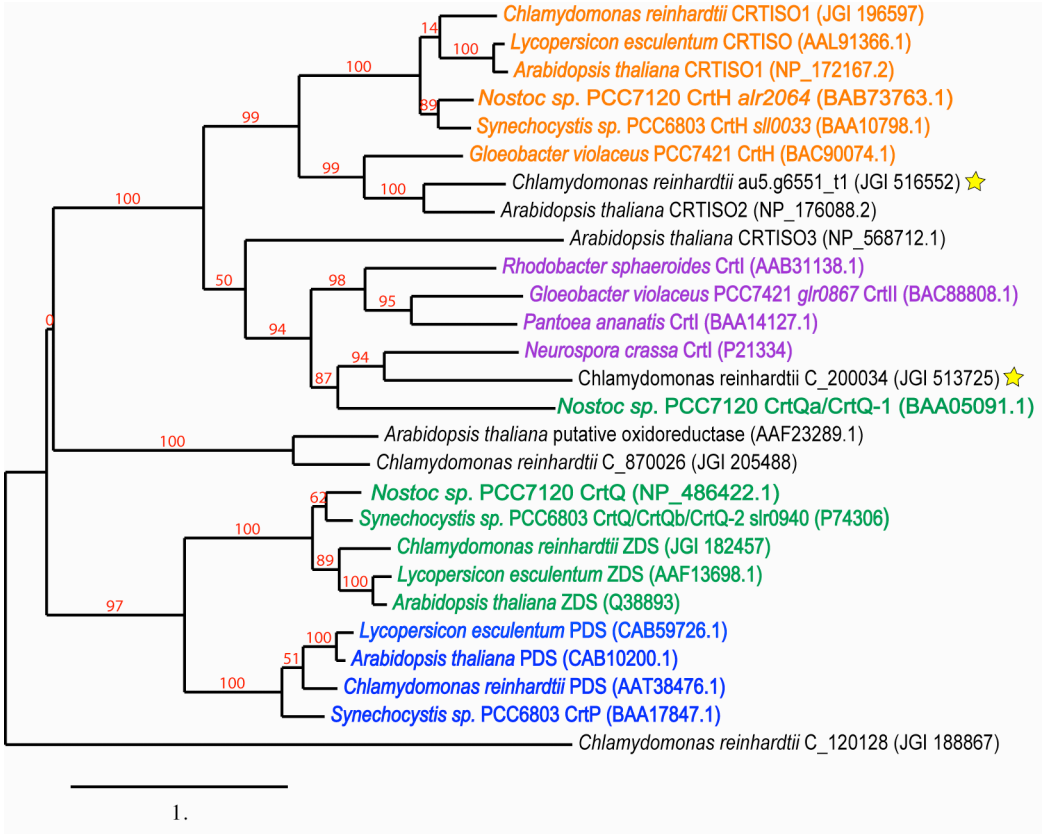

Figure 4.8. Phylogenetic tree of carotenoid desaturases and isomerases from plants, algae, bacteria, and a fungus.
Maximum likelihood tree of bacterial-type phytoene desaturase (CrtI), plant-type phytoene desaturase (PDS/CrtP), zeta-carotene desaturase (ZDS/CrtQa/CrtQb/CrtQ), and prolycopene isomerase (CRTISO/CrtH) protein sequences from plants (*Arabidopsis thaliana* and *Lycopersicon esculentum*), algae (*Chlamydomonas reinhardtii, Gloeobacter violaceus* PCC7421, *Synechocystis* PCC6803, *Nostoc* PCC7120), anoxygenic photosynthetic bacterium (*Rhodobacter sphaeroides)*, non-photosynthetic bacterium (*Pantoae ananatis* formerly *Erwinia uredovora*), and a fungus (*Neurospora crassa*). PDS sequences are colored blue, ZDS in green, CrtI in purple, CRTISO in orange, and unknown carotenoid desaturase/isomerase-like sequences in black. Protein ID from GenBank and JGI are in parentheses. Red colored numbers indicate branch support values in %. Stars show position of the two candidate desaturases chosen for qPCR analysis in *zds1-1* suppressor mutants.

Transcript levels of candidate genes in *zds1-1* suppressor mutants

The levels of RNA encoding proteins 516552 and 513725 were tested in zSup3, zSup49, and zSup63. Protein 513725 seemed an especially promising candidate, because it was found in the CrtI cluster containing the ζ-carotene desaturase CrtQa (Figure 4.8), which can convert *cis* and *trans* isomers of ζ-carotene, neurosporene, and β-zeacarotene as substrates to prolycopene, lycopene, and γ-carotene [13,14]. However, quantitative real-time PCR analysis of the RNA encoding protein 513725, did not show significant differences in expression levels for any of the three *zds1-1* suppressor mutants grown in the dark or light compared to the parental strain *zds1-1* (data not shown). Interestingly, the transcript levels were elevated two-fold compared to wild-type levels in dark-grown strains containing the *zds1-1* mutation (data not shown). Transcripts for gene model au5.g6551_t1, which encodes protein 516552, were expressed at the same level or lower in dark-grown zSup3, zSup49, or zSup63 mutants compared to control strains carrying the *zds1-1* mutation (*zds1-1*, *zds1-1 arg7-8*, and *zds1-1 arg7-1*). In vLL conditions *zds1-1* control strains expressed au5.g6551_t1 transcripts (516552) two to five-fold higher than wild-type cells under the same growth conditions. Suppressor mutants zSup49 and zSup3 had similar au5.g6551_t1 expression levels as *zds1-1* control strains. ZSup63, however, had au5.g6551_t1 transcript levels in vLL that were at least ten-fold higher than expression levels measured in wild type or in any of the *zds1-1* control strains (Figure 4.9). Based on these results, protein 516552 might be ZDS2, and its overexpression might explain zSup63's very-green-in-LL mutant phenotype.

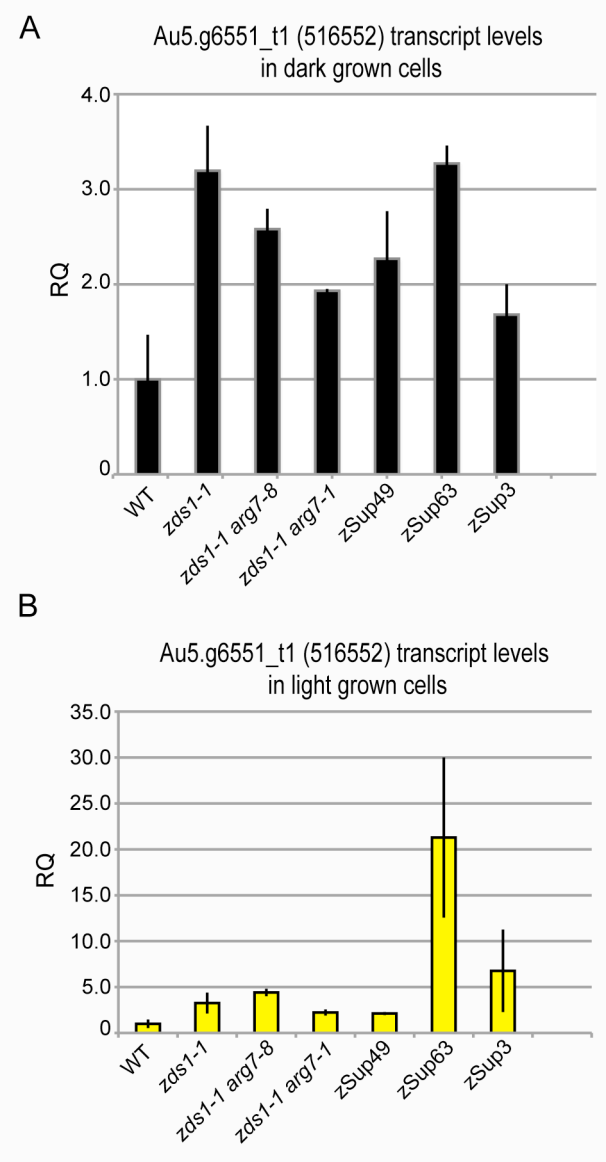

Figure 4.9. Transcript expression levels of a candidate carotene desaturase, Au5.g6551_t1 (516552), in *zds1-1* mutants with a dominant, very-green-in-LL phenotype.
Transcript levels for Au5.g6551.t1 were determined for dark-grown (A) and cultures exposed to vLL (8-12 μmol photons m^{-2} sec^{-1}) (B). RQ (relative quantification fold change) values. The reference sample was wild-type (WT). Averages and standard deviations were from three independent cultures

NCBI Conserved Domain Database (CDD) analysis (www.ncbi.nlm.nih.gov/Structure/cdd/wrpsb.cgi) of *C. reinhardtii* protein 516552 showed that it has a domain belonging to the super family of pyridine nucleotide-disulfide oxidoreducatases, which is also found in both *C. reinhardtii* PDS and ZDS proteins [26,27,28]. Conserved domain searches also found a similarity to C-3'4' desaturase (CrtD), a carotenoid biosynthesis protein found to catalyze the first committed step to myxoxanthophyll biosynthesis in *Synechocystis*

PCC6803 [29]. Protein 516552 has 34% amino acid identity to PDS, 35% to ZDS, and 31% to CRTISO from *C. reinhardtii*.

Fortunately, an DNA insertional mutant with flanking sequences from au5.g6551_t1 was identified independently in the Niyogi lab [16]. The DNA insertional mutant, CAL.028.02.09, was isolated because it exhibited sensitivity to LL, although it has a dark-green color phenotype in the dark and in vLL. Crosses with CAL.028.02.09 and *zds1-1* DNA insertional mutants are currently underway to determine if progeny carrying mutations in both genes for ZDS1 and protein 516552 will eliminate all xanthophyll biosynthesis.

DISCUSSION

Light has a stimulating effect on *zds1* mutants as evidenced by the color change of dark-grown yellow-green *zds1* mutants becoming light-green in vLL. Light could up-regulate the expression of an alternative carotene desaturase (ZDS2) and/or it could act on accumulated intermediates, modifying them into usable substrates for ZDS2. To determine what role light plays in the *zds1* mutant phenotype, *zds1-1* mutants were treated with cycloheximide under light and dark conditions (Figure 4.3, Table 4.1). This experiment showed that new cytoplasmic protein synthesis is not necessary for the light-induced conversion of accumulated ζ-carotenes into downstream cyclic carotenes. However, the light-induced accumulation of xanthophylls in *zds1-1* was blocked by cycloheximide (Figure 4.3, blue bars), suggesting that new translation of ZDS2 and/or other downstream enzymes, such as β-carotene hydroxylase, is necessary for increasead xanthophyll accumulation in the light.

Measurements of specific *cis*-isomers of ζ-carotene support a hypothesis that couples photoisomerization of substrates with light activation of ZDS2. Although the expression level in the dark of the putative ZDS2 is sufficient to allow conversion of ζ-carotenes to cyclic carotenes, light is still needed, most likely to photoisomerize accumulated ζ-carotenes into the most appropriate substrate for ZDS2. Dark-grown *zds1-1* cells treated with and without cycloheximide accumulated both 9,15,9'-*tricis*-ζ-carotenes and 9,9'-*dicis*-ζ-carotenes (Table 4.1). In the light, cells no longer accumulated 9,15,9'-*tricis*-ζ-carotenes. *In vitro* experiments with heterologous *E. coli,* daffodil chromoplasts, and substrate feeding experiments has shown that light can photoisomerize 9,15,9'-*tricis*-ζ-carotene to 9,9'-*dicis*-ζ-carotene [4,5,30,31]. Photoisomerization of 9,15,9'-*tricis*-ζ-carotenes did not result in increased levels of 9,9'-*dicis*-ζ-carotenes in light-grown cells relative to levels accumulated by cells in the dark. Instead, levels of 9,9'-*dicis*-ζ-carotenes accumulation decreased with light growth and disappeared completely after 24 hrs in LL in the presence of cycloheximide. Since total carotenoid levels in the cycloheximide experiment in the light were similar to levels found in the dark, the disappearance of 9,9'-*dicis*-ζ-carotene in cells is probably not due to photo-destruction of the carotene. The increasing accumulation of α- and β-carotenes with longer light exposure suggests that the 9,9'-*dicis*-ζ-carotene was further desaturated to form all-*trans*-lycopene which was, in turn, cyclized by β- and ε-lycopene cyclases to form α- and β-carotenes.

To determine the identity of the putative alternative carotene desaturase, screens were conducted for *zds1-1* mutants that no longer had this activity or that had higher activity than the parental strain. Screens for *zds1-1* non-greening mutants did not result in identification of mutants that no longer accumulated xanthophylls in the dark. Most likely, these screens for non-greening *zds1-1* mutants were unsuccessful because they resulted in light-sensitive mutants.

Light-sensitive mutants could include mutants impaired in other steps of carotenoid biosynthesis, photosynthesis, and repair of photodamage, just to name a few [32]. Already light-sensitive due to the *zds1-1* mutant background strains, potential non-greening mutants were difficult to distinguish from light-sensitive mutants that could still synthesize xanthophylls. Light assays and pigment analyses were dependent on the cell density of colonies and the amount of cells used in pigment analysis. Cells located in the interior colonies would receive more shading from those located on the exterior and therefore, more protection from photodamage.

A screen for gain-of-function mutants (in the *zds1-1* background) that are very green in the light was more successful. Three mutants with a dominant green-in-LL mutant phenotype were isolated: zSup3, zSup49, and zSup63. Because carotene desaturases have structural similarities, protein sequences from known phytoene desaturases and isomerases were used to construct a phylogenetic tree with candidate *C. reinhardtii* proteins that are homologous to carotene desaturases. This analysis identified two candidate ZDS2 proteins, one that clustered with CRTISO/CrtH proteins and another that clustered with CrtI proteins. Expression of the gene encoding each protein was determined for the three *zds1-1* suppressor mutants, revealing that one mutant, zSup63, over-expressed transcripts for the CRTISO-like candidate protein (JGI 516552) in the light. However, transcript levels for JGI 516552 in the dark were not elevated above the levels measured in the *zds1-1* parental strains, consistent with the lack of greening of zSup63 in the dark. This expression pattern fits my hypothesis for an alternative carotene desaturase that is expressed in the dark but that is expressed at a higher level in the light.

Though infrequent, organisms with oxygenic photosynthesis have been identified that use carotene desaturases that are more related to bacterial CrtI-type phytoene desaturases. *Nostoc* PCC7120's CrtQa/CrtQ-1 is more closely related to CrtI-type desaturases, but it was shown to use *cis*- and *trans*-isomers as substrates. When expressed in *E. coli*, CrtQa could desaturate 9,9'-*dicis*-ζ-carotenes to prolycopene, neurosporene to lycopene, and β-zeacarotene to γ-carotene [14,33]. The cyanobacterium *G. violaceus* does not have a plant-type PDS, but has a four-step CrtI-type desaturase instead [11]. The carotenogenic but non-photosynthetic bacterium, *Myxococcus xanthus*, has two CrtI-like desaturases, CrtIa and CrtIb, that in cooperation convert 15-*cis*-phytoene to all-*trans*-lycopene [34]. One desaturase, CrtIa recognizes carotenes in the *cis*-configuration while the other desaturase recognizes them in *trans*-configurations [34]. Carotenoid biosynthesis in *M. xanthus* was stimulated by blue-light [35]. Biochemical analysis of CrtQa from *Nostoc* PCC7120 and CrtIa from *M. xanthus* show that CrtI-related carotene desaturases are not strictly confined to only *trans*-configured substrates.

If a CRTISO-like ZDS does exists in addition to PDS and ZDS, *C. reinhardtii* will be the first oxygenic photosynthetic organism identified with two functional carotene desaturation pathways operating at the same time. Furthermore, the low light sensitivity phenotype of CAL.028.02.09 shows that the putative *C. reinhardtii* CRTISO-like carotene desaturase may have an important supportive role to the main plant-type PDS/ZDS carotene desaturation pathway.

To demonstrate that *C. reinhardtii* CRTISO-like protein 516552 has carotene desaturase activity, double mutants of CAL028.02.09 with *zds1-1* and also with *crtiso1* still need to be generated. Double mutants of CAL028.02.09 and either *zds1-1* or *crtiso1-1* should not accumulate xanthophylls in the dark. Pigment analysis and light sensitivity assays still need to be completed with CAL028.02.09 and any double mutants generated. Finally substrate specificity for 516552 can be determined by expressing the enzyme in *E. coli* strains that accumulate different carotenes as substrates.

REFERENCES

1. Fraser PD, Misawa N, Linden H, Yamano S, Kobayashi K, et al. (1992) Expression in *Escherichia coli*, purification, and reactivation of the recombinant *Erwinia uredovora* phytoene desaturase. Journal of Biological Chemistry 267: 19891-19895.
2. Sandmann G (2009) Evolution of carotene desaturation: the complication of a simple pathway. Archives of Biochemistry and Biophysics 483: 169-174.
3. Raisig A, Bartley G, Scolnik P, Sandmann G (1996) Purification in an active state and properties of the 3-step phytoene desaturase from *Rhodobacter capsulatus* overexpressed in *Escherichia coil*. Journal of Biochemistry 119: 559-564.
4. Breitenbach J, Sandmann G (2005) ζ-Carotene cis isomers as products and substrates in the plant poly-cis carotenoid biosynthetic pathway to lycopene. Planta 220: 785-793.
5. Chen Y, Li F, Wurtzel ET (2010) Isolation and characterization of the *Z-ISO* gene encoding a missing component of carotenoid biosynthesis in plants. Plant Physiology 153: 66-79.
6. Park H, Kreunen SS, Cuttriss AJ, DellaPenna D, Pogson BJ (2002) Identification of the carotenoid isomerase provides insight into carotenoid biosynthesis, prolamellar body formation, and photomorphogenesis. Plant Cell 14: 321-332.
7. Isaacson T, Ronen G, Zamir D, Hirschberg J (2002) Cloning of *tangerine* from tomato reveals a carotenoid isomerase essential for the production of β-carotene and xanthophylls in plants. Plant Cell 14: 333-342.
8. Li F, Murillo C, Wurtzel ET (2007) Maize *Y9* encodes a product essential for 15-cis-{zeta}-carotene isomerization. Plant Physiology 144: 1181-1189.
9. Sandmann G (1991) Light-dependent switch from formation of poly-cis carotenes to all-trans carotenoids in the *Scenedesmus mutant* C-6D. Archives of Microbiology 155: 229-233.
10. Isaacson T, Ohad I, Beyer P, Hirschberg J (2004) Analysis in vitro of the enzyme CRTISO establishes a poly-cis-carotenoid biosynthesis pathway in plants. Plant Physiology 136: 4246-4255.
11. Steiger S, Jackisch Y, Sandmann G (2005) Carotenoid biosynthesis in *Gloeobacter violaceus* PCC4721 involves a single crtI-type phytoene desaturase instead of typical cyanobacterial enzymes. Archives of Microbiology 184: 207-214.
12. Tsuchiya T, Takaichi S, Misawa N, Maoka T, Miyashita H, et al. (2005) The cyanobacterium *Gloeobacter violaceus* PCC 7421 uses bacterial-type phytoene desaturase in carotenoid biosynthesis. FEBS Letters 579: 2125-2129.
13. Linden H, Misawa N, Saito T, Sandmann G (1994) A novel carotenoid biosynthesis gene coding for ζ-carotene desaturase: functional expression, sequence and phylogenetic origin. Plant Molecular Biology 24: 369-379.
14. Albrecht M, Linden H, Sandmann G (1996) Biochemical characterization of purified ζ-carotene desaturase from *Anabaena* PCC 7120 after expression in *Escherichia coli*. European Journal of Biochemistry 236: 115-120.
15. Sandmann G (2002) Molecular evolution of carotenoid biosynthesis from bacteria to plants. Physiologia Plantarum 116: 431-440.
16. Dent RM, Haglund CM, Chin BL, Kobayashi MC, Niyogi KK (2005) Functional Genomics of Eukaryotic Photosynthesis Using Insertional Mutagenesis of Chlamydomonas reinhardtii. Plant Physiology 137: 545-556.
17. Harris EH (1989) The *Chlamydomonas* Sourcebook: A Comprehensive Guide to Biology and Labortory Use: Academic Press, San Diego.

18. McCarthy SS, Kobayashi MC, Niyogi KK (2004) White mutants of *Chlamydomonas reinhardtii* are defective in phytoene synthase. Genetics 168: 1249-1257.
19. Werner R, Mergenhagen D (1998) Mating type determination of *Chlamydomonas reinhardtii* by PCR. Plant Molecular Biology Reporter 16: 295-299.
20. Altschul SF, Madden TL, Schäffer AA, al. ae (1997) Gapped BLAST and PSI-BLAST: a new generation of protein database search programs. Nucleic Acids Research 25: 3389-3402.
21. Dereeper A, Guignon V, Blanc G, Audic S, Buffet S, et al. (2008) Phylogeny.fr: robust phylogenetic analysis for the non-specialist. Nucleic Acids Research 36: W465-W469.
22. Anisimova M, Gascuel O (2006) Approximate likelihood-ratio test for branches: A fast, accurate, and powerful alternative. Systematic Biology 55: 539-552.
23. Guindon S, Gascuel O (2003) A simple, fast, and accurate algorithm to estimate large phylogenies by maximum likelihood. Systematic Biology 52: 696-704.
24. Edgar RC (2004) MUSCLE: multiple sequence alignment with high accuracy and high throughput. Nucleic Acids Research 32: 1792-1797.
25. Chevenet F, Brun C, Anne-Laure B, Jacq B, Christen R (2006) TreeDyn: towards dynamic graphics and annotations for analyses of trees. BMC Bioinformatics 7: 1471-2105.
26. Marchler-Bauer A, Bryant SH (2004) CD-Search: protein domain annotations on the fly. Nucleic Acids Research 32: W327-W331.
27. Marchler-Bauer A, Anderson JB, Chitsaz F, Derbyshire MK, DeWeese-Scott C, et al. (2009) CDD: specific functional annotation with the Conserved Domain Database. Nucleic Acids Research 37: D205-D210.
28. Marchler-Bauer A, Lu S, Anderson JB, Chitsaz F, Derbyshire MK, et al. (2011) CDD: a Conserved Domain Database for the functional annotation of proteins. Nucleic Acids Research 39: D225-D229.
29. Mohamed HE, Vermaas W (2004) Slr1293 in *Synechocystis* sp. strain PCC 6803 Is the C-3',4' desaturase (CrtD) involved in myxoxanthophyll biosynthesis. J Bacteriol 186: 5621-5628.
30. Bartley GE, Scolnik PA, Beyer P (1999) Two *Arabidopsis thaliana* carotene desaturases, phytoene desaturase and ζ-carotene desaturase, expressed in *Escherichia coli,* catalyze a poly-*cis* pathway to yield pro-lycopene. European Journal of Biochemistry 259: 396-403.
31. Beyer P, Mayer M, Kleinig H (1989) Molecular oxygen and the state of geometric isomerism of intermediates are essential in the carotene desaturation and cyclization reactions in daffodil chromoplasts. European Journal of Biochemistry 184: 141-150.
32. Li Z, Wakao S, Fischer BB, Niyogi KK (2009) Sensing and responding to excess light. Annual Review of Plant Biology 60: 239-260.
33. Linden H, Vioque A, Sandmann G (1993) Isolation of a carotenoid biosynthesis gene coding for ζ-carotene desaturase from *Anabaena* PCC 7120 by heterologous complementation. FEMS Microbiology Letters 106: 99-103.
34. Iniesta AA, Cervantes M, Murillo FJ (2007) Cooperation of two carotene desaturases in the production of lycopene in *Myxococcus xanthus*. FEBS Journal 274: 4306-4314.
35. Burchard RP, Dworkin M (1966) Light-induced lysis and carotenogenesis in *Myxococcus xanthus*. J Bacteriol 91: 535-545.

CHAPTER 5
Conclusions

Chlamydomonas reinhardtii is a model organism for understanding carotenoid biosynthesis, evolution, and regulation in oxygenic photosynthetic organisms. The ability to culture light-sensitive mutants using heterotrophic growth conditions facilitates separation of light-induced phenotypes versus phenotypes related to carotenoid biosynthesis and regulation. In the experiments described in Chapters 2, 3, and 4, *C. reinhardtii* carotenoid-deficient mutants defective in early carotenoid biosynthesis were characterized and found to accumulate *cis*-carotene isomers (15-*cis*-phytoene, *cis*-ζ-carotenes, and 7,9,7'9'-*tetracis*-lycopene) demonstrating that the plant-type poly-*cis* carotene desaturation pathway functions in *C. reinhardtii*. The three types of *cis*-carotene-accumulating mutants had defects in phytoene desaturase (PDS), ζ-carotene desaturase (ZDS), and carotene isomerase (CRTISO) activity and had mutant phenotypes that cosegregated with their respective genes in genetic linkage analyses. Additionally, the accumulation of xanthophylls in dark-grown *zds1* and *crtiso1* mutants indicates that an alternative carotene desaturase with structural similarity to CRTISO enzymes may support primary carotenoid biosynthesis (via PDS/ZDS/CRTISO activities) in the light.

In the *zds1* suppressor zSup63, transcripts of a gene encoding a CRTISO-like protein were more highly expressed than in *zds1* and wild-type strains. If this CRTISO-like protein (516552) is responsible for dark-synthesized xanthophylls in *zds1* and *crtiso1* mutants, *C. reinhardtii* will be the first reported oxygenic photosynthetic organism with two active ζ-carotene desaturases. Furthermore, protein 516552 will be the first reported CRTISO-like protein with desaturase activity. Identification of a CRTISO-like protein with desaturase activity would add a new chapter to the story of phytoene desaturase evolution. Because CRTISO cloned from various organisms consistently clusters with bacterial-type CrtI phytoene desaturases [1,2,3,4], it is generally thought that CRTISO evolved from a CrtI-type desaturase and with its incorporation into plant-type carotene desaturation, lost its desaturase activity. A CRTISO-like desaturase with activity towards *cis*-carotenes could act as the evolutionary link between plant CRTISO proteins with only isomerase activity and bacterial CrtI-type desaturases capable of three or more desaturations. One could determine if protein 516552 has desaturase activity and substrate preference by heterologously expressing 516552 in *E. coli* strains accumulating 15-*cis*-phytoene, *cis*-ζ-carotene isomers, and *trans*-carotene isomers.

Regulation of carotenoid biosynthesis is still not well understood, as carotenoid production and accumulation in the cells are tightly bound to chlorophyll synthesis and accumulation, to plastid development, and to the presence of light [5,6,7]. Because there is a cost to synthesizing metabolites, regulation of biosynthetic pathways tends to target enzymes functioning in the beginning of the pathway. The *C. reinhardtii* mutants characterized here with blocks in steps two, four, and five of carotenoid biosynthesis will be useful for studies in regulation of the pathway. I showed that phytoene that is accumulated in the dark causes cells to grow more slowly compared to wild type and *lts1* mutants. The ability to culture *C. reinhardtii* heterotrophically and comparison with *lts1* mutants blocked in phytoene synthase allowed me to separate stress caused by photodamage from effects related to phytoene accumulation. Cells might control the flux of metabolites entering carotenoid synthesis using feedback regulation.

The *pds1* enhancer strain, P3-84 (*lts1-301 pds1-2*), might have gained a mutation in *PSY* to minimize phytoene accumulation (Chapter 2, Figure 2.4). Leaky *PSY* mutants such as *lts1-301* could be useful for studying the level of carotenoids needed for effective photoprotection, and mutants accumulating various carotenoid intermediates will be valuable for feedback regulation studies. Lutein accumulation was drastically reduced particularly for *zds1* mutants in response to the block in carotene desaturation, whereas zeaxanthin levels increased in response to lutein depression. This suggests an effect on lycopene cyclization in *zds1*. Chai *et al.* also noticed that rice *crtiso* mutant accumulated low levels of lutein and that the *zebra2* phenotype resulted in reduced transcript levels for genes upstream of lutein formation, such as *PSY1*, *PSY2*, *PDS*, *ZEBRA2*, and *LYC-E* [8].

Due to the ability of *zds1* and *crtiso1* mutants to "green" in the light, these mutants could be useful for understanding how pigment-protein complexes assemble. Pigment-protein complexes could be isolated from *crtiso1* and *zds1* cells illuminated with very low light at various time points of "photo-acclimation" and analyzed for pigment and protein content [9,10,11]. Similar experiments could also provide information on the stoichiometry of carotenoids, chlorophylls, and the proteins that bind them.

Over 150 carotenoid biosynthesis genes have been identified from various organisms and have served as the base for genetically engineering crops with improved carotenoid content and for engineering novel carotenoids [7,12,13]. Identification of the *C. reinhardtii* carotenoid genes described here will contribute to future metabolic engineering of carotenoid biosynthesis in *C. reinhardtii*, in other algae, and in plants.

REFERENCES

1. Sandmann G (2002) Molecular evolution of carotenoid biosynthesis from bacteria to plants. Physiologia Plantarum 116: 431-440.
2. Steiger S, Jackisch Y, Sandmann G (2005) Carotenoid biosynthesis in *Gloeobacter violaceus* PCC4721 involves a single crtI-type phytoene desaturase instead of typical cyanobacterial enzymes. Archives of Microbiology 184: 207-214.
3. Park H, Kreunen SS, Cuttriss AJ, DellaPenna D, Pogson BJ (2002) Identification of the carotenoid isomerase provides insight into carotenoid biosynthesis, prolamellar body formation, and photomorphogenesis. Plant Cell 14: 321-332.
4. Isaacson T, Ronen G, Zamir D, Hirschberg J (2002) Cloning of *tangerine* from tomato reveals a carotenoid isomerase essential for the production of β-carotene and xanthophylls in plants. Plant Cell 14: 333-342.
5. Bohne F, Linden H (2002) Regulation of carotenoid biosynthesis genes in response to light in *Chlamydomonas reinhardtii*. Biochimica et Biophysica Acta (BBA) 1579: 26-34.
6. Cazzonelli CI, Roberts AC, Carmody ME, Pogson BJ (2010) Transcriptional Control of SET DOMAIN GROUP 8 and CAROTENOID ISOMERASE during Arabidopsis Development. Molecular Plant 3: 174-191.
7. Farré G, Sanahuja G, Naqvi S, Bai C, Capell T, et al. (2010) Travel advice on the road to carotenoids in plants. Plant Science 179: 28-48.
8. Chai C, Fang J, Liu Y, Tong H, Gong Y, et al. (2011) *ZEBRA2*, encoding a carotenoid isomerase, is involved in photoprotection in rice. Plant Molecular Biology 75: 211-221.
9. Ruban AV, Lee PJ, Wentworth M, Young AJ, Horton P (1999) Determination of the stoichiometry and strength of binding of xanthophylls to the photosystem II light harvesting complexes. Journal of Biological Chemistry 274: 10458-10465.
10. Horton P, Ruban A (2005) Molecular design of the photosystem II light-harvesting antenna: photosynthesis and photoprotection. Journal of Experimental Botany 56: 365-373.
11. Herrin DL, Battey JF, Greer K, Schmidt GW (1992) Regulation of chlorophyll apoprotein expression and accumulation. Requirements for carotenoids and chlorophyll. Journal of Biological Chemistry 267: 8260-8269.
12. Schmidt-Dannert C (2000) Engineering novel carotenoids in microorganisms. Current Opinion in Biotechnology 11: 255-261.
13. Schmidt-Dannert C, Umeno D, Arnold FH (2000) Molecular breeding of carotenoid biosynthetic pathways. Nature Biotechnology 18: 750-753.